Title
Mycobacterium marinum actin-based motility

Author
Stamm, Luisa M

Publication Date
2005

Peer reviewed|Thesis/dissertation

Mycobacterium marinum **Actin-Based Motility**

by

Luisa M. Stamm

DISSERTATION

Submitted in partial satisfaction of the requirements for the degree of

DOCTOR OF PHILOSOPHY

in

Biomedical Sciences

in the

GRADUATE DIVISION

of the

UNIVERSITY OF CALIFORNIA, SAN FRANCISCO

Date University Librarian

Degree Conferred:

Acknowledgements

In reflecting upon all of those who have shaped my graduate school experience professionally and personally, I feel extremely fortunate; I have had a wonderful mentor, insightful colleagues, enduring friends and a loving family. I reached the completion of this degree only because of this tremendous support system.

I first thank my adviser Rick Brown for his investment in my development as a scientist. Rick possesses an enormous breadth of knowledge regarding immunology, cell biology and microbial pathogenesis, and an additional ability to easily convey complex concepts. As his student, I have benefited greatly from his guidance at all levels, from the development of experimental plans to scientific writing. He has positively influenced my critical thinking, not only in assisting me with troubleshooting and data analysis, but also in reminding me to consider the broader implications of my research. I sincerely appreciate his patience, unwavering support, and genuine interest in my personal well-being. I am also grateful to the additional members of my thesis committee, Joanne Engel, Jeff Cox and Dyche Mullins, for their thoughtful comments about this work.

The members of the Brown lab during the past four years have made it a great place to work. In particular, I am indebted to Hiroshi Morisaki, without whose keen eye and technical expertise I never would have started working on this project or made much progress. We spent countless hours at the microscope, examining hundreds of slides, scoring millions of cells, and, most importantly, building a friendship. I thank Melissa Pak for her technical expertise in molecular biology and all the energy she bought to any experiment we did together; we made a great team.

I have formed some extraordinary friendships during graduate school. Sridharan Raghavan has been a wonderful colleague and a caring friend. I appreciate all of our conversations in which he not only made me laugh, but also offered sound scientific advice. I met Marla Abodeely and Rebecca Blank during my first rotation in graduate school, and our friendship was immediate and lasting. The three of us have shared the highs and lows of graduate school, and enjoyed ourselves outside the lab.

I thank Gene, Debbie, Kate and Ian Buehler for becoming my west coast family; it has meant so much for them to make me a part of their lives. I would like to express my deepest gratitude to my mom, my dad, and Derek for all their love and support during my scientific career. My family has always believed in me, giving me the strength to pursue my goals. Lastly, I thank my best friend and husband Kenny Gray who has been a part of my life for so long that I can hardly remember it without him. He has shared in all of my frustrations and successes, and been a source of encouragement and perspective when I needed it most. I thank him for all of our adventures, and continue to value his friendship and cherish his love.

Contributions of Others to the Presented Work

Chapter 1 of this dissertation is based on material published in a review of the literature in *Microbes and Infection* (2004) 6:1418-28, titled, "*Mycobacterium marinum*: the generalization and specialization of a pathogenic mycobacterium," by copyright permission of the Institut Pasteur. The images in Figure 1.2 were kindly provided by Henry C. Sanchez, Philip E. LeBoit and Lian-Yong Gao. The figures were constructed with help from John H. Morisaki. Eric J. Brown is a co-author of this publication.

Chapter 2 is based on material published in *The Journal of Experimental Medicine* (2003) 198:1361-1368, titled, "*Mycobacterium marinum* escapes from phagosomes and is propelled by actin-based motility," by copyright permission of The Rockefeller University Press. The following co-authors contributed to this work: J. Hiroshi Morisaki, Lian-Yong Gao, Robert L. Jeng (University of California, Berkeley), Kent L. McDonald (University of California, Berkeley), Robyn Roth (Washington University), Sunao Takeshita (Washington University), John Heuser (Washington University), Matthew D. Welch (University of California, Berkeley). *M. tuberculosis* infections were performed by Sridharan Raghavan. *M. ulcerans* was provided by Pamela L. Small. Eric J. Brown supervised this work.

Chapter 3 is based on a manuscript submitted for publication, titled "Role of the WASP family proteins in *Mycobacterium marinum* actin tail formation." The following co-authors contributed to this work: Melissa A. Pak, J. Hiroshi Morisaki, Scott B. Snapper (Massachusetts General Hospital), Klemens Rottner (German Research Center

for Biotechnology) and Silvia Lommel (German Research Center for Biotechnology). Eric J. Brown supervised this work.

In Chapter 4, John E. Dueber performed pyrene assays, and the Δ*plc M. marinum* mutant was made by Melissa A. Pak under the supervision of Lian-Yong Gao. The *M. ulcerans* strains were kindly provided by Pamela L. Small.

Mycobacterium marinum **Actin-Based Motility**

by

Luisa M. Stamm

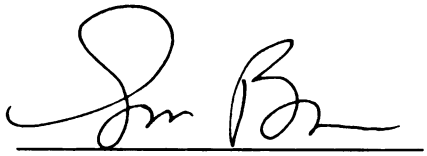

Eric J. Brown

Abstract

Mycobacterium tuberculosis infects more than one billion people and causes millions of deaths per year, but the mechanisms by which this organism causes disease are poorly understood. *M. marinum* causes a tuberculosis-like disease in fish and has been used increasingly as a model to understand the molecular pathogenesis of tuberculosis. Pathogenic mycobacteria are classical intracellular pathogens of macrophages and are widely believed not to enter the cytoplasm, but rather to exist exclusively within phagosomes. Contrary to this accepted paradigm, we found by using various microscopy techniques that intracellular *M. marinum* not only enters the cytoplasm of infected macrophages, but also is propelled by induction of actin polymerization leading to direct intercellular spread. This process of actin-based motility, although never observed previously for mycobacteria, is utilized by many bacterial intracellular pathogens such as *Listeria monocytogenes* and *Shigella flexneri* and is required for full virulence of these species *in vivo*. To polymerize actin, these

pathogens and *M. marinum* exploit a host cell signaling pathway by recruiting cytoskeletal factors leading to Arp2/3 complex actin nucleation. Using deficient cell lines and pharmacological inhibition, we demonstrate that the WASP family of proteins, including WASP and N-WASP, is critical for efficient *M. marinum* actin polymerization, whereas factors upstream of the WASP family such as tyrosine phosphorylation, Nck, WIP, and Cdc42 are not important. Through detailed analysis of the N-WASP domains able to restore *M. marinum* actin polymerization in N-WASP$^{-/-}$ cells, we found that the basic motif of N-WASP to which host cell lipids bind is required. These data indicate that *M. marinum* utilizes a mechanism distinct from other pathogens to initiate actin polymerization perhaps by using the distinct cell surface lipids present in the mycobacterial cell wall.

Table of Contents

List of Figures

List of Tables

Chapter 1

Generalization and Specialization of *Mycobacterium marinum*

Abstract

Mycobacterium marinum is being used increasingly as a model for understanding pathogenic mycobacteria. However, recently discovered differences between *M. marinum* and *M. tuberculosis*, including those presented in this dissertation, suggest that adaptation to specialized niches is reflected in unique strategies of pathogenesis. This introductory chapter emphasizes the areas in which studying *M. marinum* has made contributions to the understanding of tuberculosis, as well as the potential for using characteristics unique to *M. marinum*, in particular actin-based motility, for understanding general issues of host-pathogen interactions.

M. marinum as a Model System

The genus *Mycobacterium* causes diverse diseases in humans (Figure 1.1), the most serious being tuberculosis, which infects at least one-third of the world's population and causes two million deaths each year (1). Treatment of this disease is complicated by the requirement for long courses of therapy, leading directly to the emergence of multi-drug resistant *M. tuberculosis*. Although tuberculosis infection of humans has been traced back thousands of years (2) and its study has been a focus of microbiological research for more than a century, fundamental questions remain concerning how mycobacteria cause disease. *M. tuberculosis* is a strict human pathogen, with no other natural hosts. It can represent a considerable hazard to laboratory workers and others in the research environment, so its use in the laboratory requires stringent measures to prevent infection. At the same time, novel strategies to control tuberculosis require significant effort to improve current methods of prevention and treatment. The need to further understand the complex biology between pathogenic mycobacteria and their hosts drives research for the development of safe model systems that are easily genetically manipulated.

Mycobacterium marinum is a natural pathogen of fish that has been responsible for outbreaks of disease in both fresh and salt water in a wide geographic distribution. *M. marinum* causes a chronic progressive disease manifested by uncoordinated swimming, abdominal swelling, weight loss and occasionally skin ulcers. The disease mainly affects the liver, kidney and spleen that are marked during infection with white nodules microscopically identifiable as granulomas. Granulomas caused by *M. marinum* in fish are very similar to granulomas caused by *M. tuberculosis* in the lungs of humans,

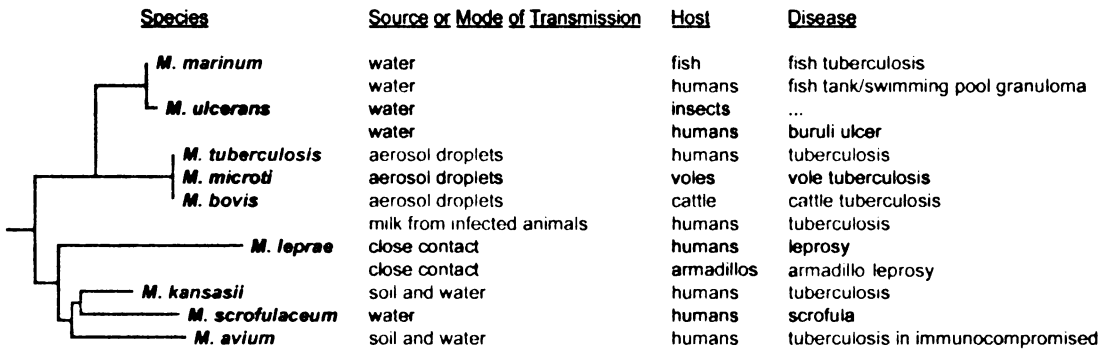

Figure 1.1 Pathogenic mycobacteria cause diverse diseases. This phylogenic tree is based on 16s rRNA sequences (8). In addition, the environmental source of the mycobacterial species or its mode of transmission, the hosts it affects and the diseases it causes in that host are shown.

including the presence of caseous necrosis in the centers of some granulomas (Figure 1.2). Transmission of *M. marinum* among fish is poorly understood. The most probable route of primary infection is either oral, as when an infected fish dies and is consumed by other fish in the population, or through injuries in the skin if the number of bacteria in the environment is high or if the fish has a poorly functioning immune system. Uptake through the gills, in a manner somehow analogous to inhalation of bacteria in transmission of tuberculosis, also remains a possibility.

M. marinum occasionally causes a disease in humans medically described as "fish tank granuloma" or "swimming pool granuloma." The granulomatous response that occurs following subcutaneous inoculation of *M. marinum* is localized to the site where it was introduced, usually in an extremity. Pathologically, the granuloma caused by a *M. marinum* dermal infection is similar to that caused by a *M. tuberculosis* lung infection (Figure 1.2). *M. marinum* is adapted to infect ectotherms, and so its optimal temperature for growth is 25-35°C (3), most likely explaining the limitation of *M. marinum* infection to the skin of immunocompetent humans. However, there have been occasional reports of *M. marinum* causing disseminated disease in severely immunocompromised patients (4), suggesting that a robust immune response is, at least in some cases, required to control disease. *M. marinum* is considered safe for use by healthy individuals under BSL2 laboratory conditions, making it an attractive organism with which to work. *M. marinum* forms colonies on agar in a week, in contrast to *M. tuberculosis* which requires 3 weeks. The pathological similarity of *M. marinum* to *M. tuberculosis* infection, combined with its increased safety, more rapid growth, and ease of use make *M. marinum* a useful model with which to study pathogenic mycobacteria.

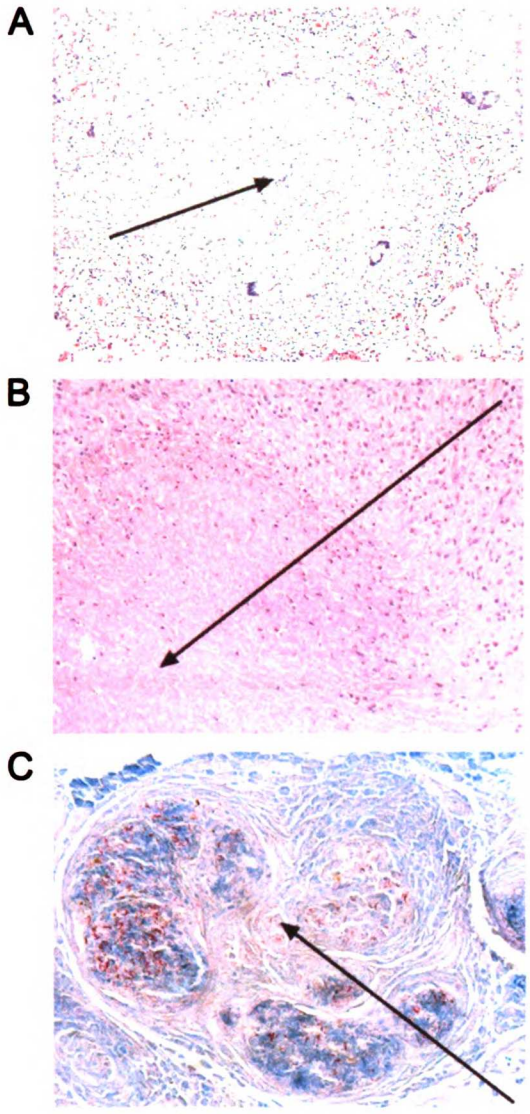

Figure 1.2 *M. tuberculosis* and *M. marinum* cause similar pathology.

(A) *M. tuberuculosis* in the human lung causes formation of a granuloma with central necrosis. (B) At a higher magnification, the central necrosis is also evident within a granuloma caused by *M. marinum* in a human dermal infection of the hand. (C) In an experimental infection of zebrafish, a granuloma was stained for the presence of acid-fast *M. marinum* found in multiple foci. Arrows of relative size in each panel indicate the center of the granuloma.

While there are undoubtedly many parallels between the pathogenic mechanisms of infection by *M. marinum* and *M. tuberculosis*, the work presented in this dissertation highlights a striking variation in the behavior of the two organisms after initiation of intracellular infection, reminding us that even these closely related organisms can demonstrate significant differences. The remainder of this introduction will focus on the state of understanding of the ways in which *M. marinum* is similar to and differs from other pathogenic mycobacteria.

Comparative Genomics

Much has been learned about pathogenic mycobacteria since the publication of the first mycobacterial genome by Cole *et al.* in 1998 (5). Currently, completed genomes include *M. tuberculosis*, *M. leprae*, and *M. bovis*. At the time of this writing the *M. marinum* genome is now assembled, but not yet completely annotated (6). The *M. ulcerans* sequencing project is also well underway (7). A brief comparison of the genomic sequences of *M. marinum* to other mycobacterial species leads to some hypotheses about how the species are related and how they have adapted to specific niches.

M. marinum *to* M. tuberculosis

According to 16S rRNA sequences of 19 mycobacterial species, *M. marinum* is the closest relative to the *M. tuberculosis* complex with a sequence homology of 99.4% (Figure 1.1) (8). Specific genes are very well conserved between *M. marinum* and *M. tuberculosis*; the expression of *M. tuberculosis* genes in *M. marinum* complements

mutations in that species suggesting that the sequence homologies extend to function (9-11). However, the predicted size of the *M. marinum* genome is 6.5 Mbp (6), differing significantly from the 4.4 Mbp genome of *M. tuberculosis* (5). Almost 50% of the *M. tuberculosis* genome appears to have arisen through duplications (5), and informal comparisons of the genomes of *M. tuberculosis* and *M. marinum* suggest that a great deal of the expansion in *M. marinum* consists of further duplications, which may be involved in species-specific adaptations to its ecological niche.

M. tuberculosis is a human-specific aerosol pathogen, in contrast to *M. marinum* that is an aquatic pathogen of multiple genera of fish. In addition, *M. marinum* can infect water-borne amoebae, at least under experimental conditions (12), suggesting that environmental protozoa may also be a host for *M. marinum* and perhaps play a role in transmission among fish in the aquatic environment. The increased size of the *M. marinum* genome may reflect requirements imposed by its increased host range compared to *M. tuberculosis*. Other differences, like pigmentation, may be required for adaptation to the aquatic environment. Additional, possibly unique, features of *M. marinum,* such as phagosome escape and actin-based motility (see below), may also contribute to the difference in genome size. The *M. marinum* genome-sequencing project, when completed, will no doubt allow testing of some of these ideas.

M. marinum *to* M. ulcerans

Of all the mycobacteria, *M. marinum* is most closely related to *M. ulcerans* (Figure 1.1)(8). *M. ulcerans* grows relatively slowly compared to *M. marinum*, taking four weeks to form colonies. Like *M. marinum*, *M. ulcerans* transmission to humans is

associated with water; however the geographic range of *M. ulcerans* is more restricted, and aquatic insects appear to be a reservoir for *M. ulcerans* in this environment (13). Although they are genetically very similar and share the same broad ecological niche, *M. marinum* and *M. ulcerans* interact with host cells in very distinct manners resulting in very different diseases. *M. ulcerans* is the cause of Buruli ulcer in Africa and Australia. In contrast to *M. marinum,* an intracellular pathogen that causes strong inflammatory and immune responses, *M. ulcerans* is an extracellular bacterium that inhibits inflammation. The toxin required for *M. ulcerans*' anti-inflammatory effects has been identified as the secreted polyketide toxin mycolactone (14). Purified mycolactone is cytopathic to host cells, including neutrophils and macrophages, explaining the absence of inflammation in *M. ulcerans* lesions (15). Mycolactone is specific to *M. ulcerans*, and not found in *M. marinum* or any other mycobacterial species (16). Subtractive hybridization of *M. marinum* and *M. ulcerans* has been used to identify the presence of a mycobacterial plasmid necessary and sufficient for the production of mycolactone (17). The acquisition of mycolactone by *M. ulcerans* has dramatically affected the clinical disease caused by the species, and alone can explain many differences between *M. ulcerans* and *M. marinum*, its genetically closest relative.

Similarities between *M. marinum* and Pathogenic Mycobacteria

M. marinum causes similar pathology in fish as *M. tuberculosis* does in humans and is closely related to *M. tuberculosis*, leading to the hypothesis that many steps in initiation and maintenance of disease are similar. A few examples that support this hypothesis are illustrated.

PE-PGRS family

The *M. tuberculosis* genome project revealed that ~5% of the *M. tuberculosis* genome is comprised of the PE-PGRS family (5), and our own informal analysis suggests that this family is also frequently found in M. *marinum*. Proteins in the family are characterized by a proline-glutamic acid (PE) amino acid sequence near the amino terminus and a carboxy-terminal domain that is rich in glycine and alanine, referred to as polymorphic GC-rich sequence (PGRS). The functions of these proteins are unknown; speculations include that PE-PGRS proteins may inhibit antigen presentation (18), or may provide antigenic variation *in vivo* (19). Several studies indicate that members of the family are found on the surface of mycobacteria (19-21).

Using a novel technique, *M. marinum* was used in a promoter trap screen to identify genes specifically expressed either after infection of macrophages or *in vivo* (22,23). Macrophages or leopard frogs were infected with the promoter-trap library of *M. marinun* and analyzed by FACs for particular subsets of genes differentially expressed within macrophage phagosomes or within granulomas (22-24). One of the macrophage-activated genes identified is a member of the PE-PGRS family of mycobacterial proteins (23). Mutants in this gene do not replicate in macrophages, do not persist in granulomas, and are out-competed by wild type bacteria 10- to 24-fold in a frog infection (23,24). It is potentially significant that mutations in single PE-PGRS genes in both *M. marinum* and *M. tuberculosis* have been found to have effects on intracellular growth despite the high degree of homology in this family of genes even within a single species of mycobacteria. This demonstrates that at least some members of the family have non-redundant, possibly direct roles in pathogenesis (20,23).

Cell Wall Synthesis

Compared to other bacterial species, mycobacteria have a very unique cell wall structure. It is composed of a thick arabinogalactan layer and an outer layer of mycolic acids. The synthesis of the mycobacterial cell wall has long been a target of anti-tuberculous therapies, including isoniazaid (INH). In examining a library of *M. marinum* transposon insertions for attenuating mutations, we found a mutant in *kasB*, a gene that encodes an enzyme required for mycolic acid synthesis (10). It and its close homologue *kasA* had been studied *in vitro* (25), but functional differences between the two enzymes were not known and no specific mutants in the enzymes existed in pathogenic mycobacteria. Using this *M. marinum* mutant, we were able to delineate a specific role for *kasB*. Surprisingly, it is required only for addition of the last 1-2 ethyl groups in these ~90-carbon fatty acids. Nonetheless, this small difference in chain length in the *kasB* mutant led to markedly abnormal permeability of the mycobacterial cell wall and increased susceptibility both to innate mechanisms of host defense, such as lysozyme, and to hydrophobic small molecules like many antibiotics. Importantly, the *kasB* defect could be completely complemented by *M. tuberculosis kasB*, but was not by either *M. marinum* or *M. tuberculosis kasA*. In fact, overexpression of *kasA* exacerbated the membrane permeability defect of the *kasB* mutant, perhaps because of a further decrease in mycolic acid length.

This has several important implications. First, it is clear that the functions of the Kas enzymes are conserved between *M. marinum and M. tuberculosis*, and the distinctions we found in function between *kasA* and *kasB* appear to be parallel in the two species. Second, it is clear that inhibition of *kasB* will affect a separate step in the

synthesis of mycolic acid from INH, a drug that inhibits cell wall synthesis at an earlier step. Thus, as a legitimate drug target, *kasB* may work synergistically with other antibiotics. Finally, these studies suggest a new approach to understanding the function of specific *M. tuberculosis* genes within the context of an intact bacterium. Because complementation of an *M. marinum* mutant with the orthologous *M. tuberculosis* gene restored function, the *M. tuberculosis* gene products can be studied in a pathogenic organism, but one with little danger to humans. This could provide an excellent method for evaluating potential new drugs with substantially fewer safety concerns that arise with the use of *M. tuberculosis* itself.

A Novel Secretion System

The region of difference 1 (RD1) is a chromosomal region known to be involved in *M. tuberculosis* pathogenesis that is deleted in all strains of *M. bovis* BCG, the attenuated vaccine strain of *M. bovis*. Recent studies have shown that removal of this region or specific genes within the region from *M. tuberculosis* leads to defective growth in macrophages and attenuation in mouse infection (26-28). Together, these publications support that the region encodes a specialized secretion system necessary for delivery of ESAT-6 and CFP-10, two prominent antigens of the early immune response. Furthermore, they suggest that ESAT-6 and CFP-10 may have roles in dampening the inflammatory response (27) or in cytolysis required for tissue invasiveness (26).

In a study that emphasizes the functional similarities between *M. tuberculosis* and *M. marinum* for virulence, our lab examined the importance of this region in *M marinum* infection (11). Consistent with the *M. tuberculosis* results, disruption of genes within the

homologous region of the *M. marinum* chromosome also causes loss of virulence of this organism in a zebrafish model of infection (11). Like *M. tuberculosis*, the *M. marinum* RD1 mutants were defective in secretion of ESAT-6 and CFP-10. These mutants originally were identified because they are defective for contact-dependent hemolysis that may play a role in *M. marinum* phagosome escape and cell spreading. Like *M. marinum*, *M. tuberculosis* and *M. bovis* both are hemolytic. Although individual RD1 gene mutants in these human pathogens have not been examined, *M. bovis* BCG is non-hemolytic, like the *M. marinum* RD1 mutants. Together, these data suggest another function for the RD1 region that links this novel secretion pathway with hemolytic activity.

Specific Adaptations of *M. marinum*

While the examples described above demonstrate significant similarities between *M. marinum* and *M. tuberculosis*, *M. marinum* does differ from *M. tuberculosis* in important ways. Since these differences may actually help in understanding pathogenic mechanisms in both organisms, it is important to understand them in detail.

Photochromagenicity

Early studies developing genetic techniques for the *M. marinum* model focused on a characteristic of *M. marinum* not shared with *M. tuberculosis*, namely its pigmentation. Unlike *M. tuberculosis*, *M. marinum* is photochromogenic, producing a characteristic yellow color when exposed to light. The expression of pigmented molecules like carotenoids is believed to confer resistance to UV damage by reducing singlet oxygen and harmful radicals, to which *M. marinum* likely is exposed when in the aquatic

environment. Because of its easily discernable phenotype, we and others focused on the pigmentation pathway to prove the validity of new genetic tools (9,29). Using expression of *M. marinum* cosmids in *M. smegmatis* (a non-photochromagen), Ramakrishnan *et al.* were able to identify *crtB* and *crtI*, genes required in the carotenoid biosynthesis pathway, and to disrupt *crtB* by homologous recombination (29). We have used an adapted *mariner* transposon for random mutagenesis in *M. marinum* and tested for disruption of photochromogenicity to substantiate random insertion of the transposon (9). This work not only confirmed the previous work on *crtI* and *crtB*, but also identified genes that are involved in the control the pigmentation pathway. Interestingly, a mutant in one of these genes was more sensitive to singlet oxygen and had decreased intracellular survival, linking pigmentation and intracellular growth, perhaps suggesting that an induced stress response pathway can be activated both in the environment and during infection.

Host Range and Animal Model Development

M. marinum is a natural pathogen of ectotherms, including frogs and fish, and its optimal growth temperature range is 25-35°C (3). Although the mouse is a very useful animal model for numerous infectious diseases and has been used extensively to study *M. tuberculosis* pathogenesis, the ability to develop a *M. marinum* murine model of infection is severely limited because the temperature restrictions to its growth prohibit systemic infection of *M. marinum* in mice. This is a shortcoming of using *M. marinum*, since the mouse immune system is well understood and it is quite clear that interactions with host immunity are very important to initial infection and persistence of mycobacteria. On the

other hand, the leopard frog, *Rana pipiens*, and the zebrafish, *Danio rerio*, have been developed as successful experimental hosts for *M. marinum* infection (30,31). These models have the advantage that, unlike *M. tuberculosis* infections of mice, fish and frogs are both naturally infected by *M. marinum*.

The zebrafish is already a well-studied organism in which genetic tools such as large-scale saturation mutagenesis screens and anti-sense DNA oligonucleotide technology are used and whose genome is currently being sequenced (32). Although classically used in developmental studies, the immunology of zebrafish has been a focus of increased investigation recently (33). Molecular homologues of many components of the mammalian immune system have been found in zebrafish, including phagocytic myeloid cells, toll-like receptors, and some cytokines. Real-time aggregation of macrophages has been observed in *M. marinum*-infected, transparent zebrafish embryos (34). The aggregates apparently are initiated by infected cells, but contain uninfected cells as well. In addition to their hypothesized role in granuloma formation, these aggregates may provide an efficient mechanism for intercellular spread during infection. Recently, it has been found that macrophage aggregation in zebrafish embryos is dependent on the RD1 region in *M. marinum* suggesting yet another role of this region in virulence (35). Zebrafish are small, relatively inexpensive, and easy to breed; in addition, relevant pathology, forward genetic techniques, and embryonic transparency make zebrafish an attractive organism in which to study *M. marinum* infection.

The optimal temperature range of *M. marinum* opens the model to another class of host organisms, namely invertebrates including amoeba and flies. Many non-pathogenic mycobacteria can exist in the soil, and it is hypothesized that pathogenic mycobacteria

evolved from these species by adapting to an intracellular lifestyle within free-living protozoa in the environment. Amoebae are highly motile and phagocytic, and this hypothesis may explain the predilection of pathogenic mycobacteria for macrophages, a motile and phagocytic cell type, in metazoan hosts. In the laboratory, *M. marinum* can infect the water-borne amoeba *Acanthamoeba castellanii* (12) and can replicate within the free-living soil amoeba *Dictyostelium* (36). *Dictyostelium* is a particularly interesting single cell system in which to study *M. marinum* infection because genetic tools are available. The utility of *M. marinum* infection of *Dictyostelium* as a model system has been demonstrated by the use of *Dictyostelium* genetics to eliminate the requirement of the actin-binding protein coronin in *M. marinum* survival (36).

Infection of *Drosophila melanogaster* with *M. marinum* has shown that *Drosophila* is extremely sensitive to *M. marinum* infection ($LD_{50} < 5$ CFU) (37) making this a potential genetically tractable model in which to study innate immunity to mycobacteria. Interestingly, in this study, *Drosophila* mutants in innate immunity, in particular in the toll and imd pathways, were not more susceptible to *M. marinum* (37). The *Drosophila* S2 cell line, derived from a fly hemocyte, can potentially be used to study the cell biology of *M. marinum* infection. Preliminary data from our lab shows that the bacteria infect and grow in these cells (I. Koo, E. J. Brown, unpublished results). The relative ease of use of siRNA in insect cells in this context may enable elucidation host cell factors important in *M. marinum* cellular infection.

Intracellular Lifestyle of *M. marinum*

Macrophages are believed to be the cell type in which pathogenic mycobacteria persist *in vivo* in metazoan hosts. The fact that these bacteria are able to exist within the phagocytic immune cells that are specialized to seek and destroy foreign invaders attests to the unique adaptations mycobacteria have made to survive within a hostile intracellular environment. While pathogenic mycobacteria, including *M. tuberculosis* and *M. marinum*, can grow in a variety of eukaryotic cell lines *in vitro*, scientists have traditionally used macrophages, both primary cells and cell lines, to study the cell biology of the host-mycobacterial interaction. Comparison of their fates after infection of macrophages illustrates both the similarities and the differences between the adaptations *M. marinum* and *M. tuberculosis* have made to survive in this unique niche.

Common Early Events

A central idea in mycobacterial pathogenesis is that the bacteria regulate trafficking within the host cell endosomal pathway, halting phagosome maturation prior to acidification and fusion with lysosomes to form the phagolysosome (Figure 1.3) (38). This model has been developed from studies that measured pH of the mycobacteria-containing phagosome, that microscopically examined the presence or absence of various markers of the host cell endosomal pathway on or in the mycobacterial phagosome, and that directly demonstrated decreased delivery of lysosomal contents to the phagosome. Like other pathogenic mycobacteria, live, but not dead, *M. marinum* prevents fusion of its compartment with the lysosome (39,40). In particular, *M. marinum* was found to exclude specific lysosomal markers such as cathepsin D and the v-ATPase required for lysosomal

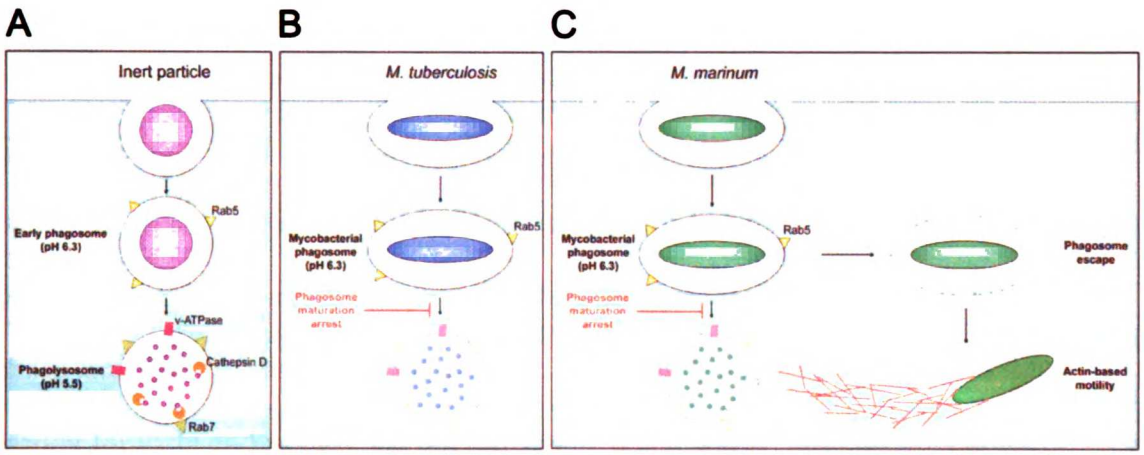

Figure 1.3 Mycobateria manipulate the intracellular environment. (A) Inert particles such as dead bacteria are phagocytosed and follow a default pathway, ending up eventually in the phagolysosome bearing the marker Rab7 on its surface and containing degradative lysosomal enzymes such as cathepsin D. This comparment possesses v-ATPase and, as a result, is acidic (pH 5.5). (B) *M. tuberculosis*, like many pathogenic mycobacteria, arrests phagosome maturaturation at the early phagsosome stage, marked by acquisition of Rab5 but not of Rab7. It does not contain mature lysosomal enzymes, and excludes v-ATPase thereby maintaining a more neutral compartment (pH 6.3). (C) *M. marinum* also arrests phagosome development like *M. tuberculosis*, and we hypothesize that it does so in a manner similar to *M. tuberculosis*. In addition, as demonstrated in Chapter 2, it is able to escape the phagosome. Once in the cytoplasm, *M. marinum* initiates actin polymerization leading to intracellular motility and direct intercellular spread.

acidification (Figure 1.3) (40). We and others have confirmed the failure of the *M. marinum* containing phagosome to acidify (10,37,41).

Work with other mycobacterial species has identified the Rab family of small GTPases as markers for phagosome progression, and emphasized the importance of not only proteins but also host lipids, such as phosphatidylinositols, and mycobacterial lipids, such as lipoarabinomannan and phosphatidylinositol mannoside, for manipulation of the phagosome by mycobacteria. For example, *M. tuberculosis* phagosomes have Rab5, a marker for early endosomes, but not Rab7, which is found on late endosomes and lysosomes; the absence of maturation apparently results from effects on host phosphatidylinositol 3-phosphate by the intraphagosomal bacteria (42). While these events have not been studied in the same detail for *M. marinum*, the similar failure of its phagosomes to mature to phagolysosomes makes it likely that the molecular mechanisms for inhibition of phagosome-lysosome fusion are quite similar for *M. marinum* and *M. tuberculosis*.

Mycobacterial Phagosome Permeability and Escape

Given all the similarities between *M. marinum* and other pathogenic mycobacteria it is surprising then that *M. marinum* can follow a unique intracellular fate, that of phagosomal escape into the cytoplasm. Nonetheless, we have found that a significant minority of intracellular *M. marinum* is capable of escape from the phagosome and initiation of actin-based motility in the cytoplasm of infected cells (Chapter 2). As reported for other pathogens that induce actin polymerization (43), this intracellular motility by *M. marinum* leads to direct intercellular spread. While the mechanism by

which *M. marinum* exits the phagosome and enters the cytoplasm is not known, *M. marinum* is hemolytic, a property of many, if not all, virulent mycobacteria (44). *M. marinum* hemolysis mutants are defective in a zebrafish model of infection, and, in addition, have decreased spreading in cell monolayers (11). These characteristics suggest that the hemolytic activity of *M. marinum* may be associated with its ability to escape from the phagosome (Chapter 4).

Although two reports have suggested that *M. tuberculosis* may exist in the cytoplasm (45,46), they are quite controversial, and it is widely believed that an intracellular *M. tuberculosis* exists exclusively within its privileged phagosome. However, there is some data to suggest that the *M. tuberculosis* phagosome could be in communication with the cytoplasm. For example, one study found that cytoplasmic fluorescently-labeled dextrans as large as 70 kDa could interact with *M. bovis* BCG in a murine cell line (47). Others have contradicted this result by showing that the mycobacterial phagosome is impermeable to 50 kDa anti-mycobacterium Fab fragments injected into the cytoplasm (48) and that fluorescently-labeled dextrans engulfed with *M. tuberculosis* by primary mouse macrophages did not leak out of the phagosome (49). The reasons for the differences between the two studies, which seem to have used very similar approaches, are unknown.

One of the oldest arguments in favor of the presence of *M. tuberculosis* in the host cell cytoplasm was the generation of MHC Class I restricted T cells in response to infection, since the "classic" pathway for Class I antigen presentation requires transport of cytoplasmic peptides into the endoplasmic reticulum. MHC class I is required for control of *M. tuberculosis* infection (50) and exogenous antigens that are taken up with

live mycobacteria are directly loaded onto MHC class I via the cytoplasm (51). However, the discovery of cross presentation pathways for generation of Class I-restricted T cells has led to a reinterpretation of these data, since it is now clear that this whole process can occur in response to intraphagosomal antigens, without the pathogen ever escaping from the phagosome (52). Nevertheless, it should be pointed out that most of these studies have not compared the extent of Class I antigen presentation by the various pathways, and it remains possible that cross presentation cannot completely explain the robust development of Class I restricted T cells in response to *M. tuberculosis* infection.

Whether *M. tuberculosis* remains completely intraphagosomal at all stages of infection is clearly an area of confusion and controversy in mycobacterial research at the moment. Although the weight of the evidence supports a phagosomal localization of *M. tuberculosis*, it is possible that phagosome escape by *M. tuberculosis* or other mycobacteria occurs in specific cell types or under circumstances *in vivo* that are not routinely reproduced in cell culture. As discussed above, *M. tuberculosis*, like *M. marinum*, is hemolytic, a property necessary for phagosome escape by *Listeria* and *Shigella* (53,54). Potentially hemolytic phospholipases C are conserved between the *M. tuberculosis* and *M. marinum* genome (6). The roles for these phospholipases in pathogenesis are unknown, but *M. tuberculosis* mutants in which three of the four phospholipase genes were inactivated had decreased virulence in a mouse model of infection, although they were not attenuated in a macrophage infection in cell culture (55). The *M. tuberculosis* phospholipases are therefore important in some manner *in vivo* that is not appreciated *in vitro*, perhaps playing a role in degradation of the phagosome

membrane at some point during animal infection. One may speculate that phagosome escape by *M. tuberculosis*, if it does occur, is very tightly regulated in a way that *M. marinum* is not, allowing more facile observation of intracytoplasmic *M. marinum* in the laboratory.

Actin-Based Motility

Because, as described above, mycobacteria are generally believed to remain within the phagosome, it was unexpected to find *M. marinum* forming actin tails in a manner similar to many other bacterial species regarded as classic intracytoplasmic pathogens such as *Listeria* and *Shigella* (Chapter 2). Whether phagosome escape and actin-based motility are unique characteristics of *M. marinum* or may be relevant to the intracellular lifestyle of other mycobacteria is not clear. We have failed to see actin tail formation by *M. tuberculosis* in conditions identical to those in which *M. marinum* forms actin tails; even the most closely related species to *M. marinum*, *M. ulcerans*, does not form actin tails when intracellular strains are tested (Chapter 2).

Studying the mechanisms of actin polymerization by cytoplasmic pathogens has led to important insights into the regulation of cell and membrane motility by eukaryotic cells. Comparisons of actin-based motility by *M. marinum* to that of other pathogens can be used as a tool to further explore cytoskeletal cell biology, such as the actin dynamics at lamellapodia and filopodia. Initial studies with *M. marinum* suggest that the bacterium involves the Arp2/3 complex for actin nucleation and branching (Chapter 2). This final step of Arp2/3 recruitment and activation is common to all actin-polymerizing pathogenic species, but there are distinct levels at which they intercept the host cell pathway

upstream of the Arp2/3 complex (Figure 1.4). The *Shigella* protein IcsA is known to indirectly activate the Arp2/3 complex by recruiting the N-WASP protein, whereas the *Listeria* protein ActA, the *Rickettsia* protein RickA, and the *Burkholderia* protein BimA mimic N-WASP and directly activate the Arp2/3 complex (43,56-58).

The above pathogens all initiate actin polymerization within the host cell cytoplasm. Other pathogens including *E. coli* species and vaccinia virus initiate actin polymerization from outside the host cell membrane leading to actin-rich formations beneath the pathogen. Like *Shigella*, these species are dependent upon the N-WASP family for actin polymerization; however they are able to use either N-WASP or WASP (Figure 1.4) (59-61). Enteropathogenic *E. coli* (EPEC) and vaccinia initiate the pathway leading to Arp2/3-dependent actin polymerization upstream of N-WASP. The EPEC protein Tir and the vaccinia protein A36R are tyrosine phosphorylated and recruit the host cell adaptor Nck; Nck leads ultimately to N-WASP activation (62,63). Additionally, in the case of vaccinia, WIP binding to N-WASP also plays a role (64). Interestingly, the Tir molecule of entrohemmorhagic *E. coli* (EHEC) is not phosphorylated and another bacterial molecule EspFU binds and activates N-WASP independently of tyrosine phosphorylation and Nck (63,65). These diverse examples suggest a convergent evolution between gram-positive, gram-negative and acid-fast species to intercept a common pathway in signaling of the host cell cytoskeleton.

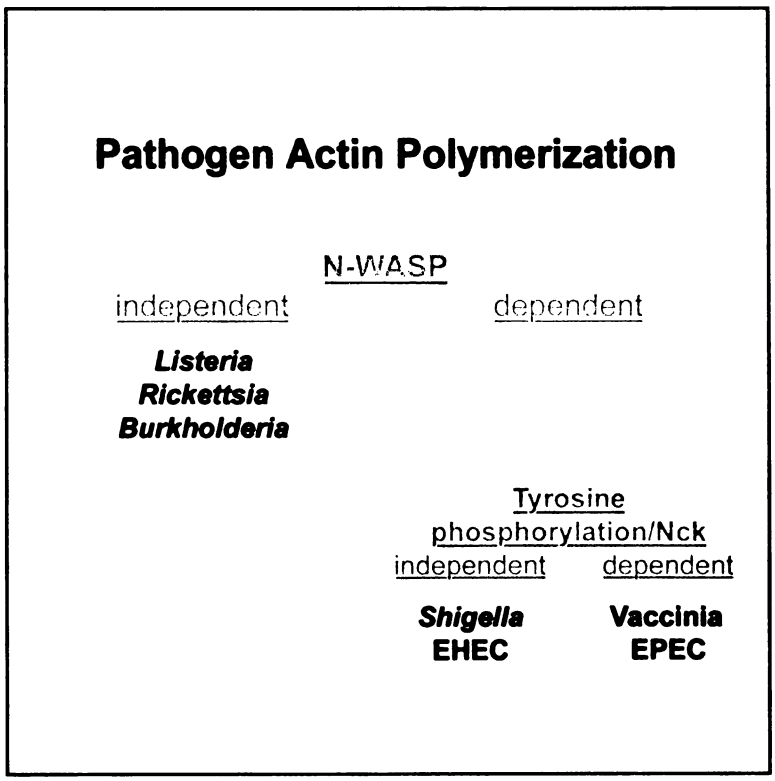

Figure 1.4 Pathogens polymerize actin by different mechanisms. *Listeria*, *Rickettsia* and *Burkholderia* initiate actin polymerization by directly activating the Arp2/3 complex, independent of N-WASP. Vaccinia virus, Enteropathogenic *E. coli* (EPEC), Enterohemorrhagic *E. coli* (EHEC), and *Shigella* require N-WASP. Vaccinia and EPEC mimic tyrosine receptor phosphorylation and require the host cell adaptor Nck, while *Shigella* and EHEC are tyrosine phosphorylation independent. *Shigella* and EHEC have been shown to directly activate N-WASP.

Conclusion

Because of the importance of tuberculosis as a global health threat, there is an obvious need for increased understanding of the molecular mechanisms of disease pathogenesis caused by the genus *Mycobacterium*. Increased drug resistance also has created a requirement for novel modes of treatment and prevention of disease. The use of *M. marinum* as a tool in this critical program is based on the genetic, pathologic, and pathogenic similarities of this organism with *M. tuberculosis*. Its safety for humans, its speed of growth, its ability to grow in a wide variety of additional hosts, and its utility for studying function of *M. tuberculosis* genes in the context of infection and even a whole organism immune response increase its appeal.

Is *M. marinum* a good model for understanding tuberculosis? Certainly, it is a great model for understanding granuloma formation and caseous necrosis *in vivo*, as well as for studying the cell biology of phagosome arrest. However, each species of mycobacteria has made unique adaptations to its ecological and pathological niche. There are characteristics of *M. marinum* that are not applicable to *M. tuberculosis*, including photochromagenicity and perhaps phagosome escape and actin polymerization. These species-specific, unique features of pathogenic mycobacteria are interesting in their own right, and comparisons of closely related bacteria can reveal roles of specific adaptations that are not shared by the genus as a whole.

In fact, cross-species comparisons may elucidate novel pathogenic strategies that enable occupation either of new niche within an existing host or a new host altogether. As an example of the former, the production mycolactone by *M. ulcerans* allows persistence in the human host in a necrotic environment devoid of an inflammatory

response, a modification unique to this species among pathogenic mycobacteria. As an example of the latter, further study of actin polymerization by *M. marinum* may help us understand not only why this is useful for intercellular spread in fish infection, but also if or why this adaptation has been maintained or lost by the human pathogen *M. tuberculosis*.

Aims of the Dissertation

The purpose of the research described within this dissertation is to investigate the process of *M. marinum* actin-based motility. The experiments described in Chapter 2 establish and explore the novel observation of motile intracellular *M. marinum*. For the reasons described above, we were initially surprised that a presumably intraphagosomal species could generate intracellular motility. We concluded that the motility was based on actin polymerization, and found that the *M. marinum* with actin tails were in the cytoplasm. The experiments described in Chapter 3 examine the host cell factors required to support actin-based motility and establish the role of the WASP family in the processes. An analysis of the N-WASP domains required for actin-based motility, as well as additional genetic and pharmacological approaches suggest that the interaction of *M. marinum* with N-WASP is direct and involves the basic motif of N-WASP. Chapter 4 addresses the microbial requirements for *M. marinum* actin-based motility, and describes our attempt to identify the bacterial molecule(s) required for N-WASP activation and subsequent actin polymerization through a yeast two-hybrid screen. In this chapter, we also use *M. marinum* RD1 mutants that are non-hemolytic to assess the role of this region in actin tail formation.

Chapter 2

Initial Characterization of *M. marinum* Intracellular Motility

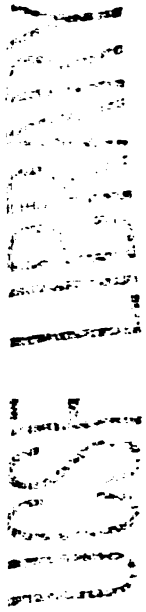

Abstract

Mycobacteria are responsible for a number of human and animal diseases and are classical intracellular pathogens, living inside macrophages rather than as free-living organisms during infection. Numerous intracellular pathogens, including *Listeria monocytogenes*, *Shigella flexneri*, and *Rickettsia rickettsii*, exploit the host cytoskeleton by using actin-based motility for intercellular spread during infection. Here we show that *Mycobacterium marinum*, a natural pathogen of fish and frogs and an occasional pathogen of humans, is capable of actively inducing actin polymerization within macrophages and epithelial cells. *M. marinum* that polymerized actin were free in the cytoplasm and propelled by actin-based motility into adjacent cells. Immunofluorescence demonstrated the presence of host cytoskeletal proteins, including the Arp2/3 complex and VASP, throughout the actin tails. In contrast, WASP localized exclusively at the actin-polymerizing pole of *M. marinum.* These findings demonstrate the ability of *M. marinum* to escape into the cytoplasm of infected macrophages, where it can recruit host cell cytoskeletal factors to induce actin polymerization leading to direct intercellular spread. The other mycobacterial pathogenic species *M. tuberculosis* and *M. ulcerans* did not polymerize actin under comparable infection conditions.

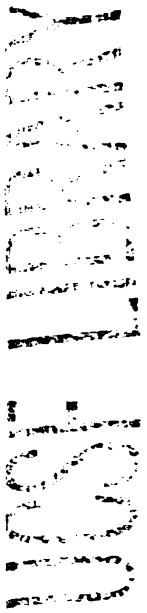

Introduction

Organisms of the genus *Mycobacterium* cause the human disease tuberculosis, as well as tuberculosis-like diseases in cattle, deer, voles, and fish. While they are recognized as classical intracellular pathogens of macrophages, the mechanism by which mycobacteria invade and persist in host cells is not well understood. *M. marinum* causes a systemic tuberculosis-like disease in its natural hosts, fish and frogs, and a localized disease in immunocompetent humans, both marked by the presence of a granulomatous host response, a hallmark of the human systemic diseases caused by mycobacteria, tuberculosis and leprosy. Like *M. tuberculosis*, *M. marinum* exists *in vivo* in host macrophages, leading to aggregation of infected cells and ultimately granuloma formation (34). *M. marinum* is closely related to *M. tuberculosis* not only in its pathology but also genetically (66), and has been used increasingly as a model for understanding the pathogenesis of tuberculosis (9,23,67).

The list of bacterial pathogens known to initiate actin-based motility is diverse and thus far includes the gram-positive bacterium *Listeria monocytogenes* and the gram-negative bacteria *Shigella flexneri* and *Rickettsia rickettsii* (43). These pathogens share the ability during intracellular infection to enter the host cell cytoplasm, induce actin polymerization, and use actin-based motility for spread between host cells. Direct intercellular spread allows these pathogens to circumvent some host immune responses, for example, antibody and complement.

In contrast to *Listeria*, *Shigella* and *Rickettsia*, pathogenic mycobacteria are widely believed not to enter the cytoplasm, but to exist exclusively within phagosomes. The infecting mycobacteria alter phagosome maturation so that these membrane-bound

compartments become suitable environments for survival and proliferation of the pathogen (38). Here we demonstrate that intracellular *M. marinum* not only enters the cytoplasm of infected macrophages, but also has the ability to be propelled by actin-based motility through induction of actin polymerization using host cytoskeletal factors. In addition to extending the ability to induce actin polymerization to a distinct type of bacterium, these studies raise the possibility that escape from the phagosome and direct intercellular spread may be significant for the pathogenesis of *M. marinum* infection.

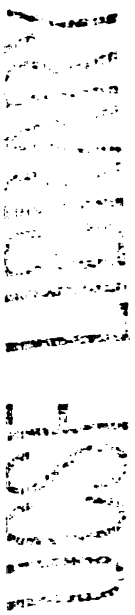

Results and Discussion

Actin Polymerization by M. marinum

During studies of phagosome maturation, we found that some *M. marinum* were motile within bone marrow-derived macrophages (BMDM; Figure 2.1). The average rate of motile *M. marinum* in BMDM was 10.69 μm/min (SD = 1.86; n = 8), comparable to that of intracellular *Listeria* and *Shigella* found previously (43). Associated with motile bacteria were phase-dense "tails" that had the appearance of polymerized actin. To determine whether bacterial motility indeed was actin based, BMDM were infected with *M. marinum* expressing green fluorescent protein (GFP) and stained for F-actin, which demonstrated the presence of actin tails (Figure 2.2A). We found actin tails following infection of the murine macrophage cell lines RAW 264.7 and J774 A.1, and the fish macrophage cell line CLC (Figures 2.2B and 2.2C). CLC cells have been used previously for *M. marinum* infection (39); this finding demonstrates that *M. marinum* polymerizes actin in macrophages of a natural host. In addition, we found that *M. marinum* can form actin tails in three different epithelial cell lines (Figure 2.3): A549 from human lung, L2 from rat lung, and HeLa from human cervix. Taken together, these data indicate that *M. marinum* can form actin tails in both phagocytic and non-phagocytic cell types from diverse vertebrate species.

Detailed kinetic analysis in BMDM demonstrated that intracellucellular *M. marinum* had a doubling time of 10 hours (Figure 2.4A). Actin tails first appeared approximately 15 hours after infection (Figure 2.4B). The number of bacteria with actin tails increased until approximately 20% of all intracellular bacteria demonstrated actin

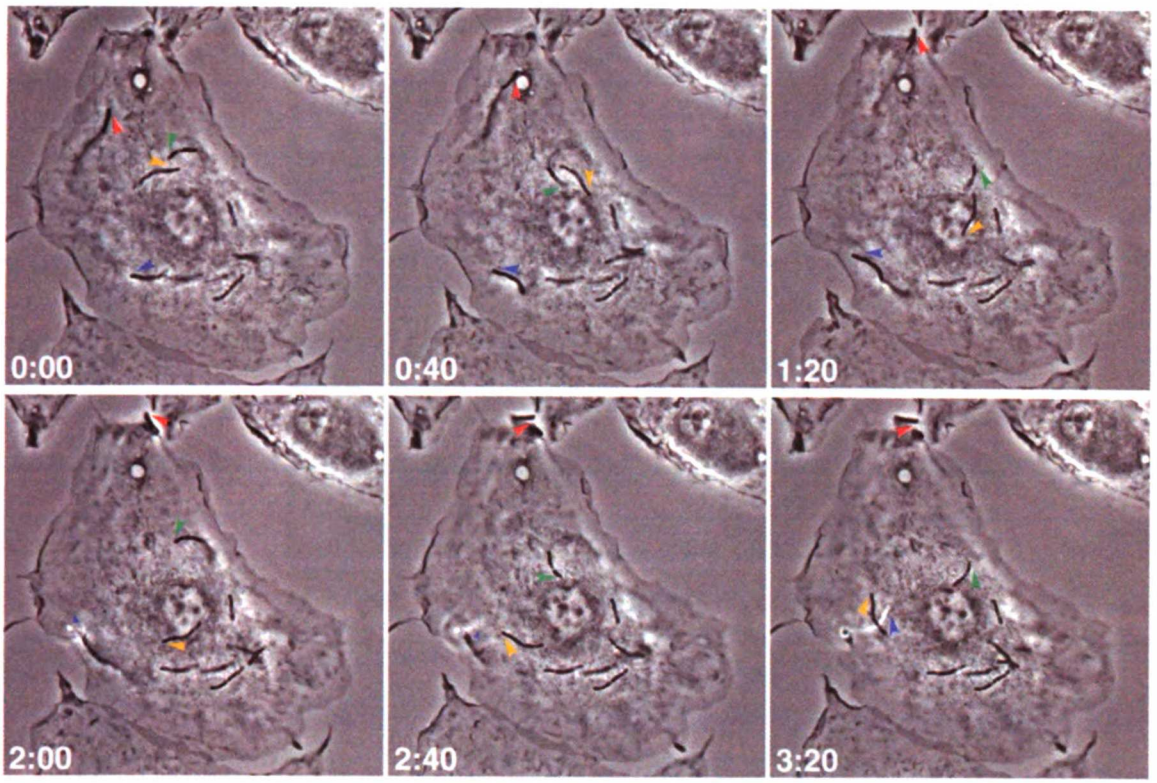

Figure 2.1 *M. marinum* are motile in primary macrophages. Time-lapse images show movement of *M. marinum* within macrophages. Select motile bacteria are followed with colored arrowheads.

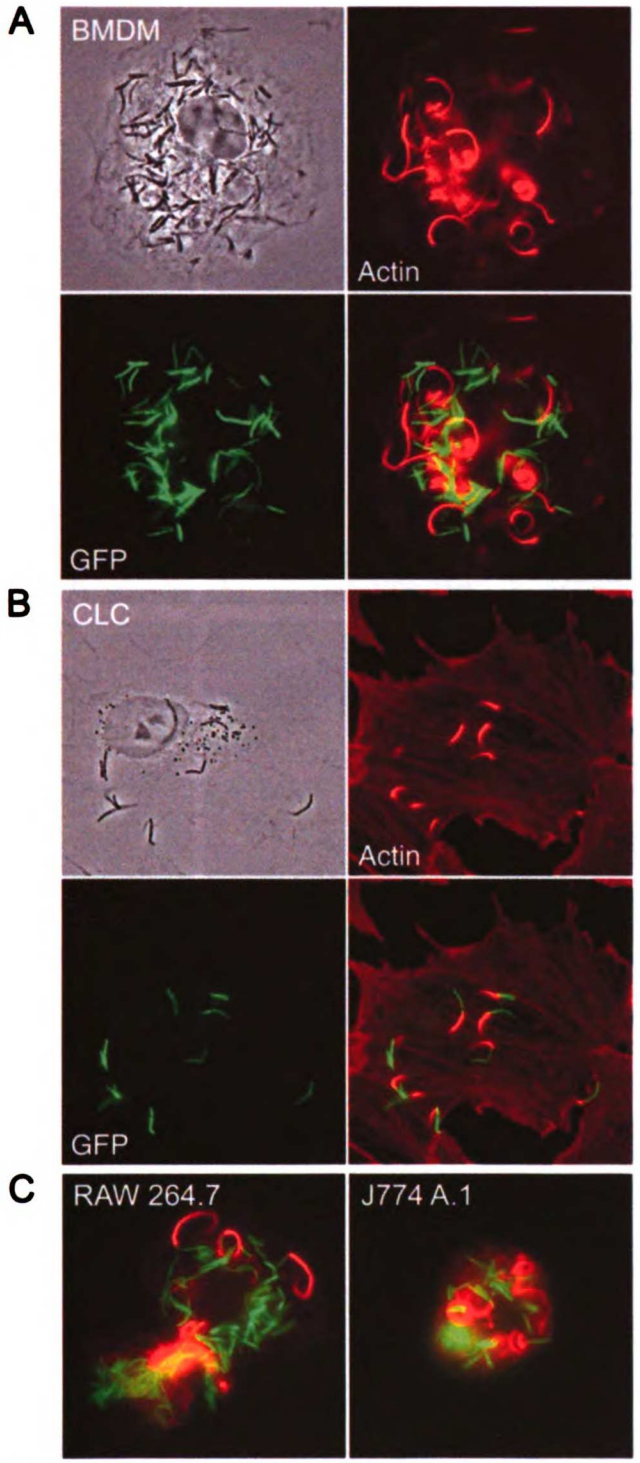

Figure 2.2 *M. marinum* form actin tails in macrophages. (A) BMDM were infected with GFP *M. marinum* and stained for actin. (B) The fish macrophage cell line CLC, and (C) the murine macrophage cell lines RAW 246.7 and J774 A.1 cells were similarly infected and stained. For RAW 246.7 and J774 A.1, only merged images are shown.

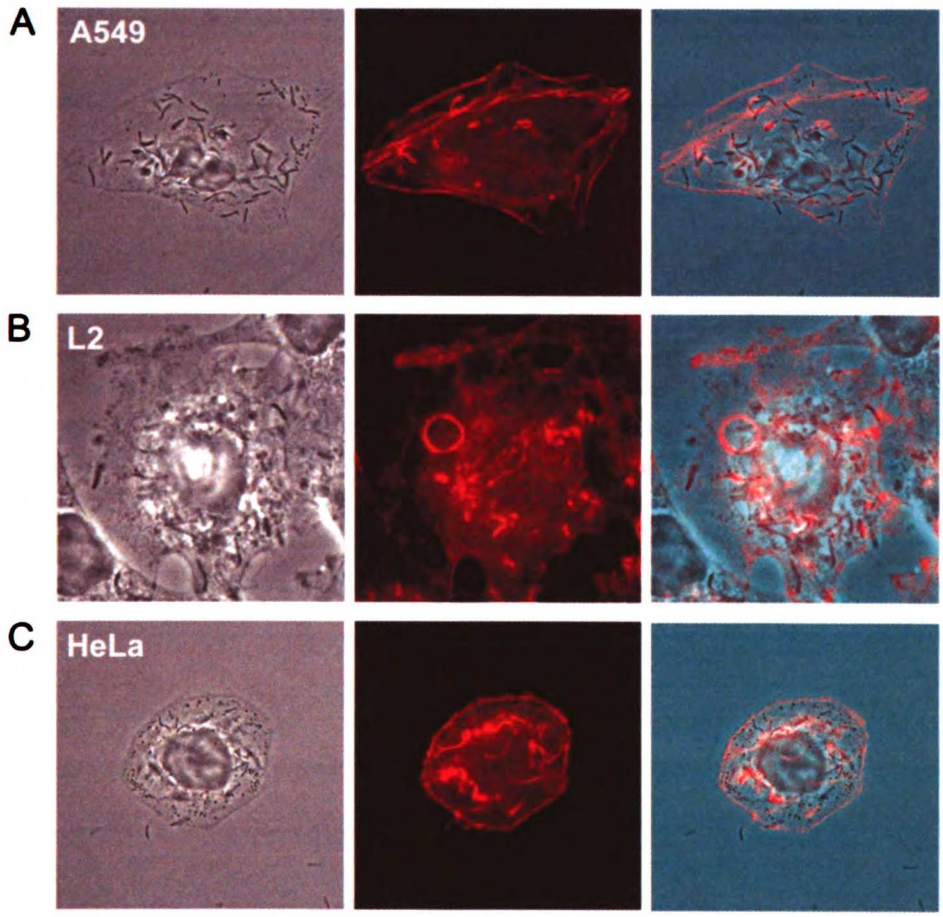

Figure 2.3 ***M. marinum*** **form actin tails in epithelial cell lines.** (A) A549, (B) L2 and (C) HeLa cells were infected with *M. marinum* (phase contrast shown in left panel) and stained for actin (shown in red in middle panel). An overlay of the fluorescence on the phase contrast is shown in the right panel for each cell type.

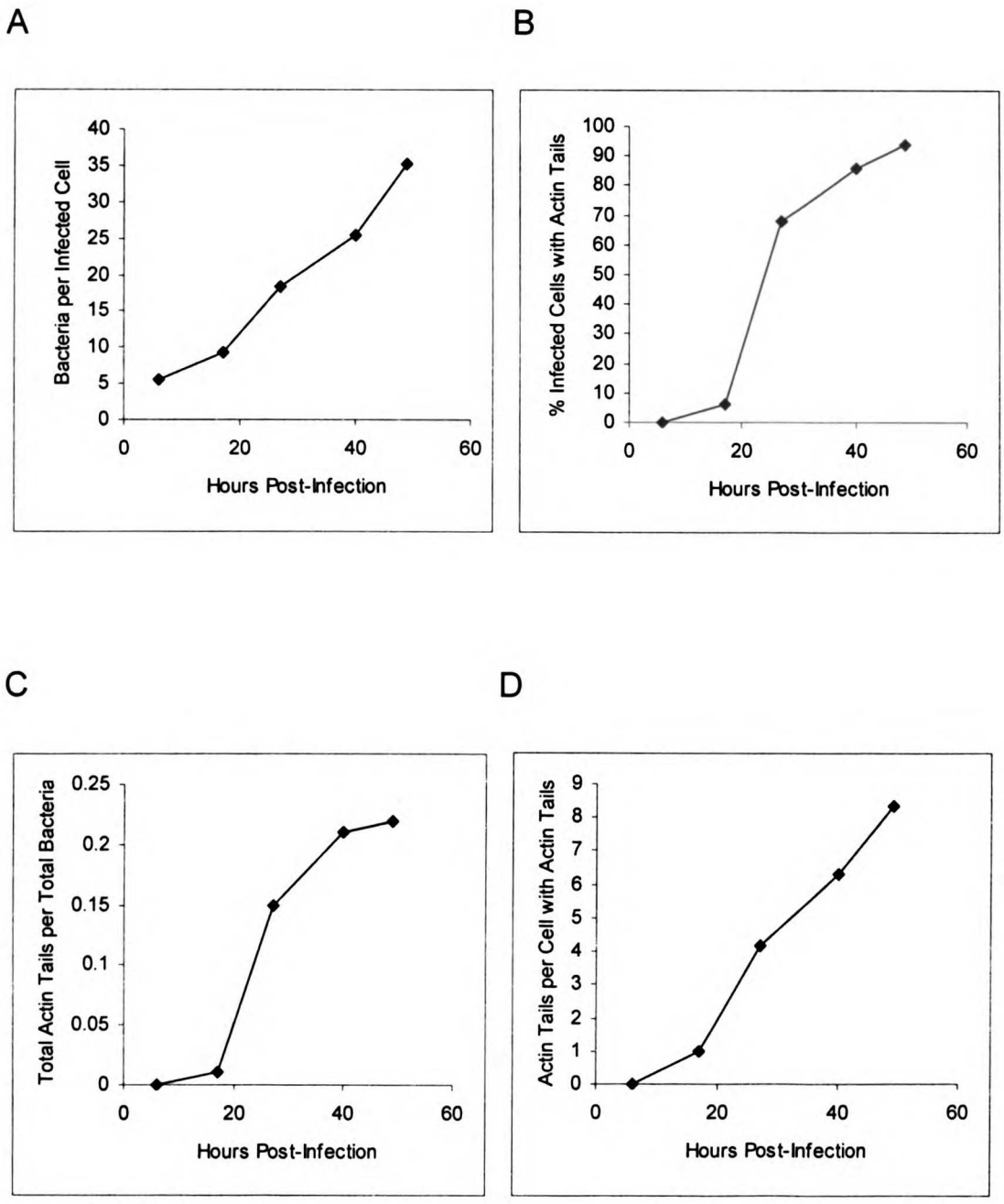

Figure 2.4 *M. marinum* actin tail formation increases over time. BMDM were infected with *M. marinum* and total bacteria and actin tails enumerated over time. Data shown are from one of two detailed experiments with similar results.

tails 48 hours after initiation of infection, after which there was marked toxicity to the BMDM monolayer (Figure 2.4C). At 48 hours, 90% of BMDM contained at least one actin-associated *M. marinum*; the average was about eight mycobacteria with actin tails per macrophage (Figures 2.4B and 2.4D). Thus, there is an initial lag prior to actin tail formation by intracellular *M. marinum*, but over time nearly all infected cells contain *M. marinum* with actin tails.

In addition to polymerizing actin during intracellular infection, *Listeria*, *Shigella* and *Rickettsia* are able to polymerize actin in cell-free extracts (68). *M. marinum* grown in standard broth conditions did not induce actin polymerization in cell-free extracts; however, *M. marinum* isolated after two days' growth in BMDM were able to polymerize actin in mouse brain extracts, forming actin clouds surrounding bacteria after 30 minutes of incubation and tails after 60 minutes (Figure 2.5A). Motility in *Xenopus* egg extracts was visualized by fluorescence time-lapse video microscopy with *M. marinum* prepared in the same manner, and the rate of movement was 17.85 μm/min (SD = 1.37; n = 4; Figure 2.5B). This suggests that expression of the bacterial surface molecule(s) required for *M. marinum* actin polymerization is enhanced in the intracellular milieu, consistent with the lag in appearance of actin tails in BMDM (Figure 2.4). Expression of the actin-nucleating proteins ActA of *Listeria* and IcsA of *Shigella* also is upregulated during intracellular infection (69,70), so enhancement of bacterial actin polymerization by the intracellular milieu may be a general phenomenon for intracytoplasmic pathogens.

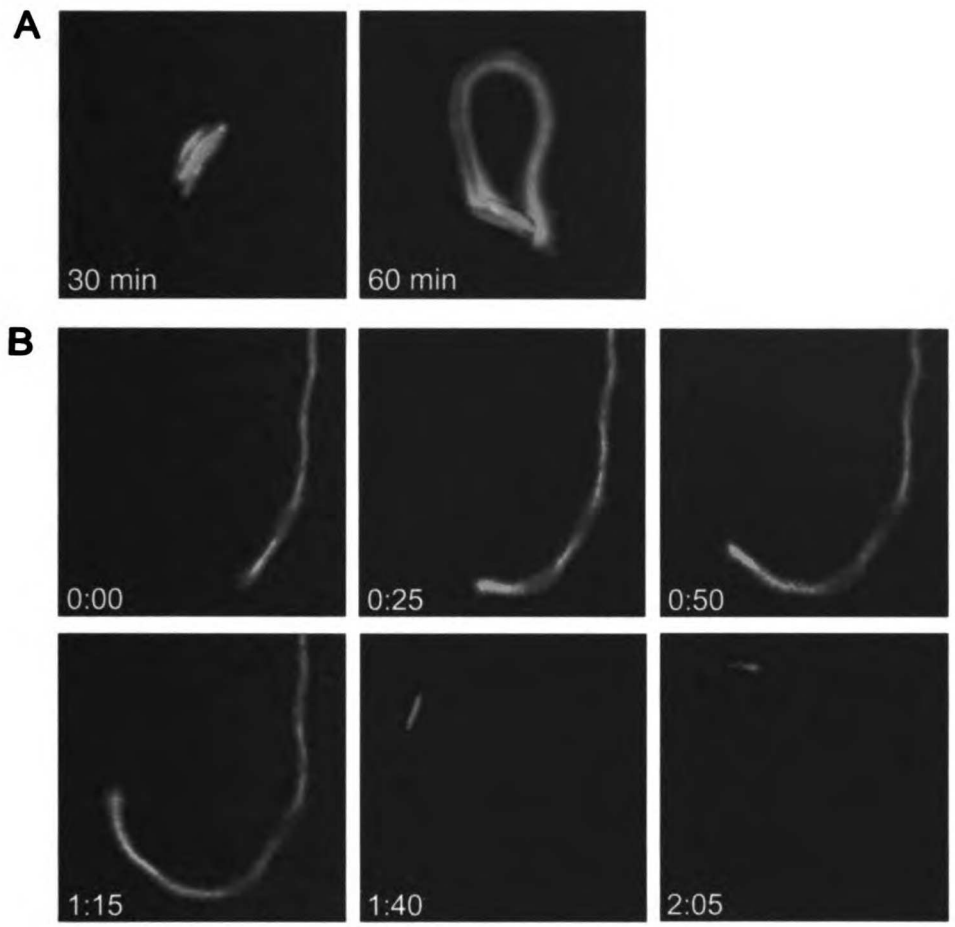

Figure 2.5 ***M. marinum*** **form actin tails in cell extracts.** (A) *M. marinum* expressing GFP (green) grown in macrophages for 48 hours were isolated and added to mouse brain extracts. Within 30 minutes, *M. marinum* polymerized rhodamine actin (red) in diffuse clouds surrounding the bacteria, and by 60 minutes *M. marinum* polymerized actin into tails at its pole. (B) Motility in *Xenopus* egg extracts was visualized by fluorescence time-lapse video microscopy shown here in the red channel for rhodamine actin and the green channel for GFP *M. marinum*.

M. marinum *in the Host Cell Cytoplasm*

Because intracellular mycobacteria are believed to exist exclusively within a phagosome while all bacteria known to initiate actin-based motility escape from phagosomes and are free in the cytoplasm, we investigated the subcellular location of the motile *M. marinum* using both light and electron microscopy. Using the lipid marker DiI under conditions that label intracellular membranes, we found that most *M. marinum* were in a membrane-bound compartment labeled with DiI (Figure 2.6A). However, none of the *M. marinum* with actin tails was associated with DiI staining, indicating either that these bacteria are in a membrane-bound compartment distinct from that occupied by non-motile bacteria and not labeled by DiI, or that the motile bacteria are in the cytoplasm. Phagocytosed heat-killed *M. marinum* were not motile in any cell type and dead bacteria were associated with DiI staining, indicating that actin polymerization was an active process induced by viable intracellular bacteria (Figure 2.6B).

Transmission electron microscopy (TEM) demonstrated that while most bacteria were separated from the cytoplasm by an electron-transparent region limited by a host cell membrane (Figure 2.7A), bacteria associated with actin tails were found in electron-dense regions indistinguishable from the cytoplasm, not surrounded by host cell membrane (Figure 2.7B). This technique also yielded interesting images that illustrate different events in the lifecycle of intracellular motile *M. marinum*, including actin polymerization from the pole and from the side of bacteria (Figures. 2.8A and 2.8B), an interaction with the nucleus that deformed upon collision (Figure 2.8C) and "pseudopod" formation at the plasma membrane (Figure 2.8D). High resolution freeze fracture electron microscopy (FFEM), used to better visualize the ultra-structural details of the

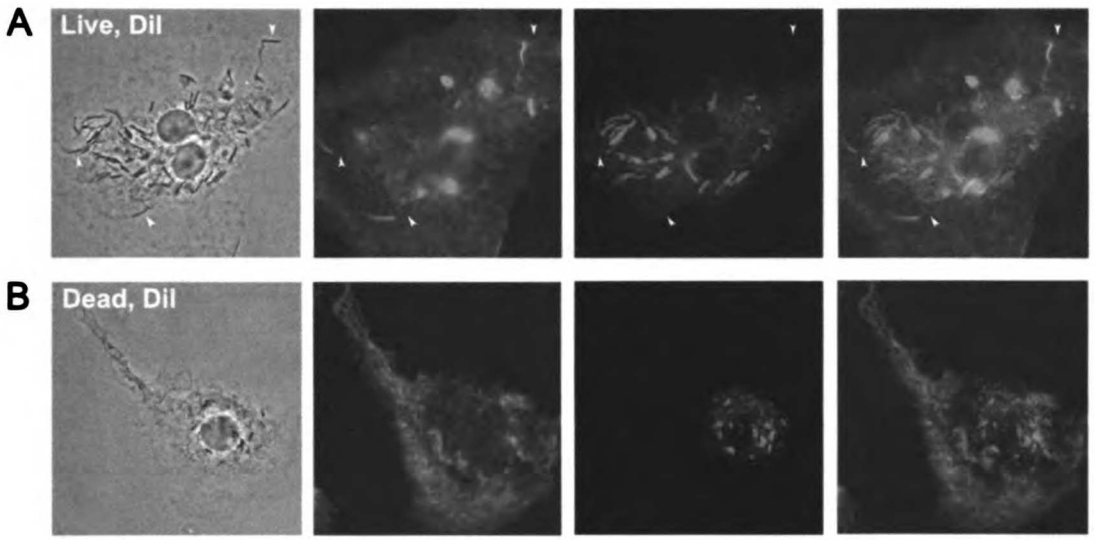

Figure 2.6 Motile *M. marinum* are not in a membrane-bound compartment.

(A) Macrophages were infected with live *M. marinum* (phase contrast in the far left panel), and stained for actin (red), and with DiI (green), a membrane marker. A merged image of the fluorescence channels is shown in the far right. Arrowheads indicate three bacteria with actin tails that are in the plane of focus and not surrounded by DiI. (B) Phagocytosed heat-killed *M. marinum* were similarly treated and stained. Dead bacteria do not form actin tails and are surrounded by DiI.

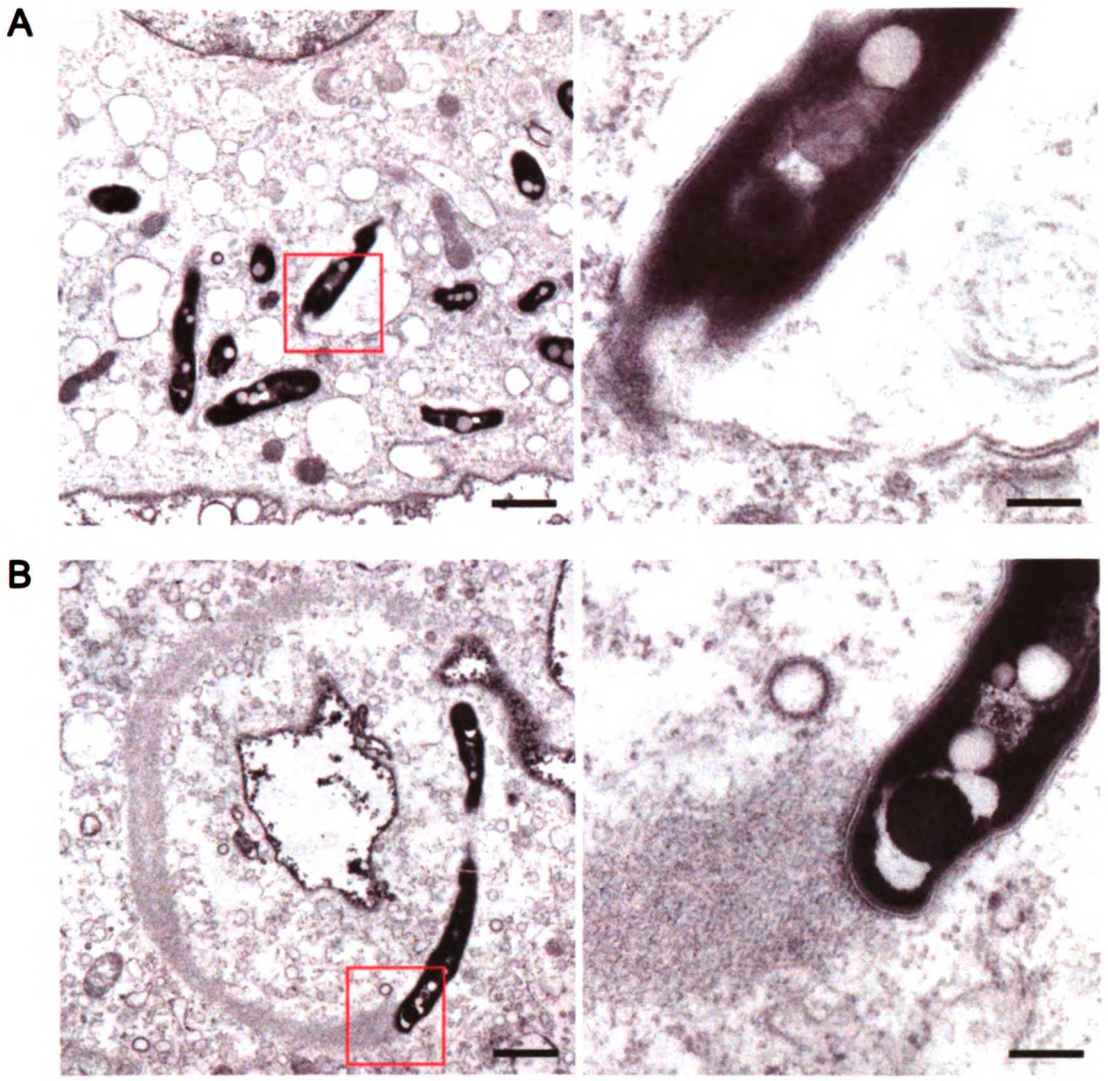

Figure 2.7 *M. marinum* with actin tails are found free in the cytoplasm.

Macrophages were infected with *M. marinum* and observed by TEM. (A) Many *M. marinum* are found in membrane-bound compartments and show no evidence of actin polymerization. Detail of boxed area is shown at right to highlight the bacterial cell wall and the host membrane lipid bi-layer. (B) An example of *M. marinum* that polymerizes actin is shown. The detail at right demonstrates the close apposition of actin filaments to the bacterial cell wall. Scale bars: left panels, 1.0 μm; right panels, 0.2 μm.

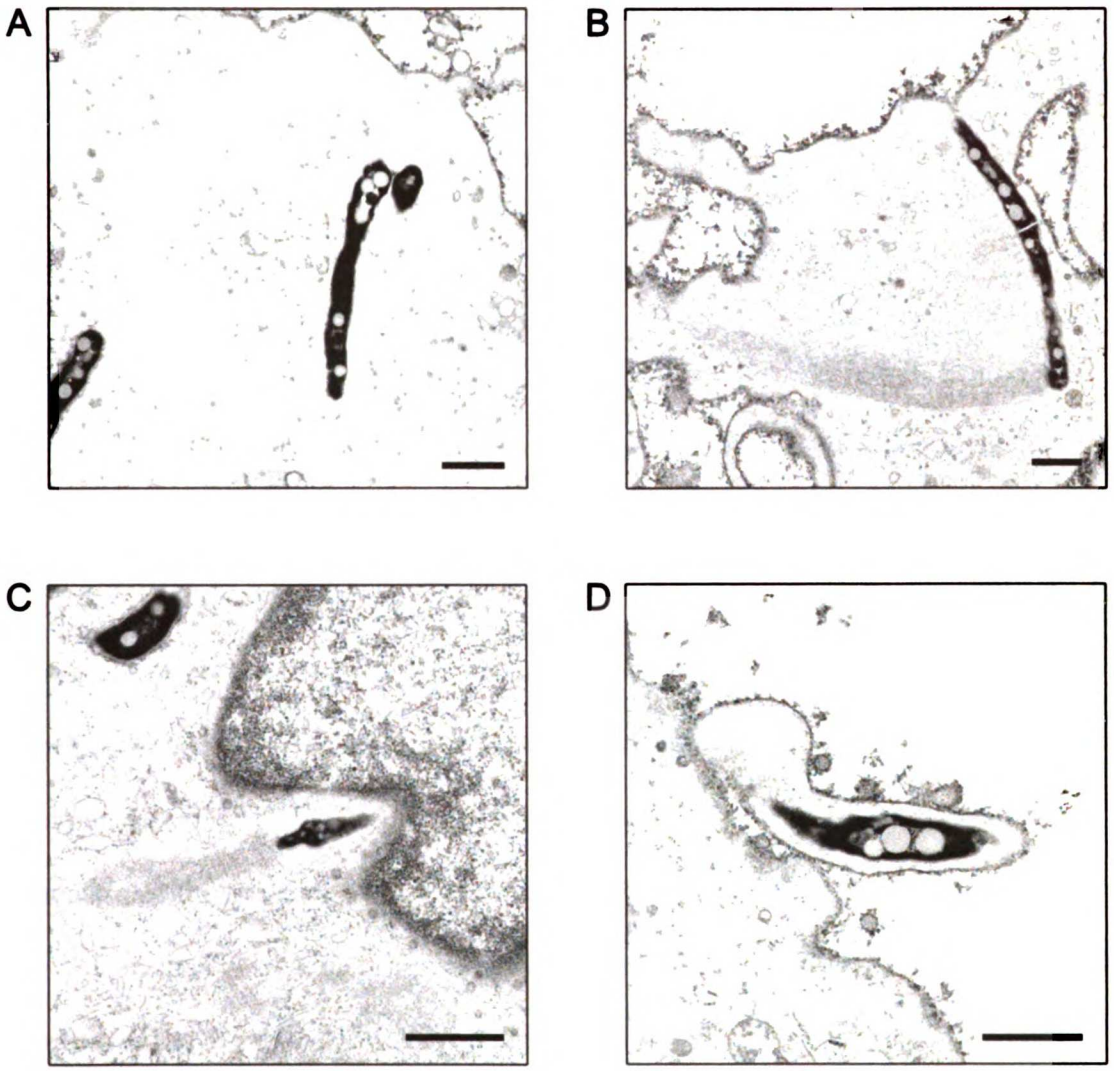

Figure 2.8 TEM illustrates events in the lifecycle of intracellular *M. marinum*. (A) The actin tails of two bacteria form an arc by polymerizing actin at the pole. The second bacterium is out of the plane. (B) Actin is occasionally polymerized from the lateral side of bacteria, resulting in a sideways motion. (C) A bacterium collides with the nucleus, and the force of the bacterial propulsion causes a deformation of organelle shape. (D) *M. marinum* polymerizing actin forms a "pseudopod" at the plasma membrane required for intercellular spread. Scale bars: 1.0 μm.

relationship between bacteria and actin tails, clearly demonstrated the intimate association of actin with the *M. marinum* surface (Figures 2.9A and 2.9B). Thus, motile *M. marinum* are found free in the cytoplasm of host cells.

WASP Recruitment to the M. marinum *Pole*

In TEM and FFEM images (Figures 2.7 and 2.9), the actin in tails behind *M. marinum* appeared to be polymerized in a branched pattern, similar to the actin polymerized by *Listeria* and *Shigella*, but unlike the parallel bundles of actin in *Rickettsia* tails (68,71). This difference has been correlated with presence or absence of the Arp2/3 complex, an essential component of one major mechanism for actin nucleation and for branching of actin filaments. Immunofluorescence using antibodies recognizing Arp3 (data not shown) or p34-Arc (Figure 2.10A), subunits of the Arp2/3 complex, demonstrated the presence of the Arp2/3 complex in *M. marinum* actin tails.

During normal actin remodeling in host cells, the Arp2/3 complex is activated by members of the Wiskott-Aldrich syndrome protein (WASP) family, which includes WASP, expressed only in hematopoietic cells including macrophages, and N-WASP, expressed ubiquitously. *Listeria* and *Shigella* have evolved independent mechanisms to induce actin polymerization that converge on this step in the activation of the Arp2/3 complex. The *Listeria* protein ActA directly activates the Arp2/3 complex by mimicking WASP, whereas the *Shigella* protein IcsA indirectly activates the Arp2/3 complex by recruiting N-WASP to the bacterial surface (43). WASP staining of *M. marinum*-infected macrophages revealed the localization of WASP exclusively at the pole of *M. marinum* where the actin tail formed (Figure 2.10B). Thus, intracellular growth induces *M.*

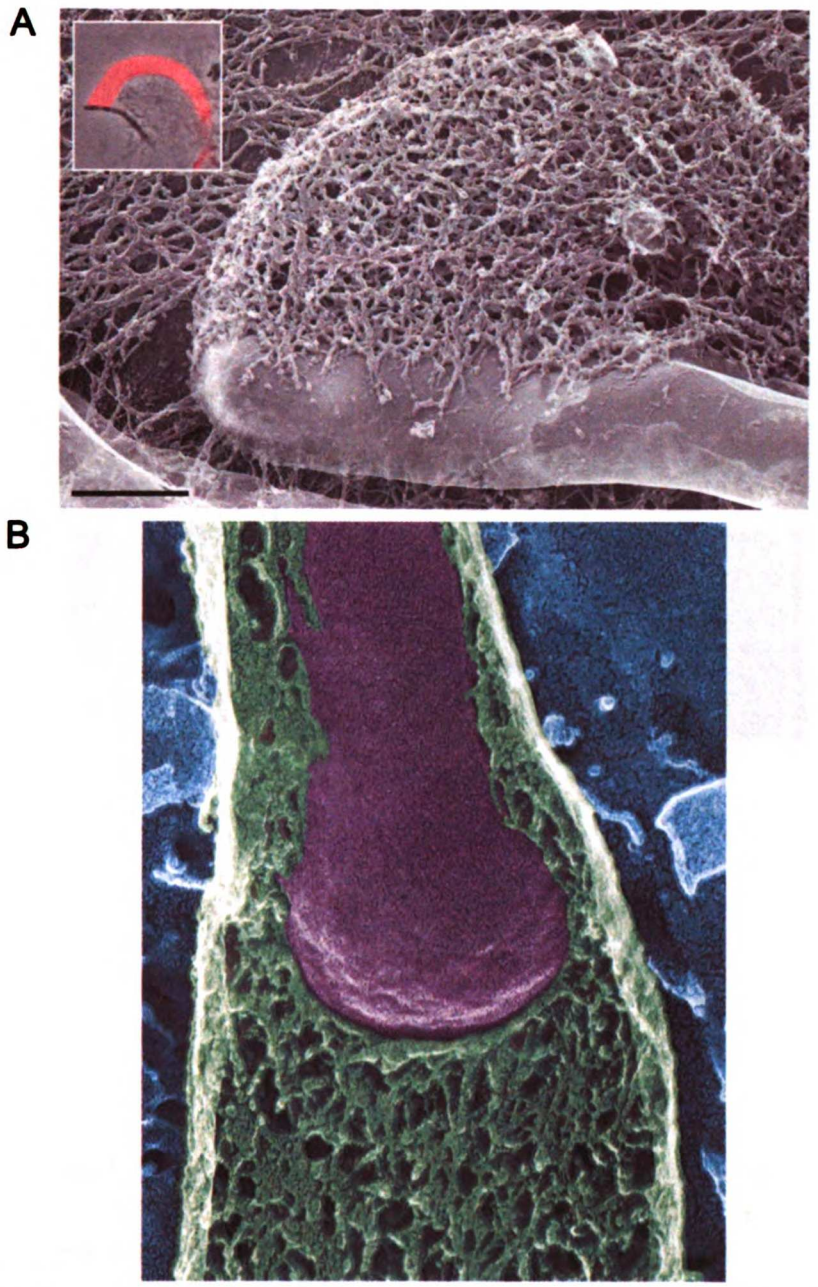

Figure 2.9 *M. marinum* is intimately associated with the branched actin tail.

***M. marinum*-infected macrophages were analyzed by FFEM. (A) Although more often found at a pole, actin polymerization can occur at the side of a bacterium.**

Scale bar: 0.5 μm. **Inset: a phase contrast image of another *M. marinum* with actin polymerized at the side, with fluorescently labeled actin superimposed in red.**

(B) *M. marinum* is **pseudocolored in purple, and the actin tail is pseudocolored in green.**

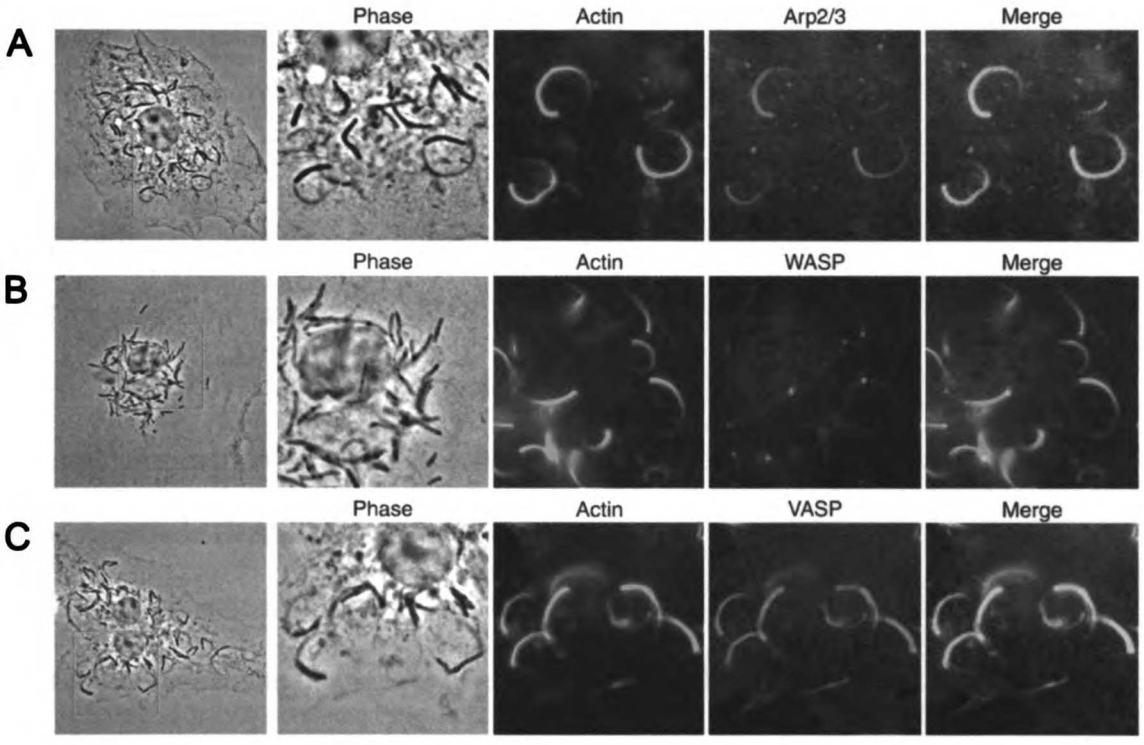

Figure 2.10 Arp2/3, WASP, and VASP localize in the actin tails of *M. marinum*. Macrophages were infected with *M. marinum* and stained with antibodies for actin (red) and for the host cell proteins (all shown in green) (A) p34-Arc, subunit of the Arp2/3 complex, (B) WASP and, (C) VASP. For orientation, the entire macrophage is shown at the left, and details of the boxed area are shown to the right. Images reveal that the Arp2/3 complex and VASP are located throughout the actin tail of *M. marinum*, whereas WASP is located exclusively at the pole at which the actin tail is formed.

marinum recruitment of WASP to its surface, an event that would be sufficient to induce branching actin polymerization and initiate intracellular motility using the Arp2/3 complex. While this is similar to induction of actin polymerization by *Shigella*, IcsA binds only to N-WASP, and *Shigella* is incapable of forming actin tails in macrophages that predominantly express WASP (72).

To explore further the similarity between *M. marinum* and *Shigella* induction of actin polymerization, we examined the localization of vasodilator-stimulated phosphoprotein (VASP) in the actin tails of cytoplasmic *M. marinum*. VASP localizes to regions of dynamic actin rearrangements in host cells, and *Listeria* ActA recruits VASP by a direct interaction that induces localization of VASP to the interface of *Listeria* with its actin tail (73). In contrast, IcsA does not bind VASP, leading to VASP staining throughout the actin tail behind *Shigella* (68) due to VASP's association with F-actin, rather than preferential recruitment to the bacteria-actin interface. Similar to *Shigella*, VASP was present throughout the length of the actin tail of *M. marinum* (Figure 2.10C), suggesting that it has no direct interaction with the accelerator of actin polymerization on the bacterial surface. Based on the staining of WASP and VASP, the mechanism of *M. marinum* induction of actin polymerization is more similar to that of *Shigella* than *Listeria,* even though mycobacteria are often grouped phylogenetically more closely with gram-positive organisms.

Direct Intercellular Spread by M. marinum

In phase contrast time-lapse microscopy, motile *M. marinum* primarily moved in arcs within the cell boundaries (see bacteria marked with orange and green arrowheads

Figure 2.1). Occasionally at earlier and often at later times, *M. marinum* was observed to move beyond the cell boundary on membranous stalks toward adjacent cells (see bacteria marked with red and blue arrowheads Figure 2.1A, and data not shown). Membranous stalks or "pseudopods" could also be seen by TEM (Figure 2.8). This phenomenon is reminiscent of *Listeria* and *Shigella* that use actin-based motility for intercellular spread between host cells without exposure to the extracellular milieu. Consistent with this role for actin-based motility, time-lapse video microscopy illustrates actin-based motility-dependent direct intercellular spread of bacteria (data not shown).

Additional evidence that *M. marinum* is capable of direct intercellular spread was provided by the pattern of bacterial growth in monolayers of host cells in the presence of amikacin to kill extracellular bacteria (Figure 2.11). Eight days after infection with a low multiplicity of infection (MOI), small fluorescent foci of infection were visible, consistent with spread of GFP-labeled *M. marinum* from an initially infected cell to adjacent cells. These results suggest a role for actin-based motility in direct intercellular spread of *M. marinum*. A similar mechanism is a known virulence factor for *Listeria* (74); it may have a similar role in the pathogenesis of *M. marinum* infection.

Inability of Other Mycobacteria to Form Actin Tails

These data show that *M. marinum* can escape from phagosomes and recruit host cell cytoskeletal factors in the cytoplasm to induce actin polymerization resulting in intracellular motility and direct intercellular spread. This observation adds *M. marinum* to the phylogenetically diverse list of pathogens that have found it beneficial to exploit the host cytoskeleton in order to spread to adjacent cells without leaving the cytoplasm.

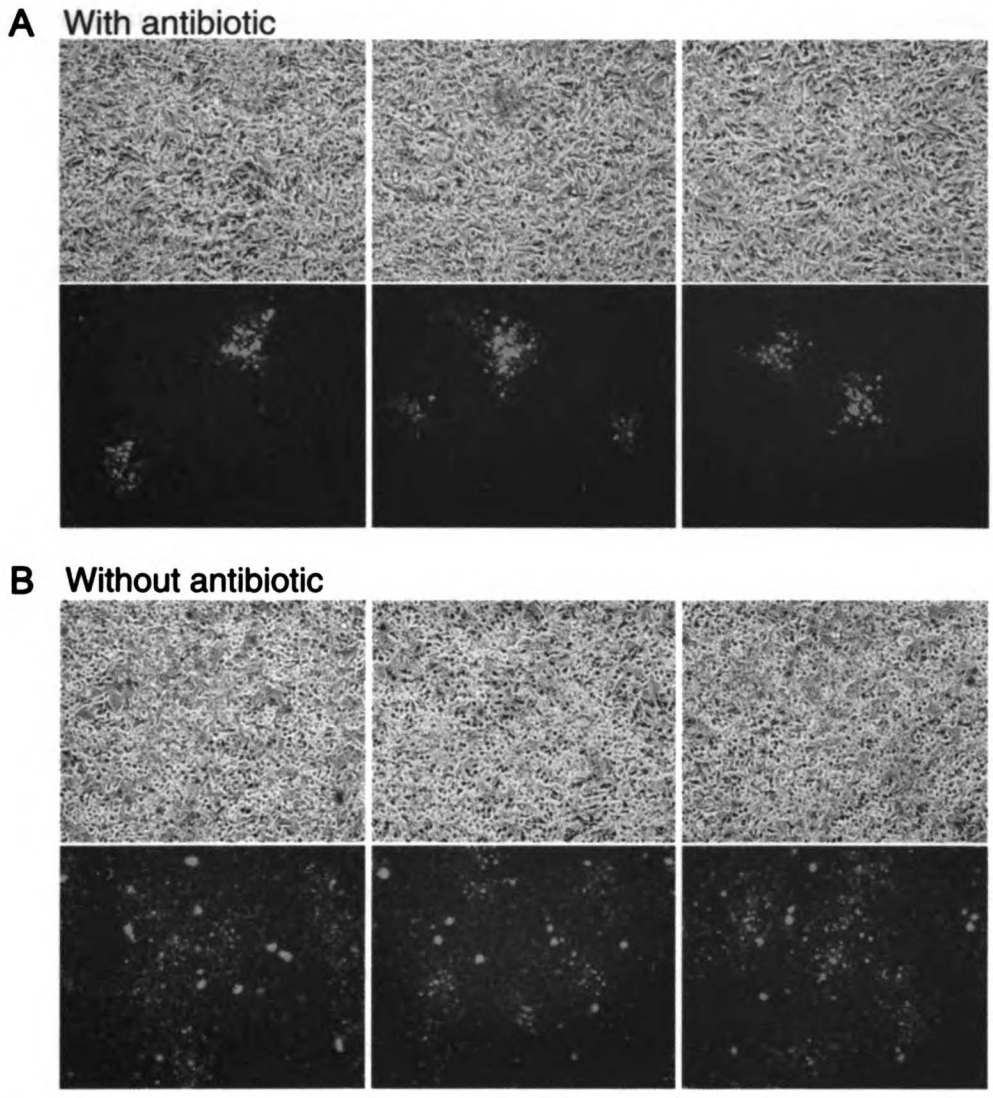

Figure 2.11 Focal growth of *M. marinum* is evidence of direct intercellular spread. A confluent cell monolayer was infected with GFP-expressing *M. marinum* and growth assessed in the (A) presence or (B) absence of amikacin to kill extracellular bacteria. (A) The top row depicts the cell monolayer in phase contrast, and directly below the corresponding fluorescence image demonstrates the focal pattern of GFP-expressing *M. marinum*. Three representative fields are shown. (B) In parallel experiments where the media did not contain antibiotics, the pattern of *M. marinum* growth is diffuse.

Only a minority of *M. marinum* exhibits this behavior; the characteristics distinguishing cytoplasmic, motile bacteria from those that remain in phagosomes are unknown.

Does the ability to escape from phagosomes and initiate actin-dependent intercellular spread extend to other mycobacteria? There is a controversial report of TEM visualization of *M. tuberculosis* free in the cytoplasm (45), as well as one report of direct *M. tuberculosis* intercellular spread in tissue culture (75). However, unlike *M. marinum*, *M. tuberculosis* has been extensively studied for decades without evidence for actin-based motility. To directly address this issue, we infected BMDM with *M. tuberculosis* under conditions identical to those in which *M. marinum* forms actin tails, and we failed to see any sign of actin tail formation by *M. tuberculosis* (Figures 2.12A and 2.12B). Even the most closely related species to *M. marinum*, *M. ulcerans*, does not form actin tails when intracellular strains are tested (Figure 2.12C). If actin polymerization has any role in *M. tuberculosis* or *M. ulcerans* infection, it likely is under conditions that differ from that of a cell culture system, and is at a site *in vivo* or at a time after initial infection that has thus far escaped close scrutiny.

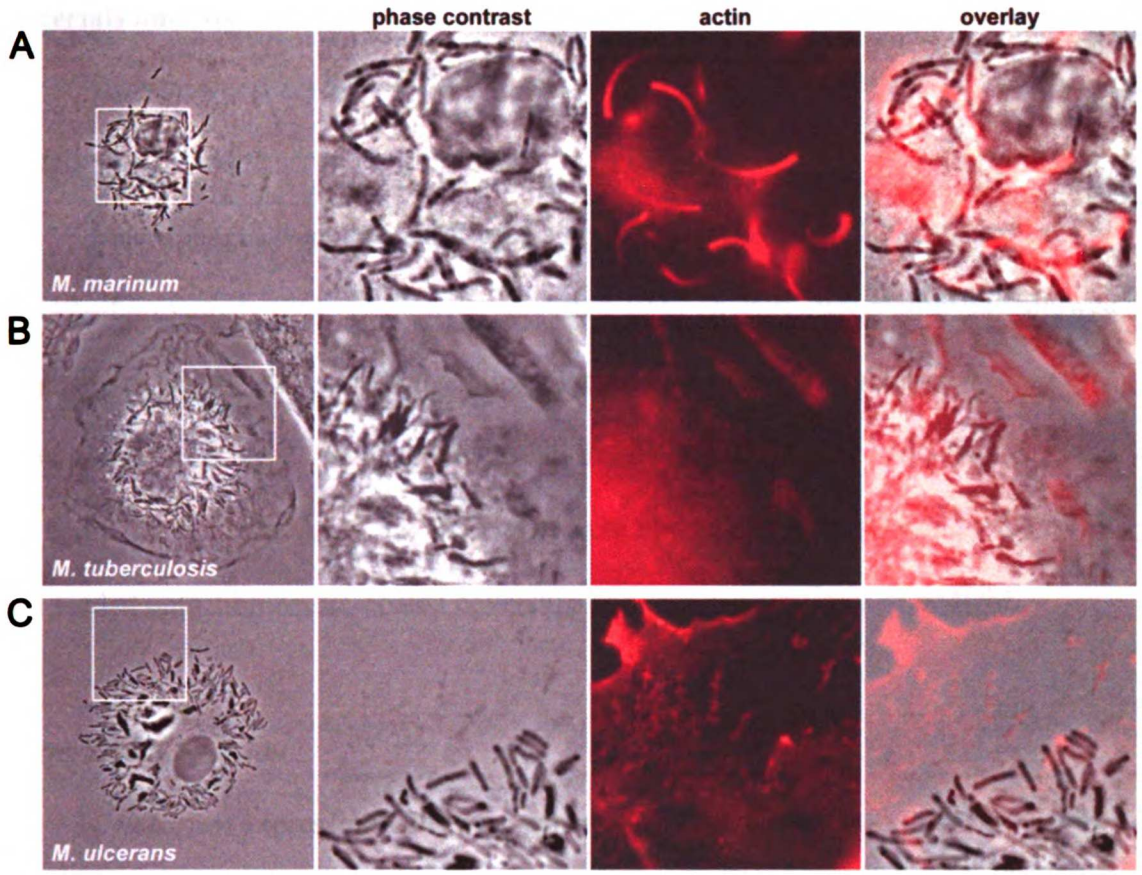

Figure 2.12 Other pathogenic mycobacteria do not form actin tails. Under comparable conditions, macrophages were infected with (A) *M. marinum*, (B) *M. tuberculosis* or (C) *M. ulcerans*, fixed and stained for actin. Actin tails indicative of intracellular motility are seen exclusively with *M. marinum*.

Materials and Methods

Cells

Macrophages were derived from the bone marrow of either 129/Sv mice as described previously (76). Cells were harvested 10 to 18 days after plating and allowed to adhere to fibronectin-coated coverslips (Becton-Dickinson) for infection with *M. marinum* the next day. The macrophage cell lines CLC, RAW 264.7 and J774 A.1, and the epithelial cell lines A549, L2 and HeLa, were maintained as suggested by the ATCC, and seeded onto fibronectin-coated coverslips and infected similarly to BMDM.

Bacteria and Infection

M. marinum expressing GFP were generated by transforming *M. marinum* with a GFP expression plasmid as previously described (9). Wild type (strain M) or GFP-expressing *M. marinum* were cultured in Middlebrook 7H9 (Difco) supplemented with 0.2% glycerol, 0.05% Tween 80, and 10% ADC enrichment (Fisher). Heat-killed bacteria were prepared by heating prepare *M. marinum* at 65°C for 30 minutes.

For infection, *M. marinum* were washed twice in serum-free cell culture media and disrupted into single bacilli by passage through a 26-gauge needle. Immediately prior to infection, BMDM and or plated cell lines were washed with serum-free medium. *M. marinum* were added to the cells at a MOI of 1, centrifuged at 500xg for 10 minutes, and incubated at 32°C (BMDM, RAW 264.7, J774 A.1 and epithelial cell lines) or 28°C (CLC) in 5% CO_2. After 2 hours, the infected cells were washed with serum-free

medium to remove extracellular bacteria. Infected cells were incubated further in their respective media for 48 hours prior to microscopy.

M. tuberculosis (Erdman) was prepared as described previously (27). The 1615A *M. ulcerans* strain used in this study has a mutation in its giant plasmid that disrupts mycolactone production allowing for intracellular growth (kindly provided by P.L. Small, University of Kentucky). *M. ulcerans* was prepared like *M. marinum*, but not passaged through a needle. Infections of BMDM with these species were carried out similarly as above, except that *M. tuberculosis*-infected cells were incubated at 37 °C. Because of the relatively slower growth of *M. tuberculosis* and *M. ulcerans*, actin tail formation was assessed by microscopy seven days post-infection.

Intercellular spreading assays were performed in confluent monolayers of A549 cells infected with *M. marinum* at an MOI of 0.1 essentially as described previously (77). In some wells, culture medium contained 40 μg/mL amikacin, a concentration that we have found does not affect the growth of intracellular *M. marinum*, but effectively kills extracellular bacteria. Media was changed every two days and monolayers were examined for pattern of infection eight days later.

In Vitro *Actin Polymerization*

Mouse brain or *Xenopus* egg extracts were prepared as described previously (78,79). For cell-free extract studies, *M. marinum* were isolated from BMDM infected for at least 48 hours. Bacteria were centrifuged, washed, and added to the extract with an ATP-containing energy mix, rhodamine actin, 1% Triton X-100, 2% methyl cellulose and a mix of glucose oxidase, catalase, and glucose, and examined microscopically after 30 minutes or 1 hour at room temperature.

Microscopy

Time-lapse video sequences were taken at 32°C using a 60x objective on a Nikon Eclipse TE 300 inverted microscope. Images were acquired at 2 or 5-second intervals with a MicroMax cooled CCD camera (Princeton Instruments) with IPLabs acquisition software (Scanalytics). Average rates of movement were determined by analysis of multiple sequential images and a stage micrometer using Adobe Photoshop for infected cells and by analysis with ImageJ Software (NIH) for bacteria in extracts.

2 μM CM-DiI (Molecular Probes) was used to label intracellular membranes by adding to infected BMDM for 1 hour prior to fixation. Labeled, infected BMDM were fixed with 3.7% paraformaldehyde and permeabilized with 0.1% Triton X-100. Alexa Fluor phalloidin (Molecular Probes) was added to coverslips for 20 minutes at room temperature to stain for F-actin. To localize host cytoskeletal proteins, infected BMDM were fixed as above and permeabilized with cold methanol. Subsequent indirect immunofluorescence was performed with anti-arp3 (80), anti-p34-Arc (81), anti-VASP (82), anti-WASP (Santa Cruz Biotechnology), anti-actin (Sigma), and species-appropriate Alexa Fluor secondary antibodies (Molecular Probes). To determine the kinetics of actin tail formation, BMDM were fixed and stained with phalloidin at various times after infection, and total bacteria per cell and bacteria with actin tails were enumerated. For electron microscopy, BMDM were examined 48 hours after infection by TEM (83) or FFEM (84).

Chapter 3

Host Cell Requirements for *M. marinum* Actin Polymerization

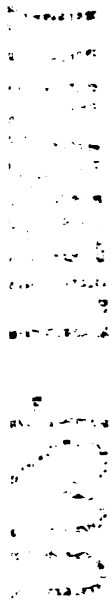

Abstract

Mycobacterium marinum, a natural pathogen of fish and frogs and an occasional pathogen of humans, is capable of inducing actin tail formation within the cytoplasm of macrophages, leading to actin-based motility and intercellular spread. We have shown previously that WASP, a major regulator of actin remodeling in hematopoietic cells, localizes exclusively at the actin-polymerizing pole of *M. marinum* in macrophages. In macrophages that are deficient in WASP but still contain the closely related and ubiquitously expressed protein N-WASP, actin tail formation by *M. marinum* is significantly reduced. In fibroblasts lacking both WASP and N-WASP, *M. marinum* is incapable of efficient actin polymerization and of intercellular spread. By reconstituting these cells, we find that *M. marinum* is able to use either WASP or N-WASP to induce actin polymerization. Inhibition or genetic deletion of tyrosine phosphorylation, Nck, WIP, and Cdc42 does not affect *M. marinum* actin tail formation, excluding the participation of these molecules as upstream activators of N-WASP in the initiation of actin based motility. In contrast, deletion of the PIP_2-binding basic motif in N-WASP eliminates its actin tail formation. Together, these data demonstrate that *M. marinum* utilizes a mechanism distinct from other pathogens to initiate actin polymerization. We hypothesize that *M. marinum* uses its cell surface lipids to subvert a normal eukaryotic mechanism for WASP family activation to initiate its own motility and cell-to-cell spread.

Introduction

In host cells, a tightly regulated signal transduction cascade normally initiates Arp2/3 complex-mediated actin reorganization of the cytoskeleton at the plasma membrane, mediated through the members of the Wiskott-Aldrich syndrome protein (WASP) and WAVE families (reviewed in (85)). The ubiquitously expressed N-WASP is a well-studied modular protein that is autoinhibited via an intramolecular interaction in its inactive state. Activation of N-WASP occurs when binding of specific molecules or post-translational modification leads to a disruption of the autoinhibitory interaction, unmasking the WASP homology 2 and Acidic (WA) domain which then allows the Arp2/3 complex to initiate *de novo* actin polymerization (86-88). Activation through binding of phosphatidylinositol 4,5-bisphosphate (PIP_2), Cdc42, Nck and Grb2 to N-WASP is a mechanism for integrating the effects of multiple signaling cascades on the cytoskeleton (87,89,90). Within the WASP and WAVE families, WASP, a protein found only in hematopoietic cells, is most closely related to N-WASP, sharing 50% sequence similarity. The two proteins are similarly organized and are controlled by the same host cell inputs. Less related to N-WASP are the WAVE proteins that contain the WA domain output region but have different activating inputs and are therefore controlled by different host cell signals (91).

Diverse pathogens have evolved mechanisms to hijack this Arp2/3-dependent pathway of actin polymerization for their own benefit (reviewed in (92)). For vaccinia virus, actin polymerization is required for viral egress from infected cells. For enterohemorrhagic and enteropathogenic *E. coli* species, actin polymerization leads to pedestal formation causing attachment and effacement lesions on gut epithelia. For

Listeria, *Shigella*, *Burkholderia*, *Rickettsia*, and *Mycobacterium marinum*, actin polymerization on the surface of cytoplasmic bacteria results in actin tails, intracellular motility and direct intercellular spread. Interestingly, in the cases where the mechanism has been identified, these pathogens use independently evolved single gene products to target different steps in the Arp2/3 activation pathway. *Listeria*, *Rickettsia*, and perhaps *Burkholderia*, have molecules that functionally mimic host cell N-WASP to activate the Arp2/3 complex directly, and actin tail formation by these species is independent of host cell N-WASP (56-59,80,93). The other pathogens capable of host actin polymerization are dependent upon the N-WASP family: *Shigella* and enterohemorrhagic *E. coli* (EHEC) have molecules that directly recruit and activate host cell N-WASP (59,60,65,94,95), whereas vaccinia and enteropathogenic *E. coli* (EPEC) initiate actin polymerization upstream of N-WASP in a manner similar to host cell receptor tyrosine kinases, which involves other host cell factors including Nck, Grb2 and WIP (62-64,96,97). Understanding how these pathogens exploit endogenous signal transduction is important to learn more about basic cell biology as well as to understand mechanisms of pathogenesis.

We have described recently the first mycobacterial species that clearly escapes from phagosomes and subsequently initiates actin tail formation in the host cell cytoplasm (Chapter 2). Immunofluorescence studies of *M. marinum* in macrophages indicated the presence of the Arp2/3 complex within the actin tail, and the localization of WASP to the pole of *M. marinum* from which actin tails formed. Here we determine the host cell requirements for efficient *M. marinum* actin polymerization, and show that it requires a member of the WASP family. *M. marinum* actin tail formation occurs

independently of known N-WASP activators including tyrosine phosphorylation, Nck, WIP and Cdc42 but involves the lipid-binding basic motif of N-WASP. The mycobacterial cell wall differs dramatically from gram-positive and gram-negative bacteria because of the existence of a thick lipid layer external to the peptidoglycan, and we propose that *M. marinum* may use this unique feature to initiate actin polymerization.

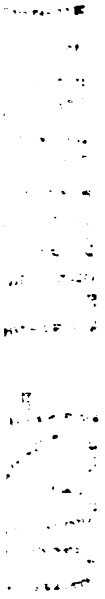

Results

Requirement of the WASP Family

Previously, we found that WASP localized to the pole behind intracellular *M. marinum* from which the actin tail formed, suggesting a potential role in initiation of motility (Chapter 2 and Figure 3.1A). To determine the requirement of WASP in *M. marinum* actin tail formation, we infected $WASP^{-/-}$ macrophages, and found a significant, approximately two-fold decrease in the number of infected cells in which bacterial actin polymerization was observed (Figure 3.1B; $WASP^{+/+}$ 72.5% $\pm$ 8.5, $WASP^{-/-}$ 35.10% $\pm$ 8.6, $p = 0.037$). Because the deficiency of WASP only partially ablated actin tail formation, we hypothesized that N-WASP might account for the residual actin tail formation. N-WASP was present in $WASP^{-/-}$ macrophages at levels comparable to $WASP^{+/+}$ macrophages (Figure 3.2). Indeed, we found that N-WASP localized to the pole of *M. marinum* with actin tails in $WASP^{-/-}$ macrophages (Figure 3.1A). *M. marinum* formed actin tails in N-$WASP^{+/+}$ fibroblasts that lack WASP and N-WASP also localized at the pole in these cells (Figure 3.3A). Most significantly, there was an almost total decrease in actin tail formation in N-$WASP^{-/-}$ fibroblasts that have neither WASP nor N-WASP (Figures 3.3A and 3.3B), demonstrating the requirement for the WASP family for efficient *M. marinum* actin tail formation. Less than 1% of N-$WASP^{-/-}$ fibroblast exhibited bacterial actin tails; this small residual bacterial motility was seen in two independently derived N-$WASP^{-/-}$ fibroblast cell lines (data not shown).

To determine whether actin tail formation is required for intercellular spread of *M. marinum*, we examined spreading of GFP-expressing *M. marinum* within a confluent

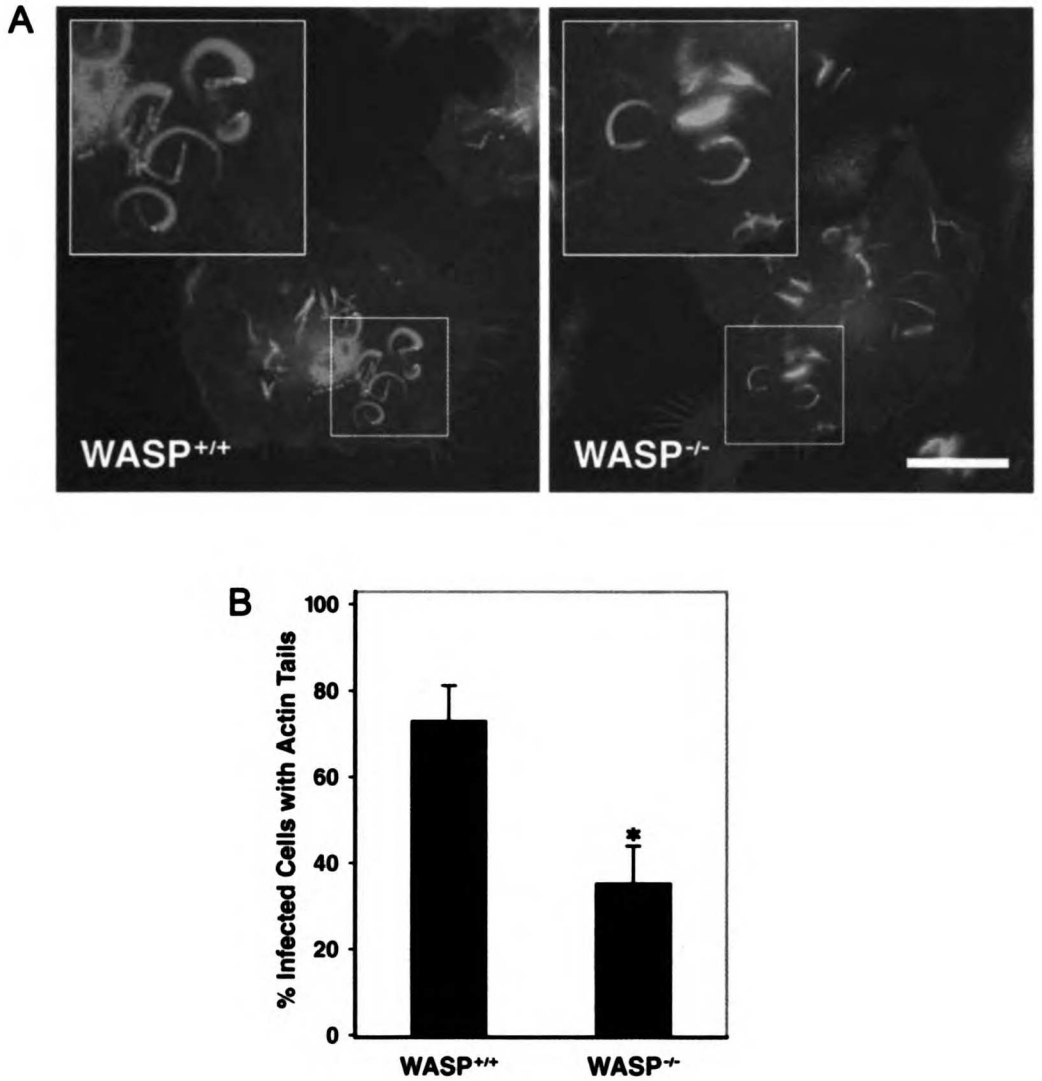

Figure 3.1 WASP$^{-/-}$ macrophages have decreased actin tail formation.

(A) WASP$^{+/+}$ macrophages (left panel) were infected with *M. marinum* (red) and stained with phalloidin to visualize actin (blue) and with anti-WASP antibodies (green). WASP$^{-/-}$ macrophages (right panel) were similarly infected and stained with phalloidin (blue) and anti-N-WASP antibodies (green). Scale bar: 20 μm. (B) The percentage of infected cells with actin tails from three independent experiments is shown; asterisk indicates a statistically significant difference.

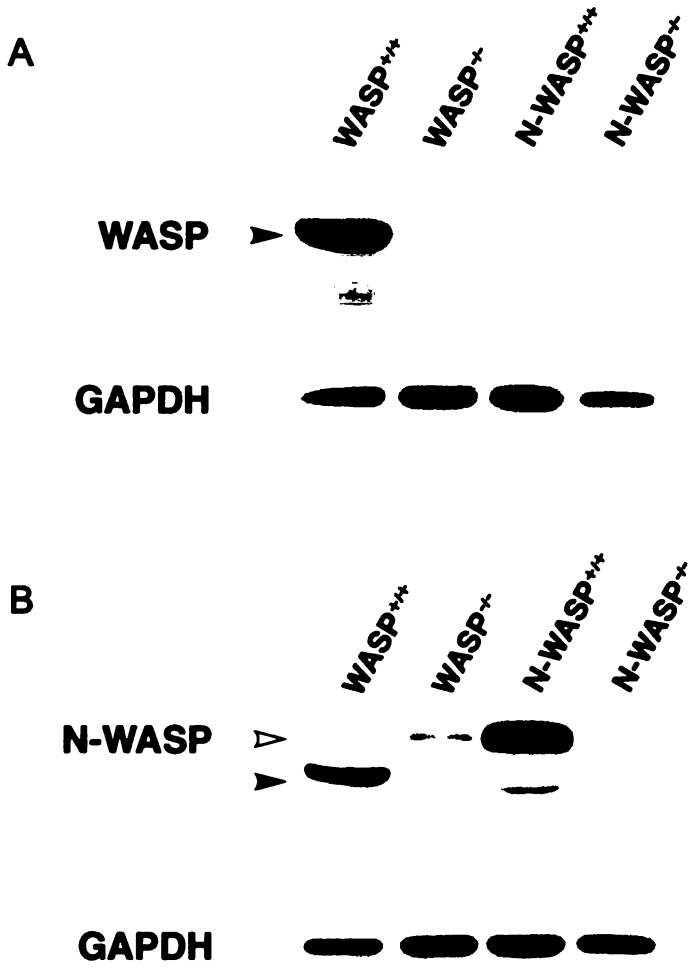

Figure 3.2 WASP$^{-/-}$ macrophages have residual N-WASP. Whole cell lysates of WASP$^{+/+}$ and WASP$^{-/-}$ macrophages and N-WASP$^{+/+}$ and N-WASP$^{-/-}$ fibroblasts were resolved by SDS-PAGE and analyzed for the presence of (A) WASP and (B) N-WASP in each cell type by Western blotting. Filled arrowheads indicate the WASP bands, while the open arrowheads indicate the N-WASP bands. The WASP antibody is specific for WASP, but the anti-N-WASP antibody is cross-reactive with WASP leading to the detection of a WASP band in the WASP$^{+/+}$ lane.

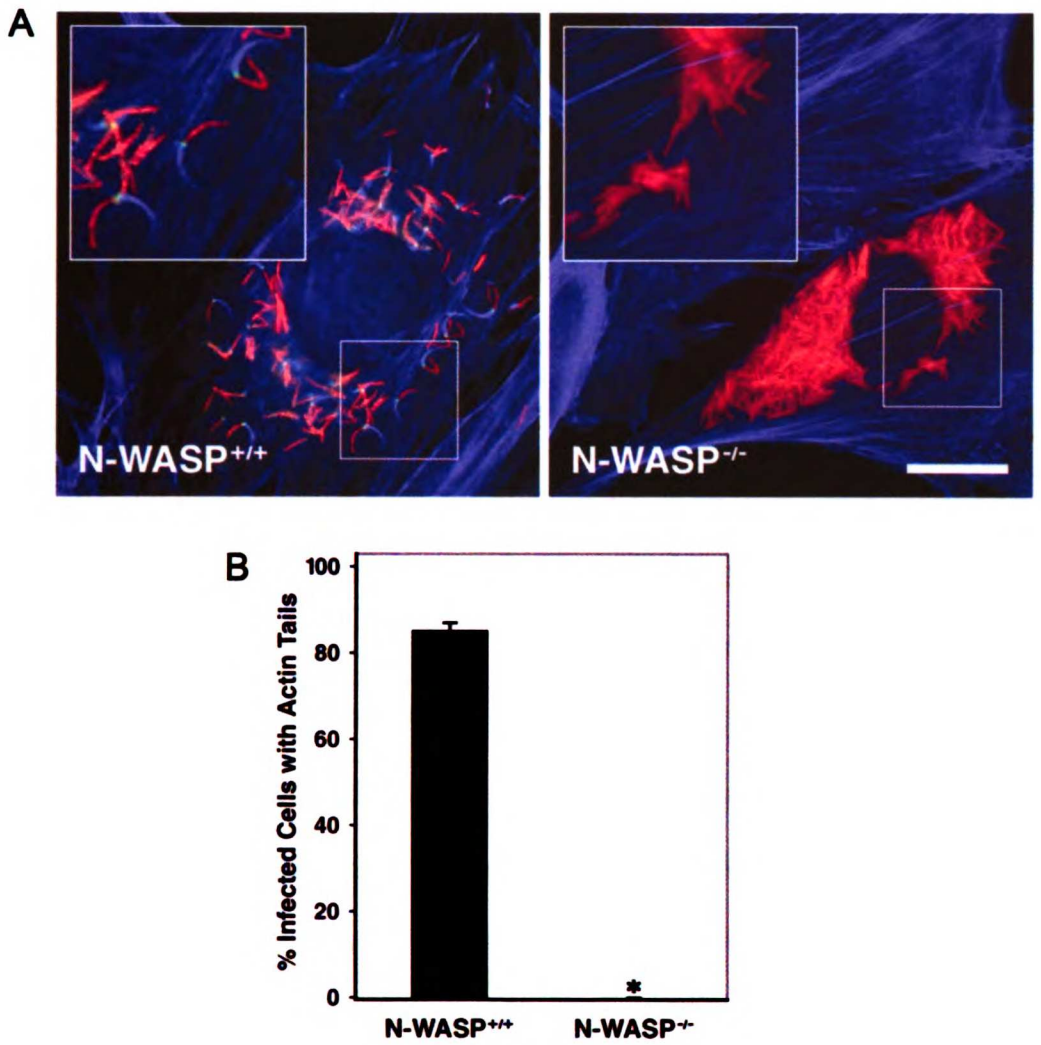

Figure 3.3 N-WASP is required for efficient *M. marinum* motility. (A) N-WASP$^{+/+}$ fibroblasts (left panel) were infected with *M. marinum* (red) and stained with phalloidin to visualize actin (blue) and with anti-N-WASP antibodies (green). A similar staining protocol revealed no tails in infected N-WASP$^{-/-}$ fibroblasts (right panel). Scale bar: 20 μm. (B) The percentage of infected cells with actin tails from three independent experiments is shown; asterisk indicates a statistically significant difference.

layer of N-WASP$^{+/+}$ or N-WASP$^{-/-}$ fibroblasts. When monolayers were infected with a low MOI of *M. marinum*, fluorescent foci of infection (FFI) (11) in the N-WASP$^{+/+}$ monolayer consisted of many cells, demonstrating that contiguously and sequentially infected cells can arise from a single originally infected fibroblast (Figure 3.4A). In contrast, FFI in the N-WASP$^{-/-}$ monolayer most often involved only a single or a few cells. As a result, FFI in the N-WASP$^{+/+}$ monolayer were significantly larger than FFI in N-WASP$^{-/-}$ monolayer (Figure 3.4B; N-WASP$^{+/+}$ 17092 $\mu m^2 \pm$ 1314, N-WASP$^{-/-}$ 1682 $\mu m^2 \pm$ 498, $p = 0.002$) although the growth of *M. marinum* in individual cells was comparable (Figure 3.3A, data not shown). This result implicates bacterial WASP family-dependent actin tail formation in intercellular spread of *M. marinum*.

We transfected the N-WASP$^{-/-}$ fibroblasts with GFP expression constructs to determine which proteins of the WASP and WAVE families can support actin tail formation (Figure 3.5). Transient expression of either N-WASP or WASP in these cells restored actin tail formation in *M. marinum*-infected N-WASP$^{-/-}$ fibroblasts (Figure 3.5). In agreement with the immunofluorescence staining of WASP and N-WASP (Figures 3.1 and 3.3), the GFP fusion N-WASP and WASP proteins localized to the pole from which the actin tail formed. However, WAVE2 failed to restore actin tail formation by *M. marinum* in these cells and failed to localize to bacterial poles (Figure 3.5) demonstrating a specificity of *M. marinum* for WASP and N-WASP among the WASP/WAVE family.

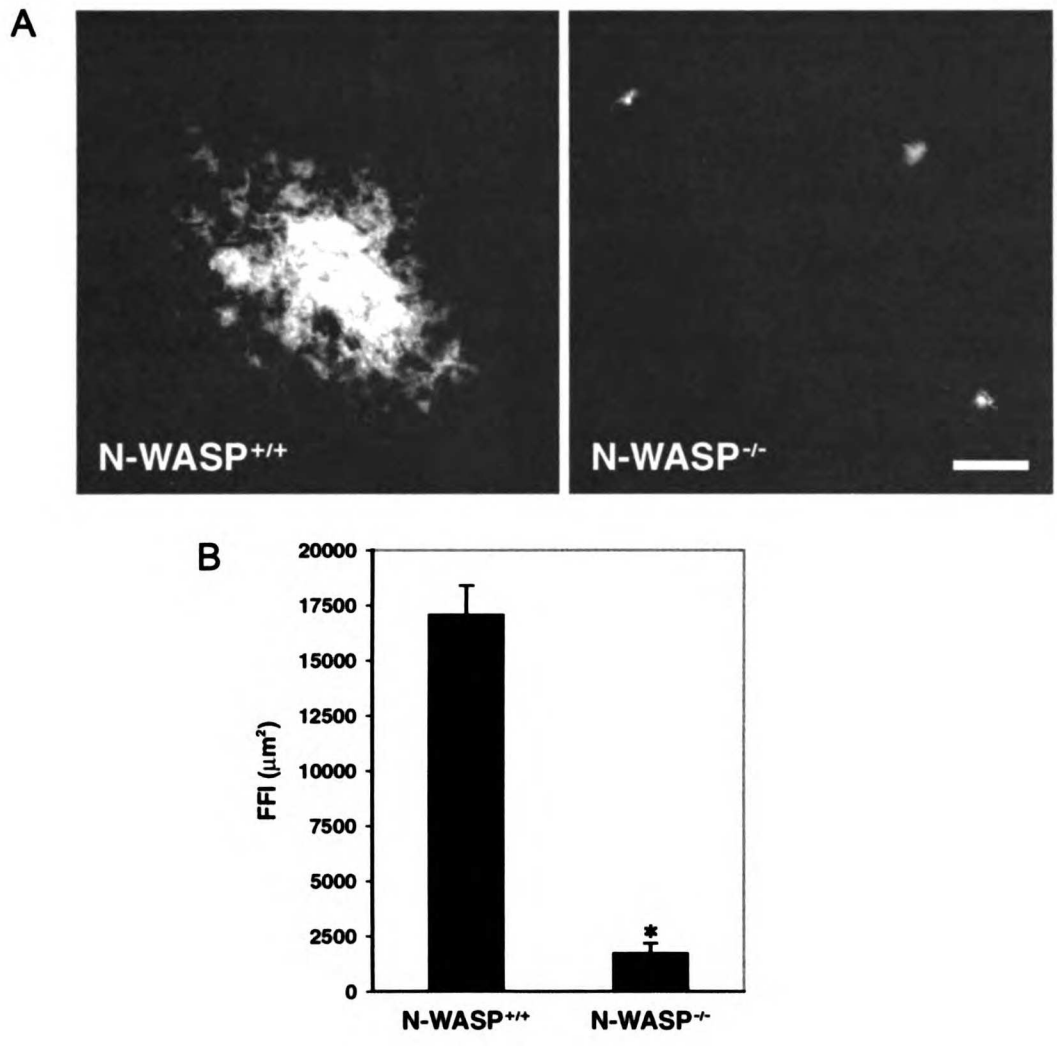

Figure 3.4 *M. marinum* do not spread in N-WASP$^{-/-}$ monolayers. (A) N-WASP$^{+/+}$ (left panel) and N-WASP$^{-/-}$ (right panel) fibroblast monolayers were infected with fluorescent *M. marinum* and foci of infection were visualized and measured 8 days later. Scale bar: 50 μm. (B) Quantitation reveals that the average size of the infection focus was much greater in N-WASP$^{+/+}$ fibroblasts ($p = 0.002$); asterisk indicates a statistically significant difference.

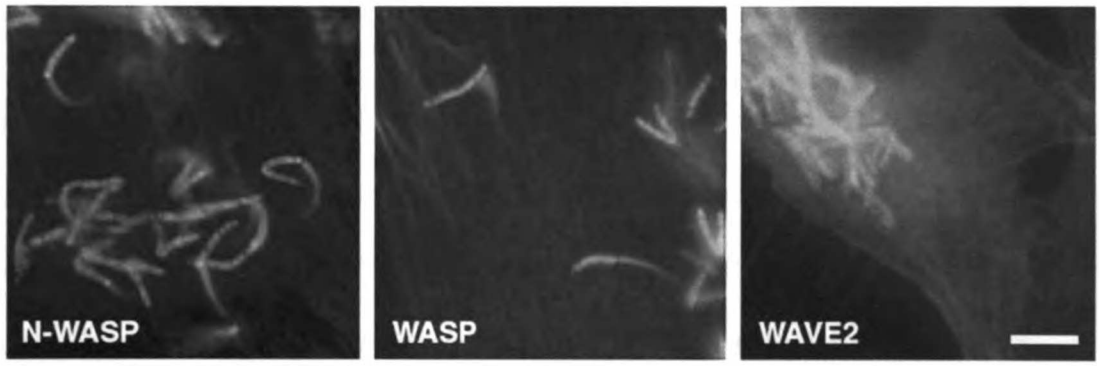

Figure 3.5 ***M. marinum*** **utilizes either N-WASP or WASP for actin tail formation.** N-WASP$^{-/-}$ fibroblasts were transiently transfected with GFP-N-WASP (left panel), WASP (middle panel) or WAVE2 (right panel) and infected with *M. marinum*. GFP is shown in green, *M. marinum* in red. Cells were fixed and stained with phalloidin to visualize actin (blue). Scale bar: 5 μm.

Independence from Tyrosine Phosphorylation, Nck and WIP

To determine how *M. marinum* recruits WASP and N-WASP, we embarked on a systematic examination of molecules known to activate and interact with proteins of the WASP family, and examination of the N-WASP domains required for actin polymerization. We first verified the necessity of the WA output region of N-WASP by transfecting the N-WASP$^{-/-}$ fibroblasts with an N-WASP construct lacking the WA domain (Figure 3.6). This construct did not restore actin tail formation, indicating that actin and Arp2/3 complex binding to the WA domain of N-WASP is required for *M. marinum* actin tail formation as suggested previously by microscopic studies (98). However, the WA domain alone of N-WASP did not restore actin tails, suggesting critical interactions with *M. marinum* in the input region of the molecule (Figure 3.6).

Vaccinia and EPEC mimic receptor tyrosine kinases by initiating an activation cascade through phosphorylation of a microbial molecule by tyrosine kinases including those of the Src family (62,99-101). Src kinases also can directly activate the WASP family, regulating its activity in hematopoeitic cells and neurons (102,103). To determine if tyrosine phosphorylation has a role in *M. marinum* actin tail formation, we first examined phosphotyrosine staining in *M. marinum*-infected macrophages and fibroblasts. Anti-phosphotyrosine antibodies showed marked staining of adhesion sites and other cellular structures (Figure 3.7). In macrophages, approximately 25% of all *M. marinum* with actin tails had phosphotyrosine staining at the pole from which the tail arose (Figure 3.7A); however, we were never able to detect any phosphotyrosine staining associated with bacteria in fibroblasts (Figure 3.7B). PP2, a Src kinase-specific inhibitor, had no effect on actin tail formation in either *M. marinum*-infected macrophages or

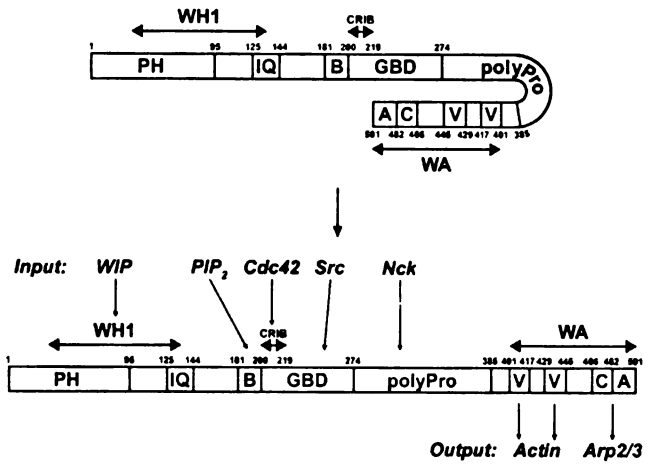

Auto-Inhibited N-WASP

Activated N-WASP

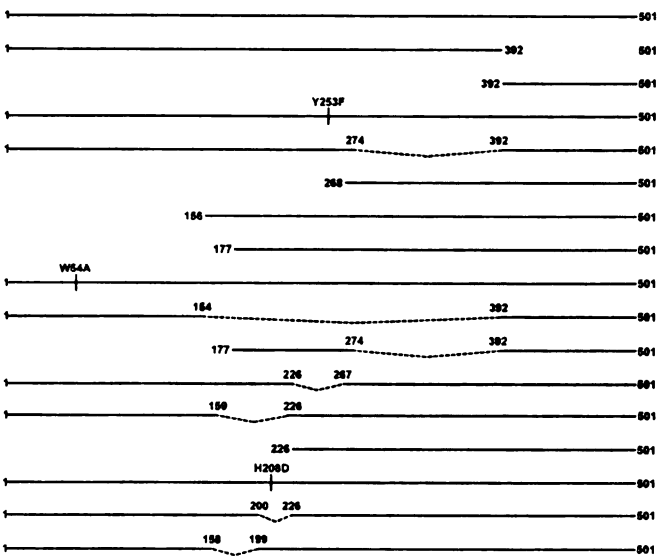

	Actin Tail Formation
N-WASP full length	+ +
ΔWA	–
WA	–
Y253F	+ +
ΔpolyPro	+
polyProWA	–
ΔWH1	+
B-WA	+
W54A	+ +
WH1+WA	–
mini-N-WASP	+
Δ226-267	+ +
Δ(B-CRIB)	–
Δ(WH1-CRIB)	–
H208D	+ +
Δ200-226	+
Δ158-199	–

WASP full length	+ +
mini-WASP	+
WAVE2	–

Figure 3.6 Actin tail formation requires specific N-WASP domains.

Top: Schematic representation of N-WASP in its autoinhibited and activated states, showing interactions relevant to function, is adapted from (60,61,104). WIP, PIP_2, Cdc42, Nck, and the Src kinase all bind to the input region and monomeric actin and the Arp2/3 complex bind to the output region. Bottom: The domain structure of N-WASP constructs used in this study and their ability to restore actin tail formation by *M. marinum* in N-WASP$^{-/-}$ fibroblasts is shown. –, +, and ++ symbols indicate efficiency of restoration ("–" represents <1 cell with tails/100 transfected, infected cells; "+" represents 2-20 cells with tails/100 transfected, infected cells; "++" represents >20 cells with tails/100 transfected, infected cells). Also included are results for full-length WASP, mini-WASP (equivalent to mini N-WASP, which is depicted), and full-length WAVE2. Each construct was tested two or more times.

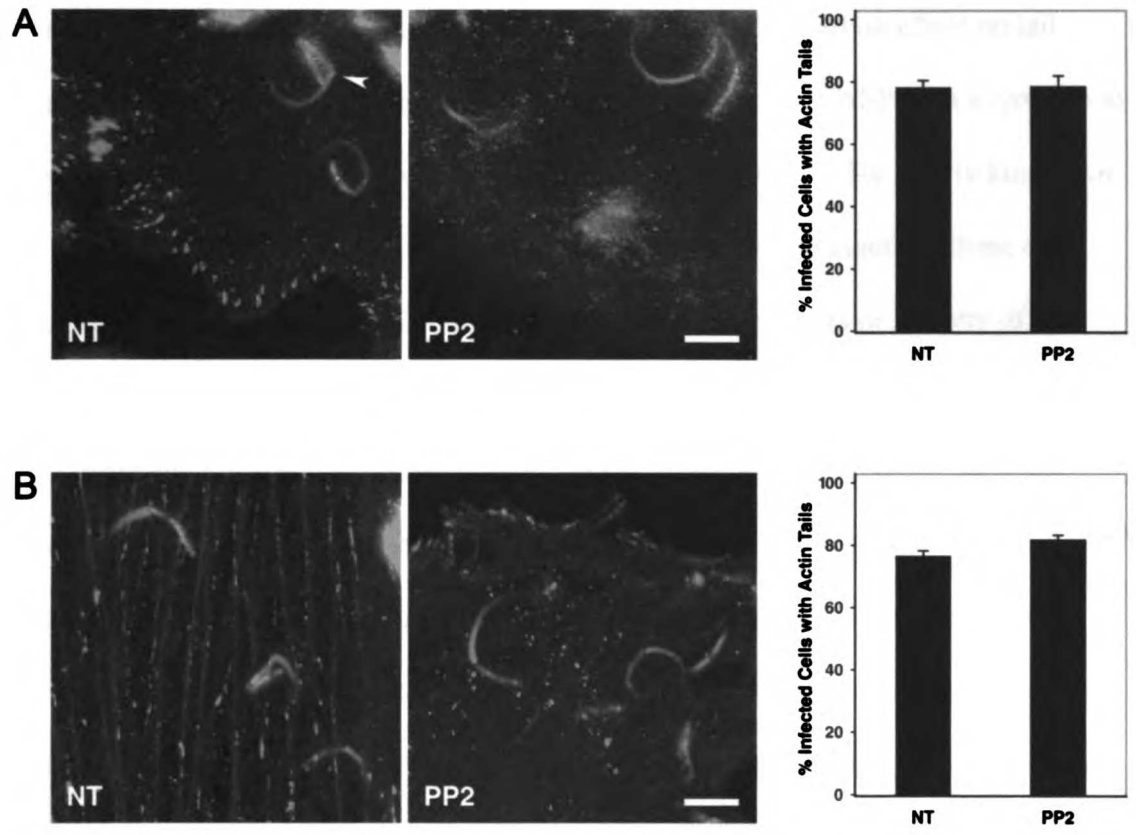

Figure 3.7 Actin tail formation is independent of tyrosine phosphorylation.

Bone marrow-derived macrophages (A) and mouse embryonic fibroblasts (B) were infected with *M. marinum* (red). Cells were not treated (NT) or treated with 100 μM PP2 for 1 hour, then fixed and stained with phalloidin to visualize actin (blue) and anti-phosphotyrosine (green). Arrowhead indicates an example of localized phosphotyrosine staining occasionally seen in macrophages. Scale bar: 5 μm. Quantification of actin tail formation from three independent experiments for each cell type under NT or PP2-treated conditions is shown to the right.

fibroblasts, but it did eliminate the occasional phosphotyrosine staining in macrophages (Figure 3.7). Genistein, a general tyrosine kinase inhibitor, also had no effect on tail formation (data not shown). In agreement with these results, N-WASP with a tyrosine to phenylalanine mutation (Y253F) that cannot be phosphorylated by Src family kinases *in vitro* (103) fully restored actin tail formation (Figure 3.6). Taken together, these data indicate that tyrosine phosphorylation, either of upstream activators or directly of N-WASP, does not play a significant role in *M. marinum* actin polymerization.

Vaccinia virus and EPEC use mainly Nck to link a phosphorylated microbial molecule to N-WASP, and Nck binding to the polyproline domain (polyPro) of N-WASP is capable of activating the protein *in vitro* (89). By immunofluorescence with two commercially available anti-Nck antibodies, Nck did not localize to the poles of any *M. marinum* with actin tails in infected macrophages or fibroblasts (Figure 3.8A, data not shown). Moreover, actin tail formation was comparable in $Nck^{+/+}$ and $Nck^{-/-}$ fibroblasts (Figure 3.8B; $Nck^{+/+}$ 79.3% $\pm$ 1.3, $Nck^{-/-}$ 82.7% $\pm$ 2.4, $p > 0.31$), and transfection of an N-WASP protein in which the polyPro region was deleted (ΔpolyPro) restored actin tail formation in *M. marinum*-infected $N\text{-}WASP^{-/-}$ fibroblasts (Figure 3.6).

The WASP-interacting protein (WIP) has been implicated in regulation of WASP and N-WASP through eukaryotic signaling cascades and in actin polymerization by vaccinia virus downstream of Nck (64). WIP did localize to the pole of *M. marinum* from which actin tails formed in both macrophages and fibroblasts (Figure 3.9A, data not shown). However, tails behind *M. marinum* in $WIP^{-/-}$ fibroblasts formed at the same frequency and had similar morphology to tails formed in wild-type fibroblasts (Figure 3.9B; $WIP^{+/+}$ 77.3% $\pm$ 2.4, $WIP^{-/-}$ 78.0% $\pm$ 3.1, $p > 0.875$). Other members of the WIP

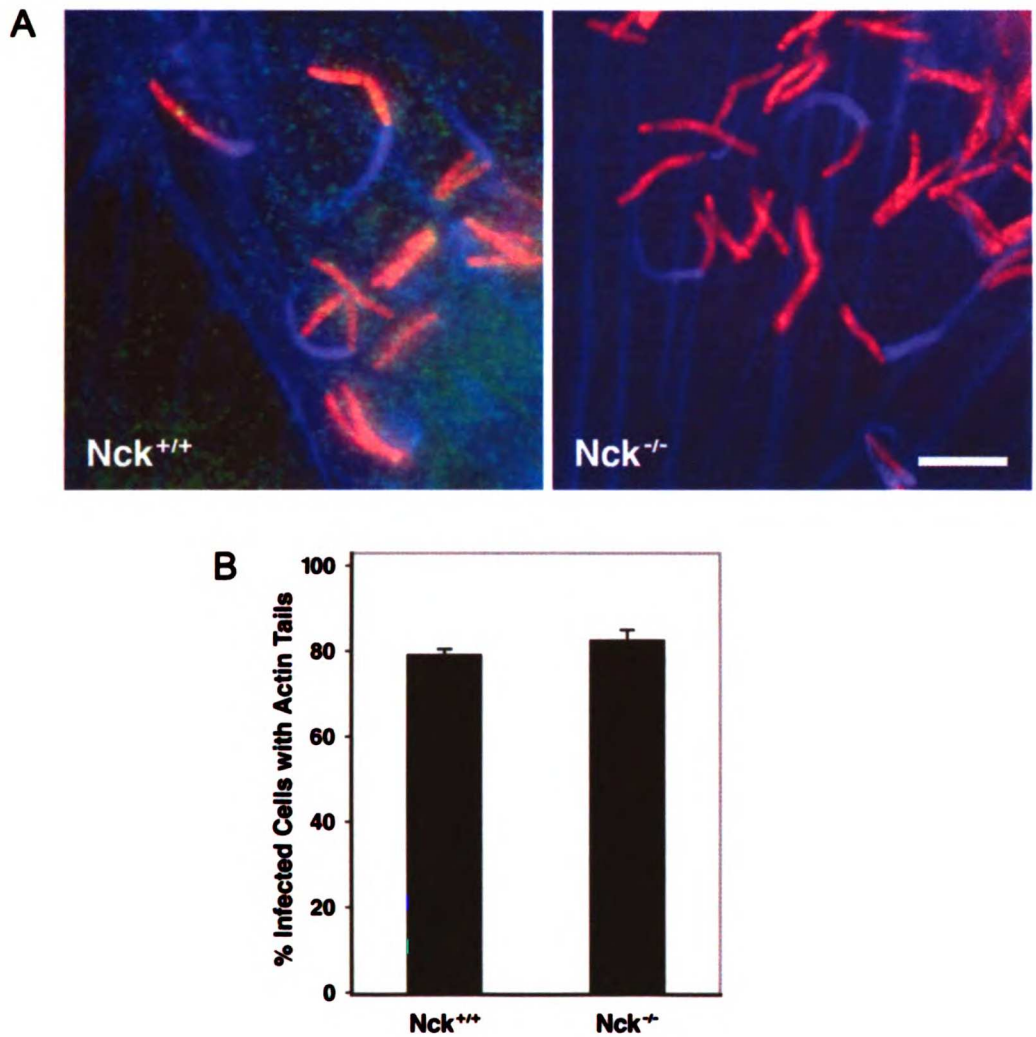

Figure 3.8 Nck is not involved in *M. marinum* actin tail formation. (A) $Nck^{+/+}$ fibroblasts (left panel) were infected with *M. marinum* (red) and stained with phalloidin to visualize actin (blue) and anti-Nck antibodies (green). $Nck^{-/-}$ fibroblasts (right panel) were similarly infected and stained. Scale bar: 5 μm. (B) The percentage of infected cells with actin tails for both $Nck^{+/+}$ and $Nck^{-/-}$ fibroblasts is shown. Quantification is the summary of three independent experiments.

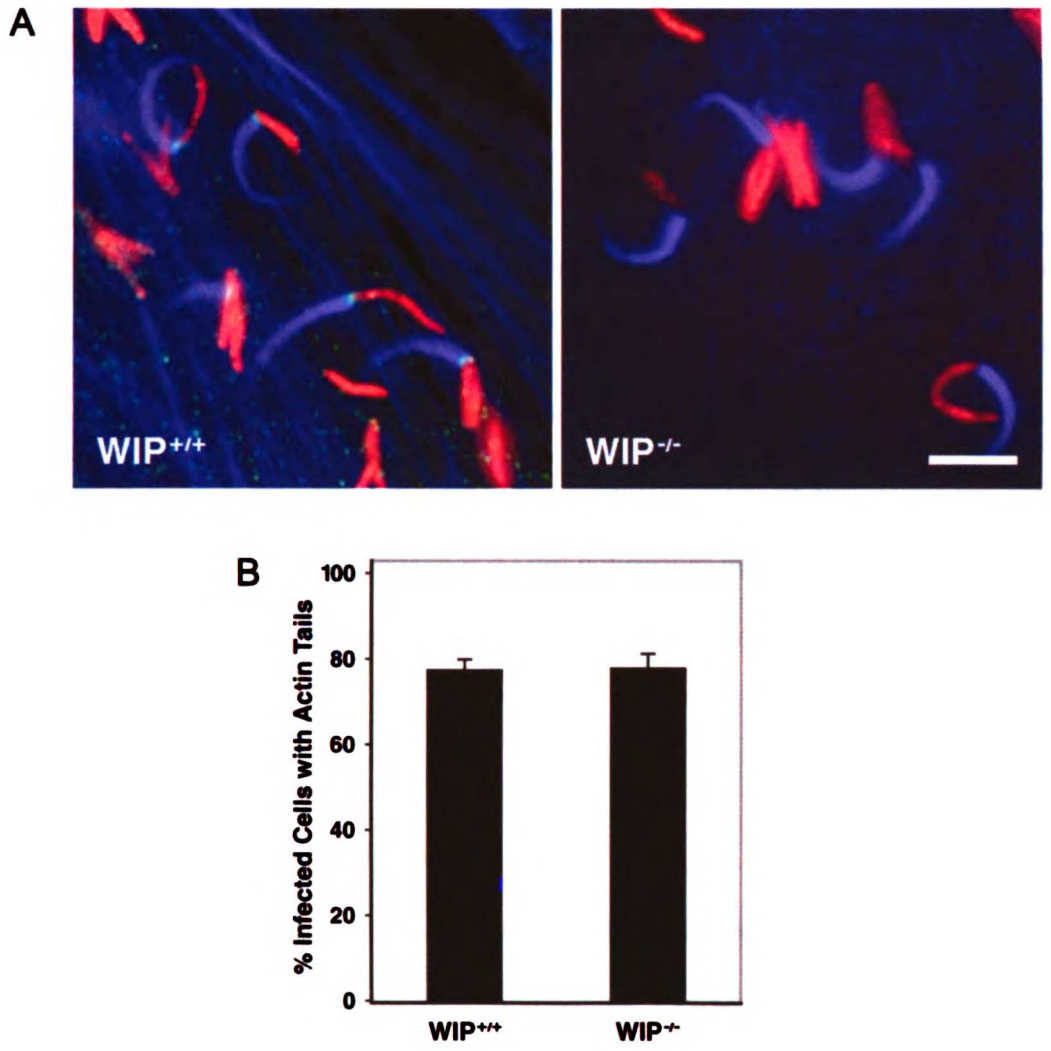

Figure 3.9 WIP is not involved in *M. marinum* actin tail formation. (A) WIP$^{+/+}$ fibroblasts (left panel) were infected with *M. marinum* (red) and stained with phalloidin to visualize actin (blue) and anti-WIP antibodies (green). WIP$^{-/-}$ fibroblasts (right panel) were similarly infected and stained. Scale bar: 5 μm. (B) The percentage of infected cells with actin tails is shown. Quantification is the summary of three independent experiments.

family of proteins, including CR16 and WICH, also bind to the WASP homology 1 (WH1) domain of the WASP family at the same site as WIP, by a mechanism requiring tryptophan 54 (105). Since these alternative family members might have a role in activation of N-WASP by *M. marinum*, N-WASP$^{-/-}$ fibroblasts were transfected with ΔWH1, B-WA and W54A N-WASP constructs. Actin tail formation by *M. marinum* in N-WASP$^{-/-}$ fibroblasts was restored by these constructs, demonstrating that the direct interaction with N-WASP of neither WIP nor a WIP-like protein is necessary for *M. marinum* actin polymerization (Figure 3.6). A construct that included only the WH1 domain and the WA domain (WH1+WA) did not restore actin tail formation; thus, the WH1 domain is neither necessary nor sufficient for *M. marinum* induction of actin polymerization (Figure 3.6).

Role of the Basic Motif within N-WASP

The mini N-WASP construct containing the basic motif and the GTPase binding domain (B-GBD) but lacking the WH1 and the polyPro domains has been shown previously to be controlled by PIP_2 and Cdc42 in a manner similar to full-length N-WASP (87). In our system, both mini N-WASP and mini WASP were sufficient to restore actin tail formation in N-WASP$^{-/-}$ fibroblasts, albeit not as efficiently as full-length constructs (Figure 3.6). The C-terminal region of the B-GBD domain has been shown previously to bind directly to the Arp2/3 complex-binding site in the WA regions maintaining N-WASP in its autoinhibited conformation (87,106). To determine if *M. marinum* activated N-WASP by binding in this area we transfected N-WASP$^{-/-}$ cells with a GFP-N-WASP Δ226-267 construct, and found that this was fully capable of restoring

actin tails. However, two constructs lacking the N-terminal portion of the B-GBD, including the Cdc42 and Rac interactive binding (CRIB) motif (ΔWH1-CRIB and ΔB-CRIB, Figure 3.6) were unable to restore actin tail formation in the N-WASP$^{-/-}$ fibroblasts (Figure 3.6) focusing our attention on that area of the protein to which Cdc42 and PIP_2 bind.

Binding of GTP-loaded Cdc42 is a major mechanism by which the WASP family proteins are activated (86). Cdc42 directly binds to the CRIB motif within the GBD of N-WASP leading to relief of autoinhibition and consequent Arp2/3-dependent actin polymerization. To determine whether Cdc42 has a role in *M. marinum* actin polymerization, we transfected N-WASP$^{-/-}$ fibroblasts with an N-WASP construct containing an H208D mutation that abolishes GTPase binding to the CRIB motif and with an N-WASP construct containing a deletion of amino acids 200-226, which includes the CRIB motif; both of these constructs restored actin tail formation by *M. marinum* (Figure 3.6), suggesting that the bacterium recruits and activates N-WASP independent of GTPases. Furthermore, we treated *M. marinum*-infected macrophages with *C. difficile* toxin B, a pharmacological inhibitor that inactivates the entire Rho family of small GTPases (Figure 3.10). Although toxin B treatment led to dramatic differences in overall actin distribution, *M. marinum* still induced actin tails at levels similar to untreated cells (Figure 3.10B; NT 85% $\pm$ 2, Toxin B 82% $\pm$ 0, $p > 0.27$). As a positive control for inhibition of actin polymerization, cytochalasin D was added to cells, and the percentage of infected cells with actin tails significantly decreased and the tails that were present were smaller (compared to NT, Cyto D 24% $\pm$ 2, $p = 0.0005$). Thus, WASP family binding of Cdc42 or a related GTPase is not required for actin polymerization.

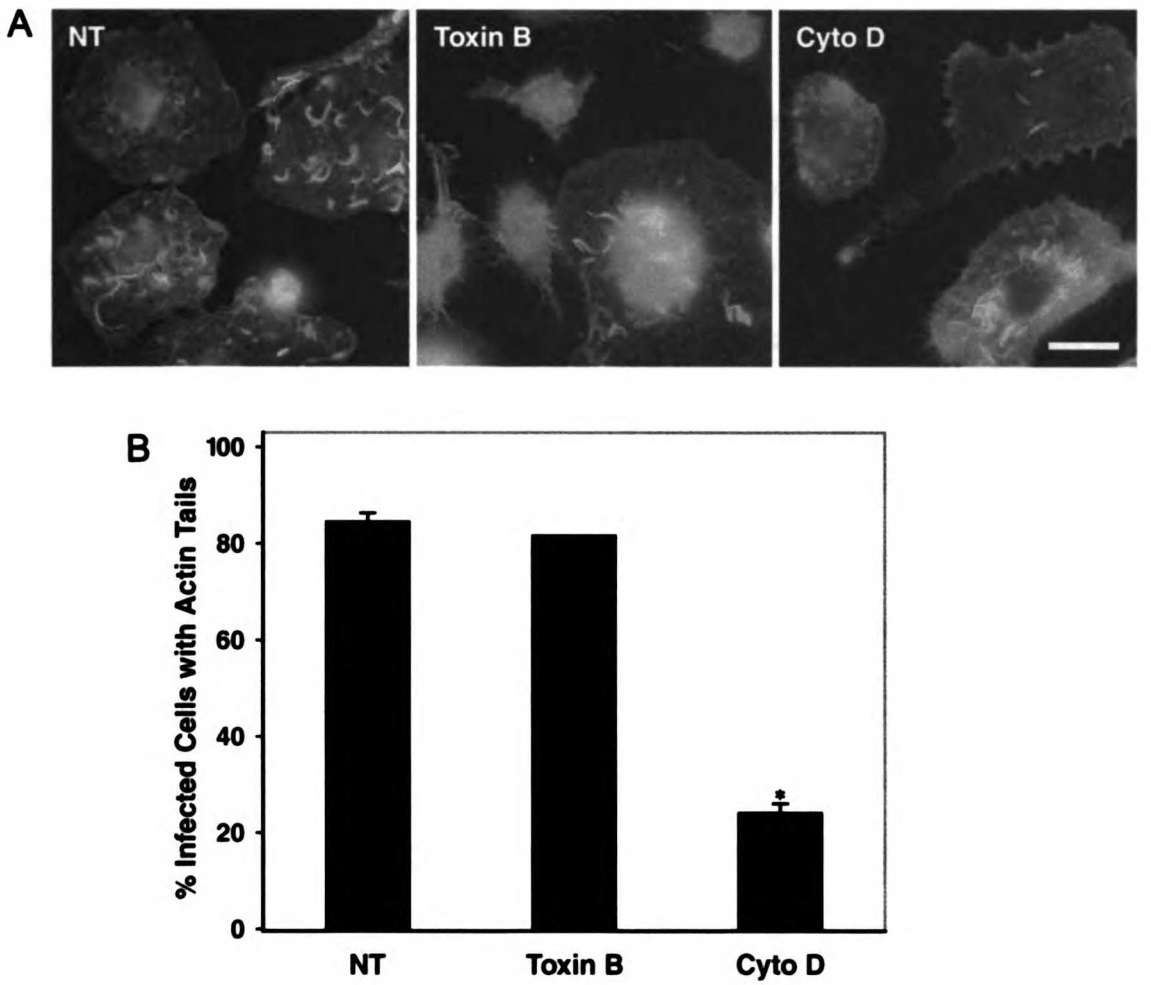

Figure 3.10 Cdc42 is not required for *M. marinum* actin tail formation.

(A) Macrophages were infected with *M. marinum* (red), and left untreated (NT) or treated with toxin B or cytochalasin D (Cyto D), and then stained for actin (blue). Scale bar: 20 μm. (B) The percentage of infected cells with actin tails under each condition was quantified in three independent experiments; asterisk indicates a statistically significant difference.

The host anionic lipid PIP_2 is known to bind to N-WASP within a basic motif in the B-GBD domain containing nine lysines. PIP_2 is capable of activating N-WASP or WASP on its own, and it can synergize with Cdc42 for highly efficient Arp2/3-dependent activation of actin polymerization (87,106,107). Transfection of an N-WASP construct containing a deletion of amino acids 158-199 that contains the basic motif was unable to restore actin tail formation in N-WASP$^{-/-}$ fibroblasts, suggesting a role for this region in *M. marinum* actin polymerization (Figure 3.6). Under some conditions, high doses of wortmannin are reported to acutely deplete host cells of PIP_2 by inhibiting PI_4 kinase (108). Adding wortmannin to *M. marinum*-infected cells had no effect on actin tail formation suggesting that the host ligand PIP_2 is not involved (Figure 3.11). Taken together, these results indicate that the basic motif of N-WASP is important in *M. marinum* actin polymerization, and that the molecule binding to this area is not host PIP_2.

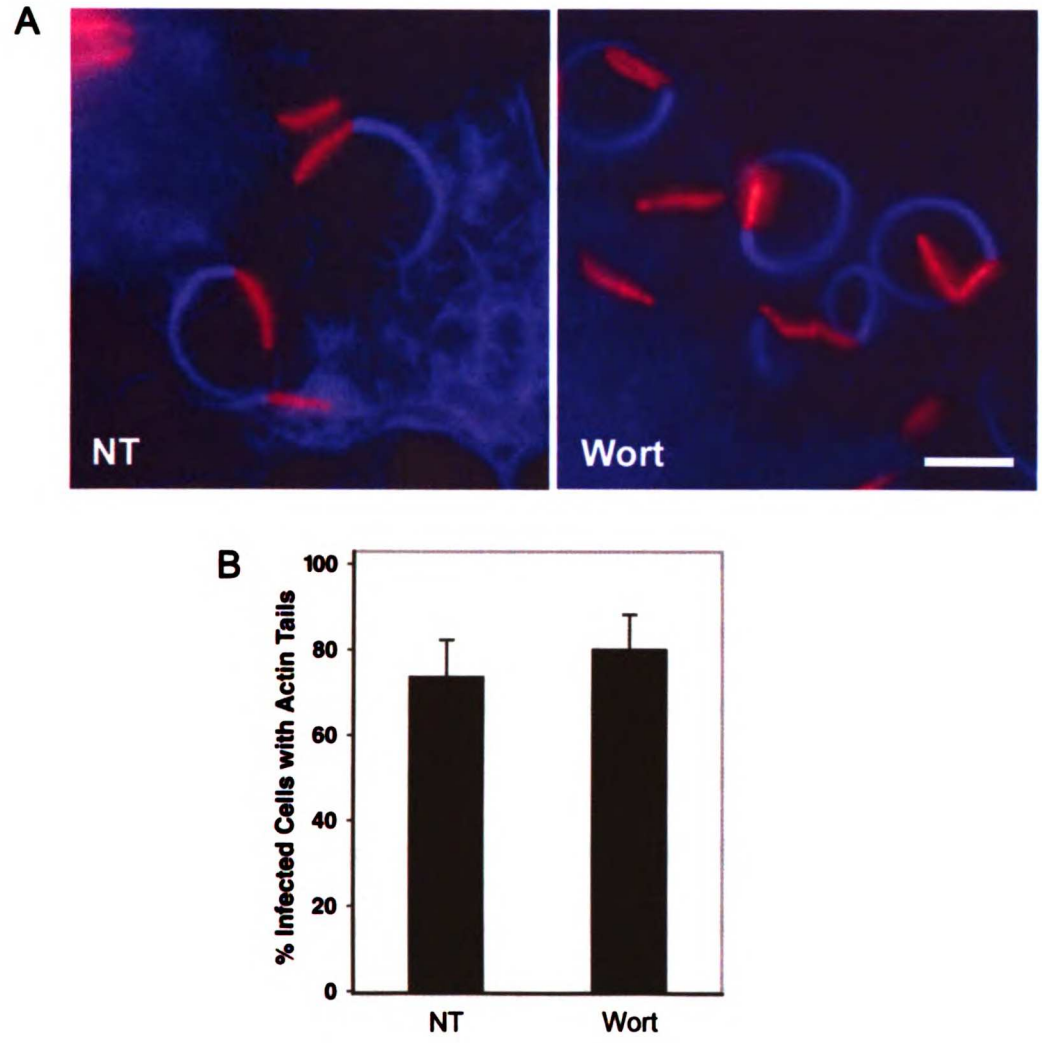

Figure 3.11 Actin tail formation is independent of host PIP_2. (A) Macrophages were infected with *M. marinum* (red). Cells were not treated (NT) or treated with wortmannin (Wort) to acutely deplete host cell PIP_2, then fixed and stained for actin (blue). Scale bar: 5 μm. (B) The percentage of infected cells with actin tails under each condition was quantified in three independent experiments.

Discussion

A diverse group of intracellular pathogens, including, surprisingly, *M. marinum*, enable efficient intercellular spread by activating actin polymerization on their surfaces within host cytoplasm. The resultant motility is used for direct intercellular spread, bypassing host defense mechanisms directed against extracellular pathogens. Intracellularly motile bacteria have evolved multiple methods for subverting the host cytoskeleton to generate Arp2/3-dependent actin polymerization. Unlike *Listeria* and *Rickettsia* that directly recruit and activate the Arp2/3 complex, we show here that efficient *M. marinum* actin polymerization is dependent on WASP or N-WASP to initiate actin polymerization. Unlike *Shigella*, which exploits only N-WASP, *M. marinum* can use either family member, depending on availability in accordance with cell type (Figures 3.1, 3.3 and 3.5). N-WASP-dependent tail formation by *M. marinum* depends on both the input and output regions suggesting that this species, like the gram-negative bacteria, has developed a mechanism of activating N-WASP that is dependent on the input region in the N terminal part of the protein, leading to unfolding of the protein and unmasking of the WA output region required for Arp2/3-dependent actin polymerization. The observation that bacterial motility was not completely eliminated by the absence of WASP family proteins suggests the existence of a second, albeit inefficient, mode of actin polymerization by *M. marinum*.

Because its role was so predominant, we sought to elucidate the mechanism by which *M. marinum* activates WASP family proteins using a variety of genetic, biochemical, and pharmacological reagents. *M. marinum* activation of N-WASP clearly differs from vaccinia and EPEC, which require tyrosine phosphorylation of pathogen-

encoded proteins, A36R and Tir, respectively, to initiate a Nck-dependent cascade for activation of N-WASP (62,63). For both vaccinia and EPEC, the WIP-binding WH1 domain is involved in actin polymerization (60,64), and WIP is thought to be downstream of Nck in the case of vaccinia but not of EPEC (61,64). For *M. marinum*, tyrosine phosphorylation, Nck, and WIP are all dispensable for actin tail formation (Figures 3.7, 3.8 and 3.9). Furthermore, the domains of N-WASP with which they interact, the WH1 and polyPro domains, respectively, can be removed without blocking actin polymerization (Figure 3.6). However, those constructs are less efficient than full-length N-WASP. It is possible that although not required for N-WASP-dependent tail formation, proteins that interact with the WH1 and polypro domains contribute to amplification of N-WASP and actin recruitment. We see that WIP localizes to the pole behind which *M. marinum* tails form (Figure 3.9). This is very similar to what has been shown for *Shigella* (64) leading to the suggestion that WIP binding to N-WASP is downstream of pathogen activation of N-WASP, and consistent with the findings that most autoinhibited N-WASP in cells is in a complex with WIP (109).

M. marinum activation of N-WASP is more similar to the mechanisms described for *Shigella* and EHEC, which are independent of tyrosine phosphorylation and also bypass Cdc42 binding to the N-WASP GBD domain (Figures 3.7 and 3.10). In contrast to EPEC Tir, the EHEC Tir is not tyrosine phosphorylated and the pathogen is not dependent upon Nck for pedestal formation (63,65). Both EHEC and *Shigella* express proteins that directly bind to N-WASP (65,72). *Shigella* IcsA most likely binds to N-WASP at several sites in the input region, including the WH1 and GBD domains (60,72). The region of the B-GBD carboxy-terminal to the Cdc42 binding site spanning amino

acids 226-274 is known to interact with the WA domain and maintain N-WASP in its inactive state (88). This region is dispensable for targeting and activation by *M. marinum* (Figure 3.6), but it is sufficient for actin polymerization by EHEC (61,65). The lack of sequence similarity between *Shigella* IcsA and EHEC EspFu, both of which directly target N-WASP, emphasizes that these pathogens have independently evolved to exploit a mechanism for activation of actin polymerization.

One way in which *M. marinum* differs from these gram-negative bacteria in activation of actin polymerization is that the basic motif of N-WASP is required for *M. marinum* activation. This region is known to bind to eukaryotic polyphosphoinositides through an ionic interaction mediated by its concentration of lysines (87,106). PIP_2 has been shown to bind preferentially to this motif in host cells, based on both its affinity for N-WASP and its concentration in cells (110). The deletion of amino acids 158-199 that contain the basic motif abolished the ability of *M. marinum* to activate N-WASP-dependent actin polymerization (Figure 3.6). In addition, acute depletion of host PIP_2 has no effect on *M. marinum* actin tail formation (Figure 3.11). This demonstrates that the basic motif, which is known to bind phosphoinositides, may mediate an interaction with the bacterial surface. Unlike other prokaryotes that activate actin polymerization, mycobacterial cell walls are rich in phosphoinositides. One of these, the multi-glycosylated lipoarabinomannan is a potential virulence factor and modulates immune responses (reviewed in (42,111)). In addition, its precursor phosphatidylinositol mannoside has been found to be associated with the bacterial surface (112). It is intriguing to speculate that mycobacterial phospholipids bind to the basic motif region of N-WASP. Alternatively, host phosphoinositides may be carried with *M. marinum* into

the cytoplasm when it escapes the phagosome or *M. marinum* may be able to modulate levels of PIP_2 on the bacterial surface by catalyzing its production. PIP_2 is not an efficient activator of N-WASP on its own, and it is believed that its major role in host cell actin polymerization is in synergy with Cdc42 or other activators. However, many intracellular pathogens, including *M. tuberculosis*, are known to control levels of host phosphoinositides for their own purposes (reviewed in (113)).

Thus, we hypothesize that *M. marinum* highjacks eukaryotic signaling for actin polymerization through the basic motif of N-WASP. This model for N-WASP activation by *M. marinum* is distinct from the mechanism of Arp2/3 complex-dependent actin polymerization thus described for other pathogens. It is unknown if actin-based motility is a characteristic unique to *M. marinum* among all mycobacteria. Future studies of actin polymerization by *M. marinum* will certainly explore its role in pathogenesis of infection, as well as further understanding of the basic biology of the actin cytoskeleton.

Materials and Methods

Host Cells

Macrophages were derived from the bone marrow of either 129/Sv or $WASP^{-/-}$ mice (114) (provided by Clifford Lowell) and cultured in 10% FBS, 100 mM HEPES, 10% CMG14-12 SN in phenol-red free DMEM at 37°C in 5% CO_2 as described previously (98). Cells were harvested 7 to 21 days after plating and allowed to adhere to fibronectin-coated coverslips (Becton-Dickinson) for infection with *M. marinum* the next day. Wild-type, $N\text{-}WASP^{-/-}$ (59,60), $Nck^{-/-}$ (115) (kindly provided by Tony Pawson), and $WIP^{-/-}$ (116) (kindly provided by R.S. Geha and N. Ramesh) embryonic fibroblast cell lines were maintained as previously described and also seeded onto fibronectin-coated coverslips prior to infection.

Bacteria and Infection

M. marinum expressing red fluorescent protein (RFP) were generated by transforming *M. marinum* with a RFP expression plasmid kindly provided by Lalita Ramakrishnan (98,117). Wild type (strain M), GFP- (98) or RFP-expressing *M. marinum* were cultured in Middlebrook 7H9 (Difco) supplemented with 0.2% glycerol, 0.05% Tween 80, and 10% ADC enrichment (Fisher).

Infections for observation of actin tail formation were carried out as described before (98). Bacteria were washed twice in serum-free cell culture media and disrupted into single bacilli by passage through a 26-gauge needle. *M. marinum* were added to host cells washed with serum-free medium at a multiplicity of infection (MOI) of 1 or 60 to

macrophages or fibroblasts, respectively, centrifuged at 500xg for 10 minutes, and incubated at 32°C, 5% CO_2. After 2 hours, the infected cells were washed well with serum-free medium to remove extracellular bacteria. Host cells were incubated further in their respective growth media at 32°C in 5% CO_2 for 32 or 48 hours prior to microscopy for macrophages and fibroblasts, respectively. For quantification, infected cells were identified by phase contrast microscopy, and actin tails were visualized by fluorescence. Each experiment was done three times, with 50 cells counted per experiment. Unpaired t-tests with Welch corrections were used to generate p values and determine statistical significance.

Intercellular spreading assays were performed in confluent fibroblast monolayers infected with *M. marinum* at an MOI of 0.1 essentially as described previously (98). Following infection, wells were overlaid with agar and culture medium contained 40 μg/mL amikacin. Media was changed every two days and monolayers were examined for pattern of infection eight days later. Quantification of FFI was performed using IPLab analysis software (Scanalytics).

Expression Constructs and Transfection

The WAVE2 and many of the GFP-tagged murine N-WASP expression constructs have been described (60,61,104). GFP-tagged full-length and mini human WASP expression constructs were kindly provided by John Dueber (UCSF). The pEGFP-C1-N-WASP Y253F mutant was generated from full-length N-WASP using the quickchange site directed mutagenesis kit (Stratagene) and restriction cloning and

confirmed by sequencing. The constructs pEGFP-C1 N-WASP polyProWA, pEGFP-C3 N-WASP WH1+WA, and pEGFP-C1 N-WASP Δ226-267, pEGFP-C1 N-WASP Δ200-226 and pEGFP-C1 N-WASP Δ158-199 were generated by restriction cloning and confirmed by sequencing. Expression of an appropriate size molecule was monitored by immunoblotting for all constructs. All constructs here scored as negative for *M. marinum* are functional in other systems (S. Lommel, unpublished results). Fibroblast cell lines were transfected 24 hours after plating on fibronectin-coated coverslips with Fugene (Roche) according to manufacturers' specifications. Transfected cells were infected 18 hours after transfection.

Pharmacological inhibitors

Infected macrophages and fibroblasts were treated with inhibitors 30 or 48 hours post-infection, respectively. To study the effect of the rho family of GTPases on *M. marinum* actin tail formation, toxin B (1 μg/mL, Calbiochem) was added to infected cells for 1.5 hours prior to fixation. As a positive control for inhibition of tail formation, cytochalasin D (1.3 μM, Sigma) was added to infected cells. PP2 (100 μM, Calbiochem) or genistein (250 μM) were added to infected cells for 1 hour prior to fixation and staining to study the effect of tyrosine kinase inhibition. To acutely deplete host PIP2, wortmannin (100 μM, Calbiochem) was added to infected cells for 20 minutes prior to fixation.

Microscopy

Infected cells were fixed with 3.7% paraformaldehyde for 10 minutes and permeabilized with 0.1% Triton X-100 for 5 minutes. Alexa Fluor phalloidin (Molecular Probes) was added to coverslips for 20 minutes at room temperature to stain for F-actin. To localize host cytoskeletal proteins, indirect immunofluorescence was performed with anti-N-WASP (provided by Jack Taunton), anti-Nck (Uspstate, BD Transduction Labs), anti-WIP (Santa Cruz), anti-phosphotyrosine (PY99, Santa Cruz; 4G10, Upstate Biotech) and species-appropriate Alexa Fluor secondary antibodies (Molecular Probes). Coverslips were mounted with Prolong anti-fade reagent (Molecular Probes). Images were acquired on a Nikon Eclipse TE300 microscope with an Evolution QEi cooled CCD (Media Cybernetics) with IPLab acquisition software (Scanalytics).

Chapter 4

Microbial Requirements for *M. marinum* Actin-Based Motility

Abstract

Pathogens have evolved diverse ways of subverting the host signaling pathway to lead to actin polymerization. Researchers have identified these various pathogenic factors in different ways, including screening assays and homology searching. In this chapter, we discuss our approaches to identify the microbial molecules involved in *Mycobacterium marinum* phagosome lysis, actin polymerization and intercellular spread. A large part of this work involved creation of a *M. marinum* genomic prey library, and screening this library in yeast with N-WASP as bait. This method proved unsuccessful, most likely because the molecule required for *M. marinum* actin polymerization may be a lipid rather than a protein. We also began a preliminary analysis of mutants from a transposon library that originally were identified as defective in hemolysis. These mutants all have insertions in the RD1 region of the *M. marinum* genome. We show here that these mutants have variable colony morphology and defects in intracellular growth in macrophages. Most of them have delayed actin tail formation in primarily infected cells, except for two of the most attenuated strains that were quite defective for tail formation even at the later time points. Thus, a locus implicated in virulence of *M. tuberculosis* is required for optimal phagosome escape. Together, these data suggest that the molecular mechanisms of *M. marinum* phagosome escape, actin tail formation, and intercellular spread will most likely involve many genes and multiple molecules.

Introduction

An amazingly diverse group of pathogens have evolved molecules to highjack the Arp2/3 complex to induce actin polymerization in host cells (43) (92). A brief survey of the discovery of the molecules involved in this process aids our understanding of reasonable ways to look for novel genes. The first molecules identified, those of *Shigella* and *Listeria*, were discovered by evaluating mutants for screenable phenotypes. The *Shigella* IcsA protein was identified by transposon mutagenesis within a *Shigella* virulence plasmid and screening for mutants that did not form plaques in a cellular monolayer (118,119). IcsA is a 110 kDa protein that contains an auto-transporter motif common in gram-negative bacteria that mediates its own translocation across the outer membrane. It has a β domain anchoring it in the outer membrane and α domain that contains the regions required for actin polymerization and direct binding of N-WASP.

The *Listeria* protein ActA was identified by screening of transposon mutants for the absence of phospholipase C activity on egg yolk agar plates (120). Fortuitously, phospholipase C (plc), listeriolysin O (LLO) and ActA are in an operon, and this mutant also was negative in actin tail and plaque formation. ActA contains an N-terminal signal sequence and C-terminal transmembrane domain. Like N-WASP, ActA contains WASP homology 2 domains (WH2, also called verprolin homology (V) domains) that bind to monomeric actin and an acidic domain that directly binds the Arp2/3 complex. ActA also contains an extensive polyproline region consisting of four repeats to which VASP binds. VASP binds profilin, which binds and recruits monomeric actin. Although not required for motility *in vitro*, its presence increases the rate of *Listeria* movement in some cases (121).

The second way that proteins involved in pathogen actin polymerization have been discovered is by genome searching. For example, the polyproline region present in ActA was used to search the *Rickettsia* genome to find RickA (56,57). RickA also contains WH2 and acidic domains and is found only in the genomes of *Rickettsia* species that form actin tails. The *Burkholderia* protein BimA was identified by searching the genome for autosecretory proteins containing polyproline motifs (58). Like ActA and RickA, the other molecules known to initiate actin polymerization independently of N-WASP, BimA contains WH2 motifs; however, unlike ActA and RickA that are known to directly bind the Arp2/3 complex, BimA has no acidic motif, and its mechanism of initiating actin polymerization remains unclear.

The third successful way to identify novel microbial proteins involved in actin polymerization is to utilize additional data about how the protein may function to narrow the search to a certain subset of proteins. For example, it was known that tyrosine phosphorylation was required for actin-based motility of vaccinia virus (122), and A36R was originally identified as a phosphotyrosine protein that localized to the site of actin assembly; it was later confirmed to be necessary and sufficient for vaccinia actin polymerization (62).

Lastly, the enteropathogenic *E. coli* (EPEC) Tir protein was discovered indirectly and fortuitously during studies focused on another issue. It had been known that EPEC intimin bound a tyrosine-phosphorylated protein in the host cell membrane, but it was originally thought to be of host origin. In trying to purify this protein investigators found that antibodies against EPEC were cross-reactive with this protein, and subsequent studies identified it as Tir, the bacterial factor translocated by the type-three secretion

apparatus to initiate a signal cascade resulting in actin polymerization and pedestal formation (97). Soon after, the enterohemorrhagic (EHEC) Tir was identified using by homology searching and utilitizing antibodies against EPEC Tir (123). However, EHEC Tir alone could not initiate pedestal formation suggesting that EHEC requires an additional bacterial protein (124). Recently, EHEC EspFu (or TccP) was identified by combining the methods described above: by screening mutants with deletions in known pathogenicity islands (65) and by searching the genome for proline-rich proteins present in EHEC, but not in EPEC.

These examples demonstrate that several different methods to identify microbial genes required for actin polymerization have been successful. It is notable that in two cases, the identification was based on fortuitous coincidence. Given that the bioinformatics approach was useful in several others, we first sought homologies within the *M. marinum* genome with domains from IcsA from *Shigella* and EspFu from EHEC. This strategy was based on the fact that these two pathogens function similarly to *M. marinum* by directly recruiting N-WASP for actin polymerization. At the time of this writing, the sequencing of the *M. marinum* genome is complete (6). However, we were unable to identify strong candidates by this method (data not shown). There are a couple of important reasons why the bioinformatic approach may have failed. First, there is no significant homology between IcsA and EspFu, supporting the hypothesis that these pathogens have independently evolved the respective molecules to induce actin polymerization. Second, neither IcsA nor EspFu interaction with N-WASP has been studied in detail, so we could not focus our search on smaller potentially relevant moftifs. Most importantly, by assays with N-WASP deletion and mutation constructs, it seems

that *Shigella*, EHEC and *M. marinum* target different domains within N-WASP ((60,61), S. Lommel unpublished results, Chapter 3), and so it is logical that the factors would be significantly different. Furthermore, because *M. marinum* requires the basic motif of N-WASP (Chapter 3), we hypothesize that the *M. marinum* molecule, if it directly binds to N-WASP, may be a lipid, a category of molecule that is not directly searchable in genomic databases.

We also tried a conceptually directed method to identify the *M. marinum* N-WASP activator. Because N-WASP was required for *M. marinum* actin polymerization and upstream molecules were not (Chapter 3), we believed that the *M. marinum* microbial factor would interact directly with N-WASP. So, we used full-length N-WASP as bait to screen a *M. marinum* genomic library. To our knowledge, this is the first attempt to use a host cell protein as a bait to discover a microbial molecule. This approach is fraught with caveats: the interaction must be a direct, protein-protein interaction, and that fusion proteins in the library may not be expressed or localized correctly. The failure of this technique to identify *M. marinum* actin initiator as described in this chapter may be because it is a lipid rather than a protein.

One would predict that there are three critical steps for direct intercellular spread: escape from the phagosome of primarily infected cells, actin polymerization, and escape from the double membrane compartment of secondarily infected cells. In the case of *Listeria*, these processes are linked in an operon that is upregulated intracellularly under the control of the PrfA promoter (125). In addition to the molecule(s) required to initiate *M. marinum* actin polymerization, we are also interested in the process of escape from the phagosome, particularly since this property is novel for *M. marinum* among pathogenic

mycobacteria. Good candidates for this process are hemolysins because the ability to lyse red bloods cells *in vitro* potentially correlates with lysis of intracellular membranes. Previously, a screen of an *M. marinum* transposon library for defects in hemolysis identified mutants with insertions the Region of Difference 1 locus (RD1) (11). RD1 has been a focus of intense study recently and is a known virulence cluster (26-28). In both *M. tuberculosis* and *M. marinum*, the RD1 locus encodes a specialized secretion system for ESAT-6 and CFP-10, and may have roles in modulation of the immune response (27) cytolysis (26) and granuloma formation (11,35). Here we show that most of these mutants have delayed actin tail formation in primarily infected cells. The strains most attenuated for intracellular growth form fewer tails even at later time points, perhaps because they were killed prior to phagosome escape.

In *Listeria*, LLO is necessary and sufficient for phagosomal escape in the primarily infected cell. In secondarily infected cells where the invading bacteria are located within a double membrane, phospholipases C are required (126). *M. marinum* has phospholipases C which are conserved with *M. tuberculosis* (6). In *M. tuberculosis*, *plcA*, *plcB*, and *plcC* are clustered while *plcD* is in a different region. In *M. marinum*, there is a single predicted open reading frame with similarity to *plcA* and *plcB* that is upstream of plcC; plcD is in a different region (L.Y. Gao, unpublished results). The role for these phospholipases C in mycobacterial pathogenesis is unknown; a *M. tuberculosis* mutant in which *plcA-C* were deleted had decreased virulence in a mouse model, but was not attenuated in a macrophages (55). Because of its potential role in pathogenesis, *M. marinum* a Δ*plc* strain that contains a deletion of the *plcA/B*, and *plcC* was constructed (M.A. Pak and L.Y.Gao, unpublished data), and here we demonstrate that this gene

Results and Discussion

Yeast Two-Hybrid Screen

A library was made using a random partial digest of *M. marinum* genomic DNA (see Materials and Methods). We calculated the number of clones required to ensure adequate representation with statistics based on the Poisson distribution using the equation: $N = \ln(1-P)/\ln[1-(I/G)]$

where N is the number of independent clones that must be screened to isolate a particular sequence with probability P, where I is the size of the average cloned fragment and G is the size of the target genome. In our case, to have a 0.99 probability with a genome size of 6.5×10^6 bp, and an average cloned fragment of 2.5×10^3 bp, N is 1.2×10^4 clones. Our *M. marinum* genomic DNA prey library contained 2.5×10^5 total clones which should have complete and sufficient coverage assuming total randomness.

We created several bait plasmids (Table 4.1) and used full-length N-WASP and CFP-10 in two large-scale screens of the *M. marinum* genomic DNA library using the Matchmaker GAL4 Two-Hybrid System 3. The CFP-10 bait yielded a very promising candidate that was intensely blue on the high stringency plate containing X-galactose. However, we were never able to isolate the plasmid from *E. coli* to sequence it and confirm its identity as a mycobacterial protein known to interact with CFP-10 (i.e., ESAT-6 or the *M. marinum* homologue of Rv3871 (27)). In the first screen with the full-length N-WASP bait, 10 colonies were found on 50 plates with the full-length N-WASP bait. Twice the amount of bait and prey DNA were used in the second screen and a

Bait (pBGKT7)	5' primer (RE site)	3' primer (RE site)
FL N-WASP	CATATGAGCTCGGGCCAGCAG (NdeI)	CTGCAGGGTCTTCCCACTCATC (PstI)
Mini N-WASP	CATATGAACATCTCCCACACCAAAGAA (NdeI)	CTGCAGGGTCTTCCCACTCATC (PstI)
FL WASP	CATATGGGAGGAAGGCCCGG (NdeI)	GGATCCCGTCATCCCATTCATC (BamHI)
Mini WASP	CATATGCCTAGCCCAGCTGATAAGA NdeI)	GGATCCCGTCATCCCATTCATC (BamHI)
CFP-10	CATATGGCAGAGATGAAGACCGATG (NdeI)	GGATCCCGAAGCCCATTTGC (BamHI)
Overexpression (pLYG206)	**5' primer (RE site)**	**3' primer (RE site)**
Mh3405c No or V5 tag	TGGCCACTACAGGTTCGGCAATCCGTTCTC (MscI)	AAGCTTTCAACCGCGACCTGAGGGCTCG (HindIII)
Mh3405c His or EGFP tag	TGGCCACTACAGGTTCGGCAATCCGTTCTC (MscI)	AAGCTTCACCGCGACCTGAGGGCTCGAT (HindIII)
Expression (pET-15b)	**5' primer (RE site)**	**3' primer (RE site)**
Mh3405c His tag	CATATGGTGACTACAGGTTCGGCAATCCGTTCTCG (NdeI)	AAGCTTTCAACCGCGACCTGAGGGCTCG (HindIII)
ΔMh3405c (pLYG304)	**5' primer (RE site)**	**3' primer (RE site)**
US Mh3405c	GCACGGTGATCGCGCTGGTCATGC (BamHI within)	CGATATCCACACGCTACACTAGCCGATGTAGTC (EcoRV)
DS Mh3405c	CGATATCTGACGCCCACACCTTGG (EcoRV)	CTCTAGACTGCACGGTGCCCGCTAC (XbaI)

Table 4.1 Primers used in this study. The above primers were used to construct bait plasmids for the yeast two-hybrid screen, Mh3405c overexpression plasmids for *M. marinum*, and bacterial expression plasmids for recombinant Mh3405c protein. Also shown are the primers used to amplify upstream (US) and downstream (DS) regions of Mh3405c required to make the deletion strain.

recovery time was added increasing transformation efficiency and yielding 359 colonies on 50 plates (Table 4.2). By PCR, sequencing and yeast colony hybridization these 369 colonies pulled out using the full-length N-WASP bait belonged to 21 distinct classes. Of these, ten candidates had sequences that had >15 amino acids in-frame with the yeast activation domain, and had a *M. marinum* sequence that has a start codon, i.e. predicted to be an expressed protein (Table 4.3). Intriguingly, several of these candidates were in PPE8, a gene of which there are two copies in the *M. marinum* genome and a member of a large family that comprises ~2% (68/4000) of *M. tuberculosis* genome. These proteins have been localized to cell surface (21). Although their function is unknown, it has been suggested that they may play a role in inhibition of antigen processing and antigenic variation (18,19). None of these 10 candidates activated reporter genes when transformed into yeast alone (Table 4.4). However, all but one of the candidates activated the reporter when mated with yeast containing the binding domain alone (Table 4.4) suggesting that PPE8 family was a class of false positives in our yeast two-hybrid screen.

The single candidate (Class IV) that interacted specifically with full-length N-WASP contains all but the first nine amino acids from a 21-kDa (191 amino acid) protein from *M. marinum* named Mh3405c since it is homologous to *M. tuberculosis* Rv3405c (Figure 4.1). Rv3405c is annotated in the *M. tuberculosis* genome as a "possible transcriptional regulatory protein" because it contains a weak helix-turn-helix motif. For Mh3405c, the helix-turn-helix domain begins at amino acid 15 and has a 50% probability of binding DNA using the Network Protein Sequence Analysis (http://npsa-pbil.ibcp.fr/). In the *M. marinum* genome, the genes flanking Mh3405c, Mh3401 and Mh3406, are speculated to be involved in metabolic processes. Interestingly, the *M.*

	Screen 1	Screen 2
Efficiency (CFU/μg)		
Bait Transformation	5.8×10^3	1.6×10^7
Library Transformation	6.0×10^3	9.8×10^6
Co-transformation	1.7×10^4	2.5×10^4
Clones screened	4.2×10^6	1.2×10^7
Colonies on 50 plates	10	359

Table 4.2 Yeast two-hybrid screen efficiency results. Full-length N-WASP was used as bait, and efficiency was determined using nutritional selection. Compared to Screen 1, Screen 2 utilized twice the DNA and an additional recovery time.

Class	*M. tuberculosis* homologue	Description
II	Rv1629	Polymerase/Conserved Hypothetical
III	Rv0355	PPE8a
IV	Rv3405c	Transcriptional/Conserved Hypothetical
VII	Rv0885	TM protein/Conserved Hypothetical
XI	Rv0355	PPE8b
XV	Rv2572c	tRNA synthetase
XVII	Rv2572c	Conserved Hypothetical
XVIII	Rv3449	Membrane-anchored Mycosin
XX	Rv1722	Possible Carboxylase
XXI	Rv0355	PPE8a

Table 4.3 Preliminary candidate classes from the yeast two-hybrid screens. The candidates from the screens were grouped by class (I-XXI) based on their sequence. The above classes were considered further because of their in-frame sequence and prediction to be translated. Additionally, their *M. tuberucolosis* homologue and description are shown.

	-L	-L-H-A	-L-T	-L-T-H-A	Conclusion
pCL1	+	+	NA	NA	Control
T/LAM	+	-	+	-	Control
T/53	+	-	+	+	Control

	-L	-L-H-A	-L-T (BD)	-L-T-H-A (BD)	-L-T (N-WASP)	-L-T-H-A (N-WASP)	Conclusion
AD	+	-	+	-	+	-	Control
II	+	-	+	+	+	+	BD interaction
III	+	-	+	+	+	+	BD interaction
IV	+	-	+	-	+	+	Good
VII	+	-	+	+	+	+	BD interaction
XI	+	-	+	+	+	+	BD interaction
XV	+	-	+	-	+	+/-	Weak interaction?
XVII	+	-	+	+	+	+	BD interaction
XVIII	+	-	+	+	+	+	BD interaction
XX	+	-	+	+	+	+	BD interaction
XXI	+	-	+	+	+	+	BD interaction

Table 4.4 Validation of specific interactions with full-length N-WASP. Control plasmids or plasmids isolated from the classes were transformed into yeast to validate a specific interaction by mating with yeast containing BD or BD with full-length N-WASP (N-WASP). Nutritional selection was used for prey (-leucine, -L), bait (-tryptophan, -T), and reporter activation (-histidine-adenine, -H-A). Only Class IV had a specific interaction.

```
                                                -------HTH motif------

Mh3405c         VTTGSAIRSRKTPTGREEVAAAVLEAAADLFAERGPAATSIRDIAARSKVNHGLVFRHFG 60
Rv3405c         MTTRPATDRRKMPTGREEVAAAILQAATDLFAERGPAATSIRDIAARSKVNHGLVFRHFG 60
                :** .*   ** **********:*:**:********************************

Mh3405c         AKEQLVGAVLDYLGTHLTELLRAGTPADDLERALDRQMRVWARTLLDGYPAEQLQTRFPN 120
Rv3405c         TKDQLVGAVLDHLGTKLTRLLHSEAPADIIERALDRHGRVLARALLDGYPVGQLQQRFPN 120
                :*:********:***:**.**:: :*** :******: ** **:******. *** ****

Mh3405c         VAELLGQVRVHHGDDTTARLAVANAIALRLGWRLFEPMLRSATGLDELADADLRQAVTDE 180
Rv3405c         VAELLDAVRPRYDSDLGARLAVAHALALQFGWRLFAPMLRSATGIDELTGDELRLSVNDA 180
                *****. ** ::..*  ******:*:**::***** ********:***:. :** :*.*

Mh3405c         VARIIEPSGRG 191
Rv3405c         VARILEPH--- 188
                ****:**
```

Figure 4.1 Mh3405c aligns with Rv3405c. Using CLUSTAL W (1.82) multiple sequence alignment, Mh3405c and Rv3405c are very similar and both contain a weak helix-turn-helix (HTH) motif at their N terminus. All but the first nine amino acids of Mh3405c are present in Class IV.

marinum region is missing two *M. tuberculosis* genes of unknown function Rv3402c and Rv3403c.

The interaction between the Class IV insert with the AD and the full-length N-WASP, with the BD was confirmed by β-galactosidase activity, although quantitatively it was about half of the positive controls (Figure 4.2). However, Class IV did not activate the reporter with WASP, mini N-WASP or mini WASP as we would predict for a true positive given our results with restoration of actin tails in N-WASP$^{-/-}$ fibroblasts (Chapter 3). When the full-length N-WASP BD and Class IV AD domains were switched, the yeast no longer grew on high stringency nutritional selection indicating that the interaction between in the system was due to artifact. In addition, when full-length N-WASP with the BD was tested with the full-length Mh3405c including the first nine amino acids with the AD, the yeast again did not grown on minimal media (data not shown). Preliminary assays to assess a protein-protein interaction by co-immunoprecipitation with *in vitro* transcribed and translated proteins, tranfected cell lysates, and recombinant protein were unsuccessful (data not shown).

Since *M. marinum* grown in macrophages but not in broth culture could form actin tails in cell extracts (Chapter 2) we hypothesized that the gene required for actin polymerization may be upregulated intracellularly, and tested this hypothesis by overexpressing untagged or tagged Mh3405c in *M. marinum* (Table 4.1). Western blot and fluorescent microscopy confirmed the presence of the tagged strains in transformed mycobacteria (data not shown). Subcellular fractionation demonstrated that his-tagged Mh3405c was both in the cytoplasm and the cell wall (Figure 4.3). However, *M. marinum* overexpressing Mh3405c were not able to form tails in cell extracts (data not shown).

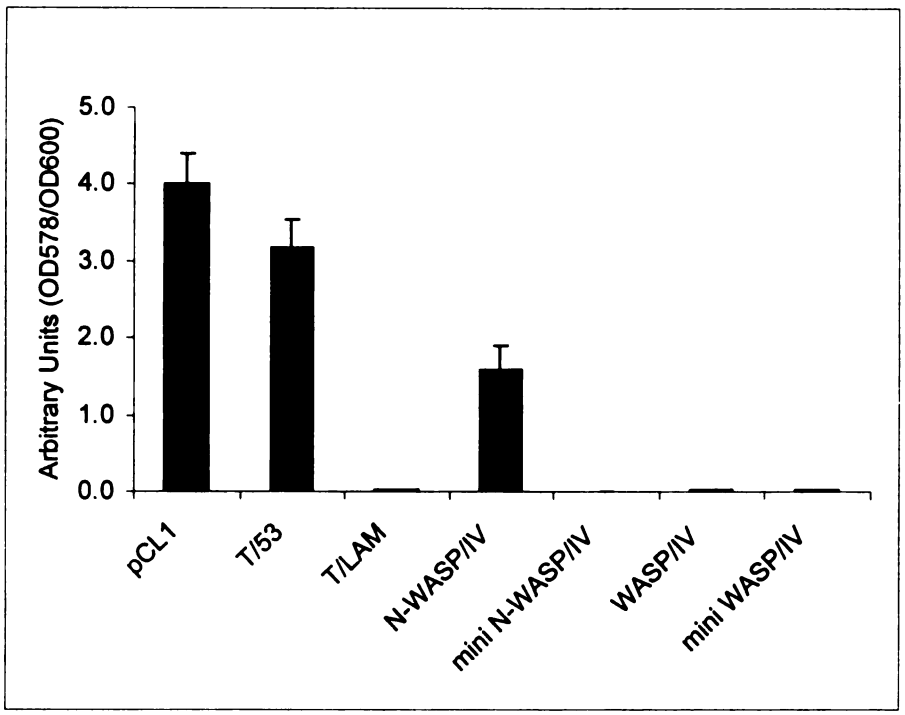

Figure 4.2 Class IV activates full-length N-WASP by β-galactosidase assay. Positive (pCL1 and T/53) and negative (T/LAM) controls and Class IV were tested for activation of the β-galactosidase reporter. Class IV induced β-galactosidase production with full-length N-WASP but not with other bait plasmids.

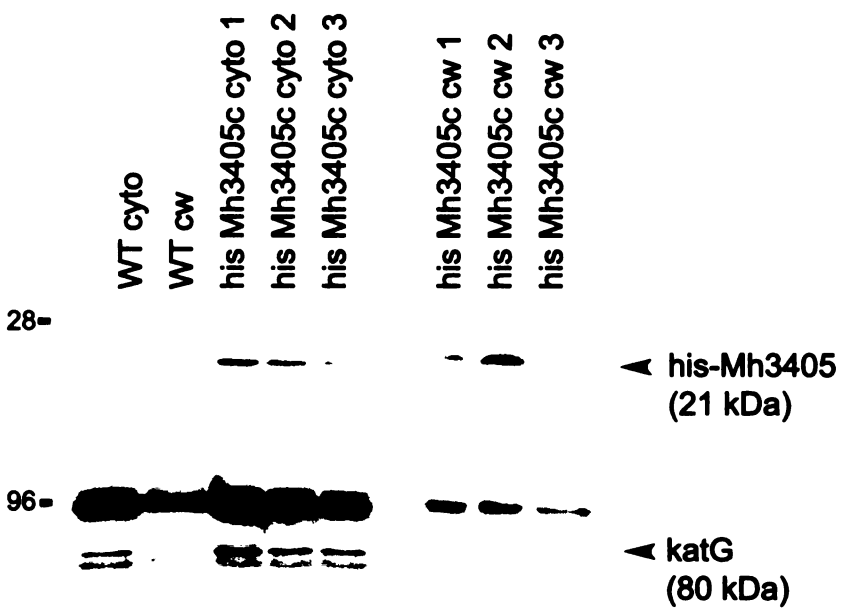

Figure 4.3 Overexpressed Mh3405c is in the cytoplasm and in the cell wall. Either wild type (WT) *M. marinum* or *M. marinum* overexpressing his-tagged Mh3405c were lysed and separated into cytoplasmic (cyto) or cell wall (cw) fractions. These fractions were resolved by SDS-PAGE, and analyzed by Western blot. The top row was blotted for the his tag, and the bottom panel was blotted for katG, a cytoplasmic enzyme.

For evaluation of its ability to polymerize actin *in vitro*, recombinant Mh3405c was made (Table 4.1 and Figure 4.4A). Although this protein was difficult to maintain in a soluble form, we tested recombinant Mh3405 in a pyrene assay. Control IcsA and EspFu proteins were able to induce actin polymerization using ΔWH1 N-WASP and the Arp2/3 complex consistently in multiple experiments, but Mh3405c was not (Figure 4.4B). However, it is difficult to estimate the actual concentration within an experiment because of the insolubility of the protein.

To definitively determine the role of Mh3405c in *M. marinum* actin-based motility we generated a deletion strain that replaced Mh3405c with the kanamycin gene (Table 4.1). The strain was confirmed by PCR on both sides of the insert to ensure that it represented a double-crossover event. The Δ*Mh3405c* strain grew like wild type *M. marinum* in broth culture (data not shown) and within macrophages (Figure 4.5A). However, it also formed actin tails like wild type when stained with phalloidin (Figure 4.5B). Taken together, this single candidate from the yeast two-hybrid screen is unlikely to be involved in actin polymerization. It is most likely that the interaction of Class IV with full-length N-WASP was due to an artifact, particularly in light of the fact that the swapping of the BD and AD domains led to a loss of interaction in yeast, and that full-length Mh3405c fused to the AD did not interact with full-length N-WASP. Its annotation as a transcription factor may be correct, due to its helix-turn-helix motif. If so, this transcription factor is not required for growth in 7H9 broth or in macrophages. Importantly, data from Chapter 3 acquired long after the initiation of this screen suggests that the *M. marinum* molecule(s) involved may be, in fact, lipid(s). This, of course,

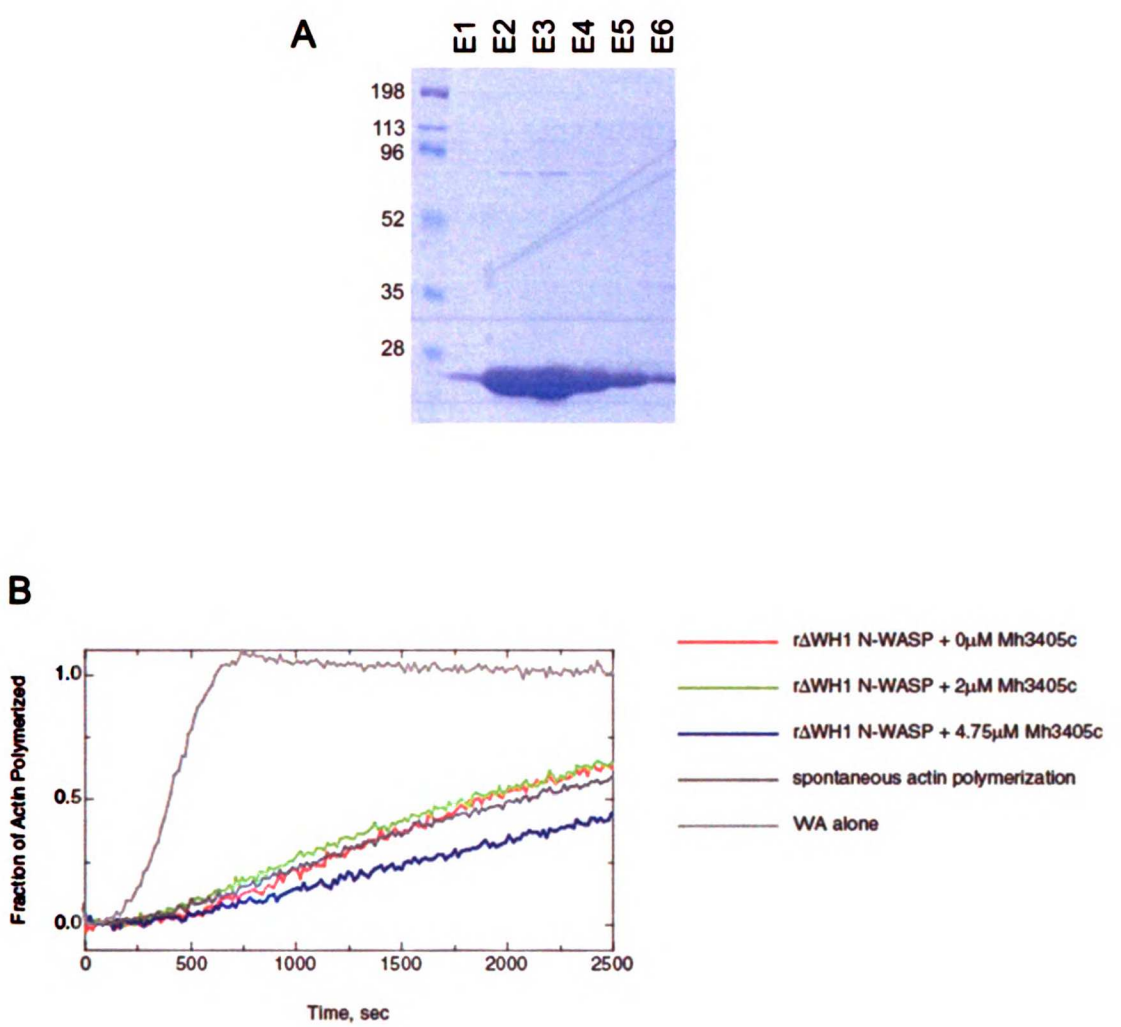

Figure 4.4 Recombinant Mh3405c does not induce actin polymerization.

(A) Recombinant his-tagged Mh3405c (21 kDa) was purified from a nickel column and a coomassie-stained gel of clean elution fractions (E1-E6) is shown. (B) Mh3405c was added with recombinant ΔWH1 N-WASP and Arp2/3 complex in a pyrene assay to measure its effect on *in vitro* actin polymerization. The WA domain of N-WASP is shown as a positive control.

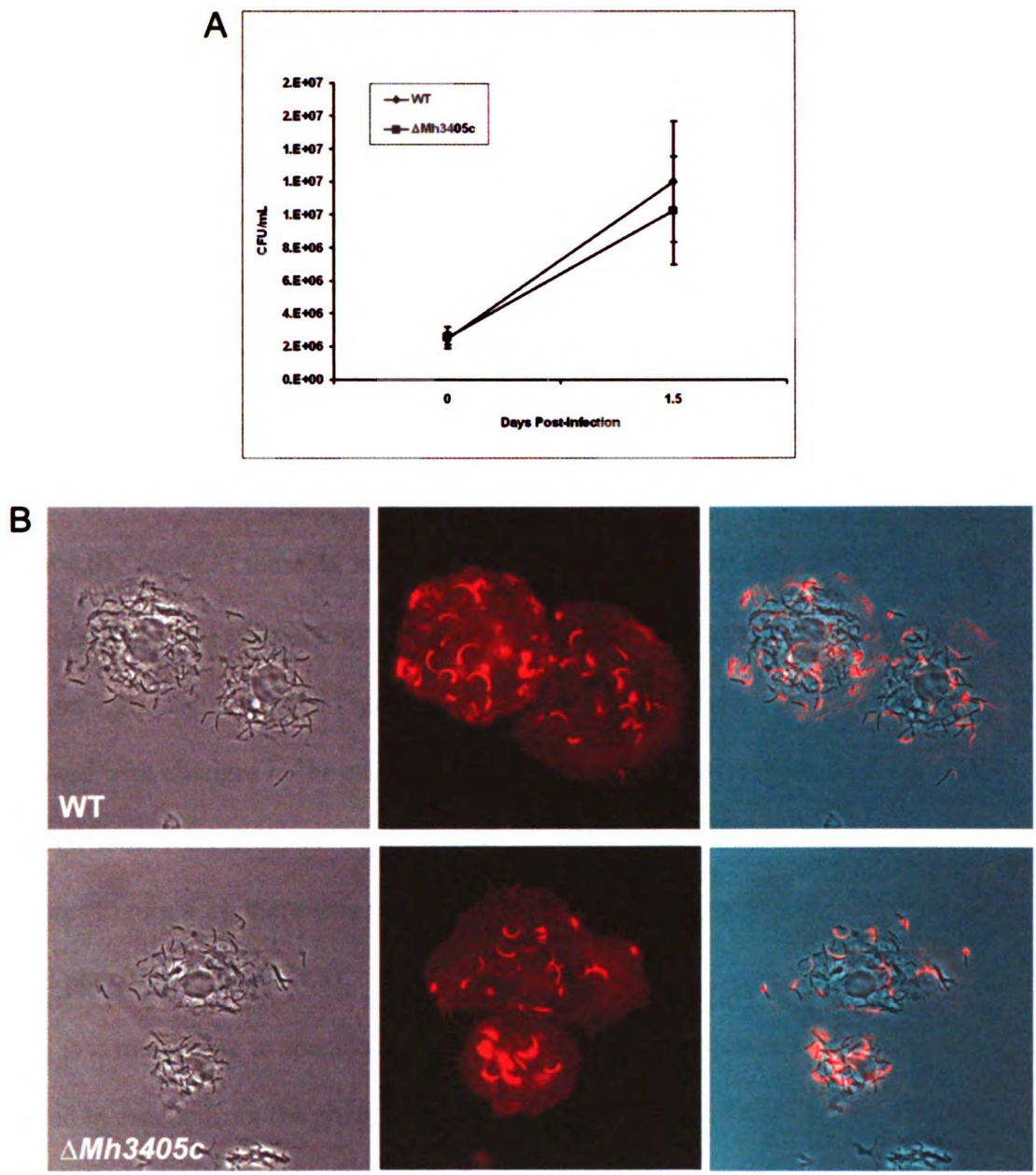

Figure 4.5 Δ*Mh3405c* grows well and forms actin tails in macrophages.

(A) Macrophages were infected with wild type (WT) or Δ*Mh3405c M. marinum* and assessed for growth. The data are representative of two experiments. (B) Infected cells (phase contrast shown in left panel) were fixed and stained for actin (shown in red in middle panel). An overlay of the fluorescence on the phase contrast is shown in the right panel.

provides an explanation for the failure of the yeast-two-hybrid screen, a technique which relies upon a direct protein-protein interaction.

Role of the RD1 Region in Phagosome Escape

An *M. marinum* transposon library comprised of approximately 1,000 mutants was preliminarily screened for defects in photochromogenicity, intracellular growth and hemolysis (9-11). Interestingly, most of the mutants that lacked hemolysis had insertions within the RD1 region that is highly conserved between *M. marinum* and *M. tuberculosis* (Figure 4.6). Some of these *M. marinum* mutants and the ΔRD1 mutant (35) had alterations in colony morphology compared to the rough colonies of the wild type strain grown on agar (Table 4.5 and Figure 4.7). Smooth colonies have been shown to be associated with changes in the cell wall and with attenuated growth in cells (127,128). Although some RD1 mutants had decreased growth in macrophage at 30 hours post-infection (Figure 4.8), there was no correlation between the morphology and attenuated growth phenotypes (Table 4.5).

It is interesting to speculate that RD1-dependent secretion of factors may be involved in escape from the phagosome, so we tested the RD1 mutants with respect to actin tail formation. At 20 hours post-infection all RD1 mutant-infected cells had less actin tails than wild type infected cells suggesting that this region is important in efficient phagosome escape and actin polymerization (Figures 4.9 and 4.10). However, by 30 hours post-infection, all of the mutants except for the ΔRD1 and *Mh3881c*::Tn formed actin tails like wild type (Figures 4.9 and 4.10). These two mutants were the most defective for growth in macrophages (Figure 4.8), and perhaps they were unable to form

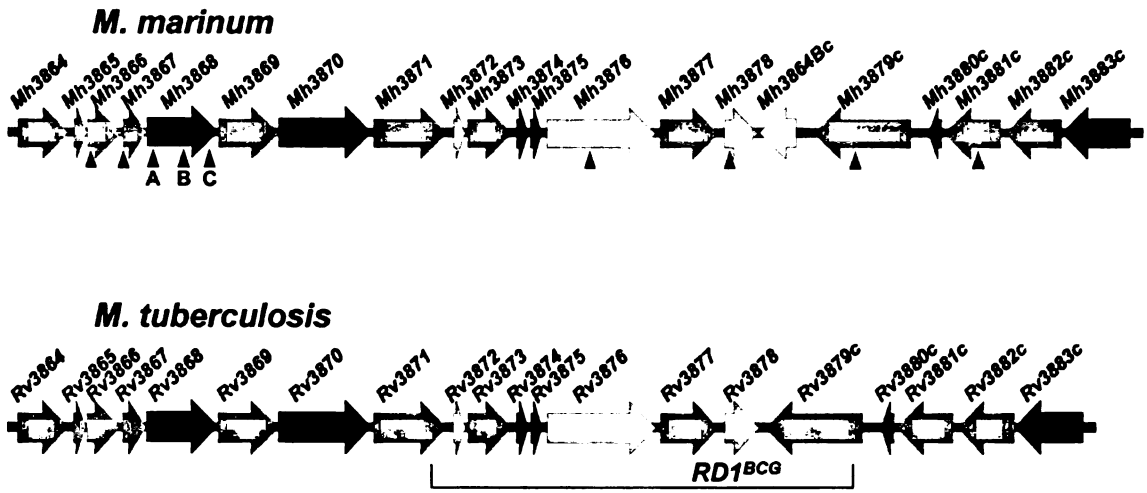

Figure 4.6 The RD1 region is conserved between *M. marinum* and *M. tuberculosis*. The RD1 regions of *M. marinum* and *M. tuberculosis* are shown as diagrammed in (11). The *M. marinum* ΔRD1 mutant used in this study lacks the genes indicated by the bracket (35). Transposon insertions in RD1 mutants are indicated by triangles. Colors filling the arrows are indicative of sequence similarity: black >90%, dark grey 70-89%, light grey 55-69% and open <54%.

Strain	Morphology	Growth in Cells	Actin Tails
WT	Rough	+	+
ΔRD1	Smooth	-	-
Mh3866::Tn	Rough	+	+
Mh3867::Tn	Smooth	+	+
Mh3868A::Tn	Rough	+	+
Mh3868B::Tn	Smooth	-	+
Mh3868C::Tn	Rough	-	+
Mh3876::Tn	Rough	-	+
Mh3878::Tn	Smooth	+	+
Mh3879c::Tn	Smooth	+	+
Mh3881c::Tn	Smooth	-	+/-

Table 4.5 Summary of RD1 mutant phenotypes. Morphology, intracellular growth and ability to form actin tails was assessed for wild type (WT) and the RD1 mutant strains. The data summarized here are presented in detail in Figures 4.7, 4.8, 4.9, and 4.10.

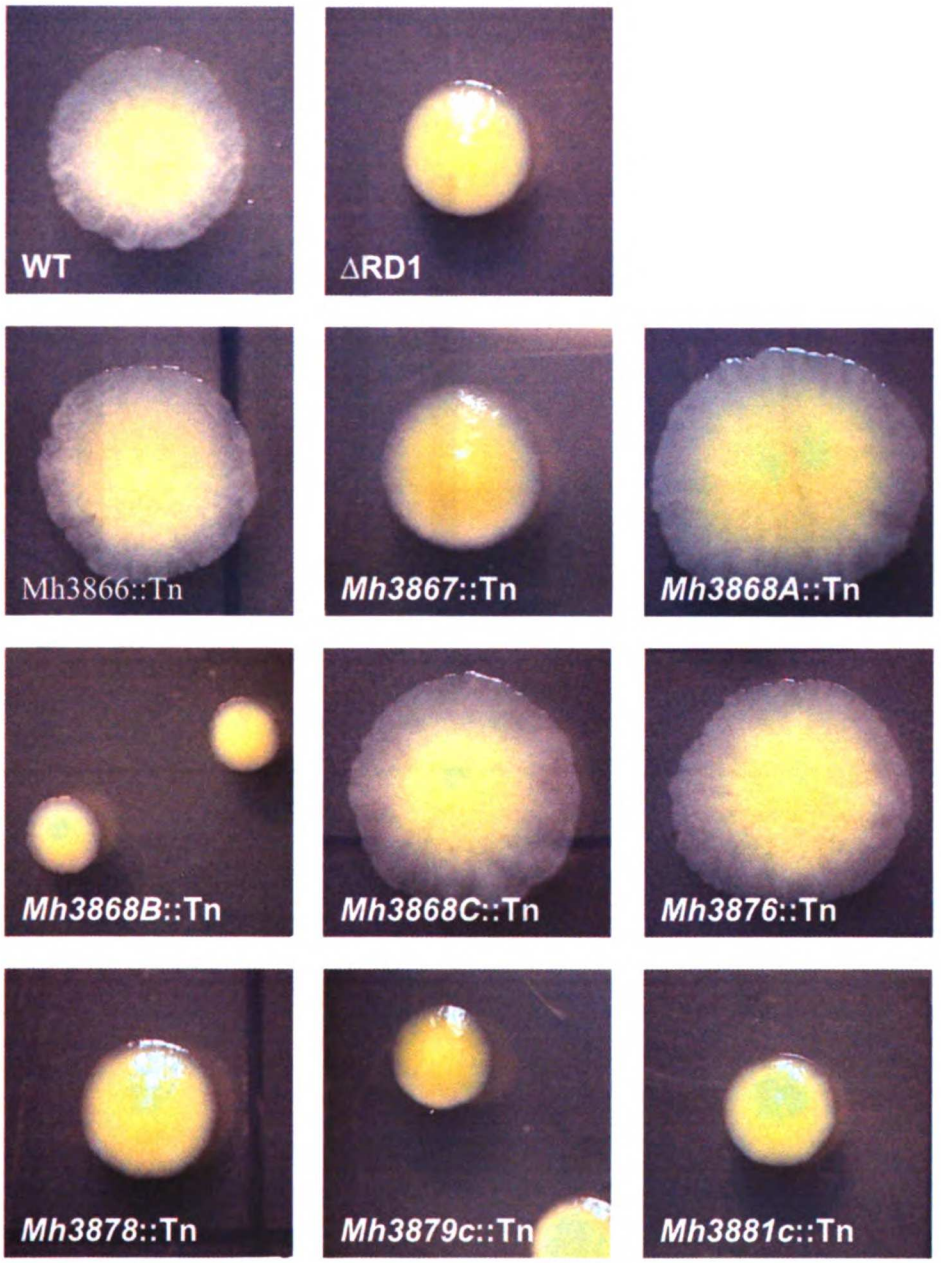

Figure 4.7 RD1 mutants have altered colony morphology. Wild type (WT) *M. marinum* and RD1 mutants were grown on 7H10 agar, and colony morphology was documented.

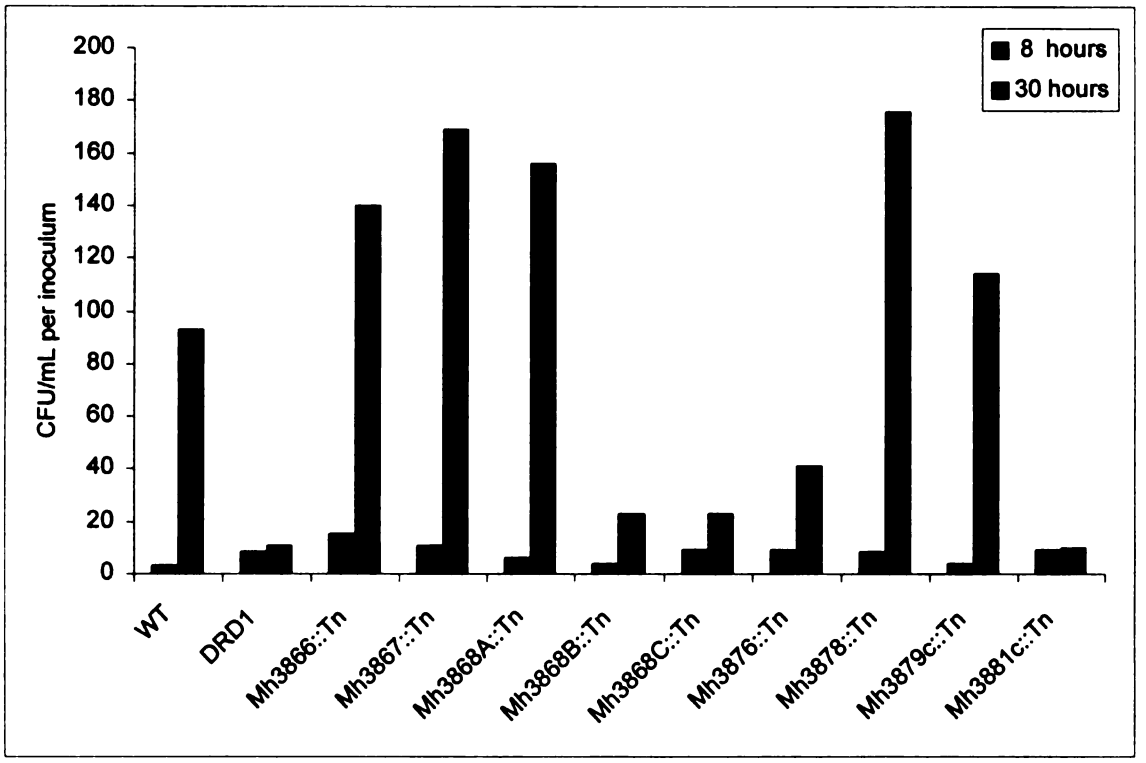

Figure 4.8 RD1 mutants are attenuated for growth in macrophages. Macrophages were infected with the wild type (WT) *M. marinum*, or RD1 mutant strains and intracellular growth was quantitated. At 8 and 30 hours post-infection, infected macrophages were lysed and plated on 7H10 in serial dilutions. Colony forming units per mL of suspension were standardized to the original inoculum.

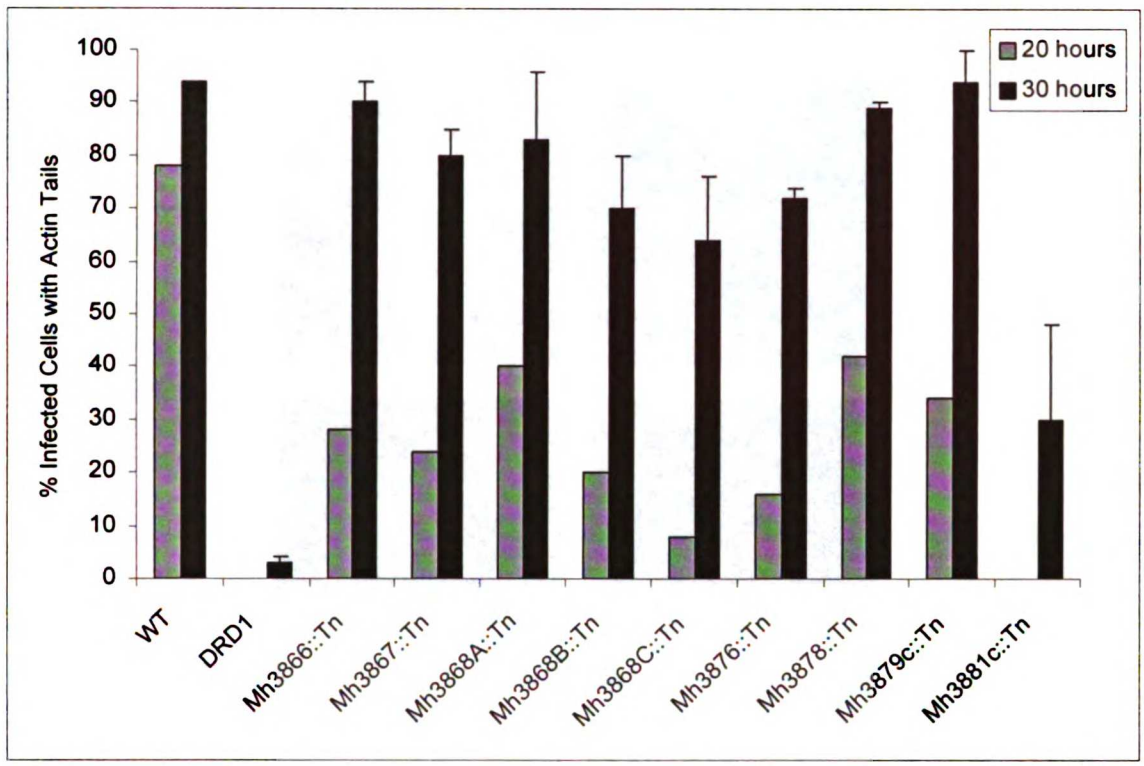

Figure 4.9 RD1 mutants have decreased and delayed actin tail formation.

Macrophages were infected with wild type (WT) and RD1 mutant strains and stained for F-actin 20 and 30 hours post-infection. The percentage of infected cells with actin tails was quantified. Fifty cells were counted per experiment; the 30-hour time point was done twice and the mean $\pm$ SEM is shown for the data set.

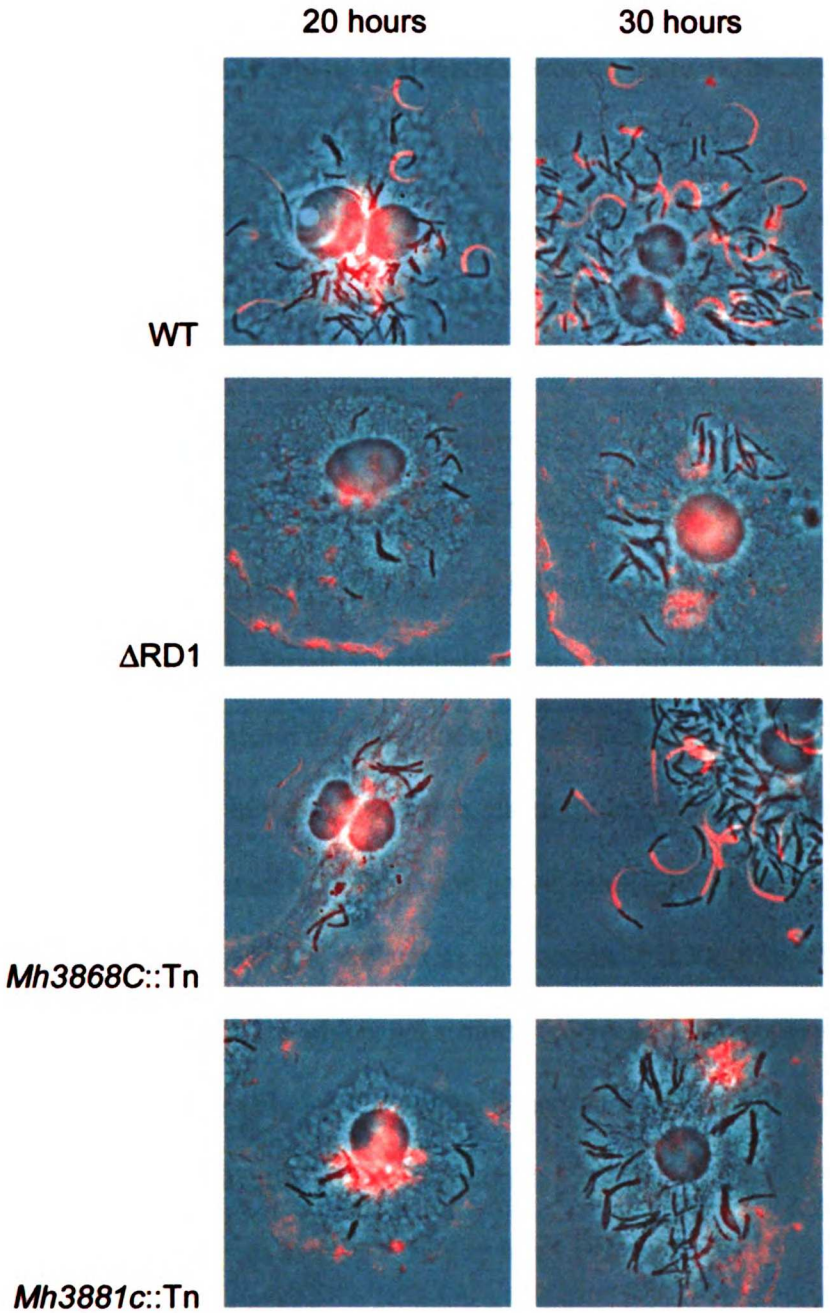

Figure 4.10 Actin staining shows defective tail formation by RD1 mutants.

Macrophages were infected with wild type (WT) *M. marinum*, and RD1 transposon mutants as in Figure 4.9. Representative images of actin (red) overlaid on phase contrast are shown.

actin tails because they were dead, similar to heat-killed bacteria (Chapter 2). However, this is unlikely to be a complete explanation because there are several mutants that also did not grow well (i.e., *Mh3868*B::Tn, *Mh3868*C::Tn, *Mh3876*::Tn, Figure 4.8) that were fully capable actin tail formation (Figures 4.9 and 4.10). It is possible that ΔRD1 and *Mh3881c*::Tn are unable to prevent phagosome acidification and that the *M. marinum* protein required for escape cannot function in that compartment, similar to the case of *Listeria* where LLO has a strict pH optimum (129).

We also tested *M. ulcerans* isolates for their ability to form actin tails in primarily infected cells. All African, Malaysian and Australian *M. ulcerans* strains have deletions in the RD1 region (P.L. Small, unpublished results). Strain 1615A is a spontaneous variant of an African strain that also does not secrete ESAT-6 or CFP-10 that has a spontaneous deletion in the mycolactone plasmid. In contrast, strain 5143 is from Mexico, and has an intact RD1 locus and grows intracellularly because it has a deletion in the giant plasmid encoding mycolactone production. Like the Tn119 strain shown in Chapter 2, neither of these additional strains, 1615A or 5143, formed actin tails in infected macrophages (Figure 4.11) suggesting that other genetic differences outside the RD1 region are responsible the for the phenotypic differences between *M. marinum* and *M. ulcerans* with respect to their ability to form actin tails.

In addition to their defects in hemolysis, the *M. marinum* RD1 mutants are also defective when assayed for phospholipase activity (L.Y. Gao, unpublished results). Because of this and because phospholipases have reported roles in the phagosomal escape of other pathogens, we tested a Δ*plc* mutant *M. marinum* strain for actin tail formation in macrophages. This strain had colony morphology similar to wild type, grew well

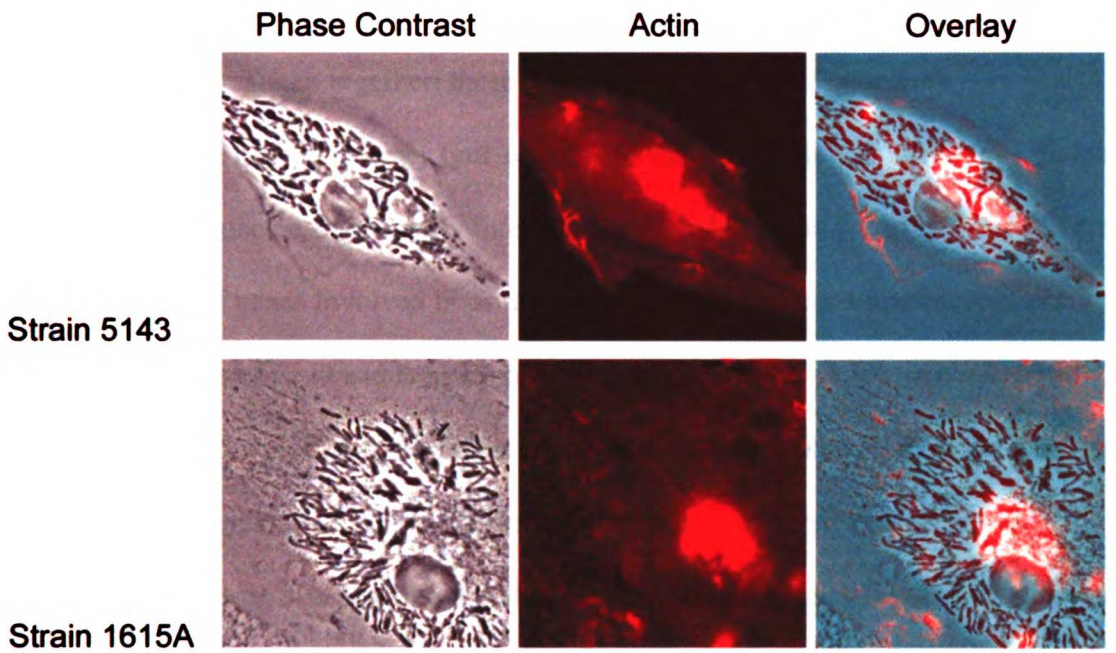

Figure 4.11 The RD1 region has no effect on *M. ulcerans* actin tail formation.

Macrophages were infected with *M. ulcerans* strain 5143 which has intact RD1 region and strain 1615A which has deletions in the RD1 region. Cells were fixed and stained with for actin 5 days post-infection. Phase contrast, actin and overlay images are shown.

intracellularly in the first 30 hours post-infection and formed tails equivalently to wild type (Figure 4.12). Taken together, these data suggest that the *M. marinum* phospholipases are not the primary lytic effector of the RD1 region required for efficient escape of the phagosome in primarily infected macrophages. It is possible that there are two distinct sets of genes involved in primary and secondary phagasome escape, similarly to the distinct roles of LLO and the phospholipases C in *Listeria* (130). Although not absolutely required, the RD1 region most likely is involved at some level in the first step since the RD1 mutants have delayed actin tail formation compared to wild type *M. marinum*. In addition, it is possible that the RD1 region and phospholipases may have a role in *M. marinum* escape from the double membrane of secondarily infected cells. In fact, some of the RD1 mutants and the Δ*plc* mutant have small fluorescent foci of infection in an adapted plaque assay indicative of defective intercellular spread ((11), L.Y. Gao, unpublished results). Further microscopic studies are needed to confirm that these mutants are trapped within double membranes in secondarily infected cells.

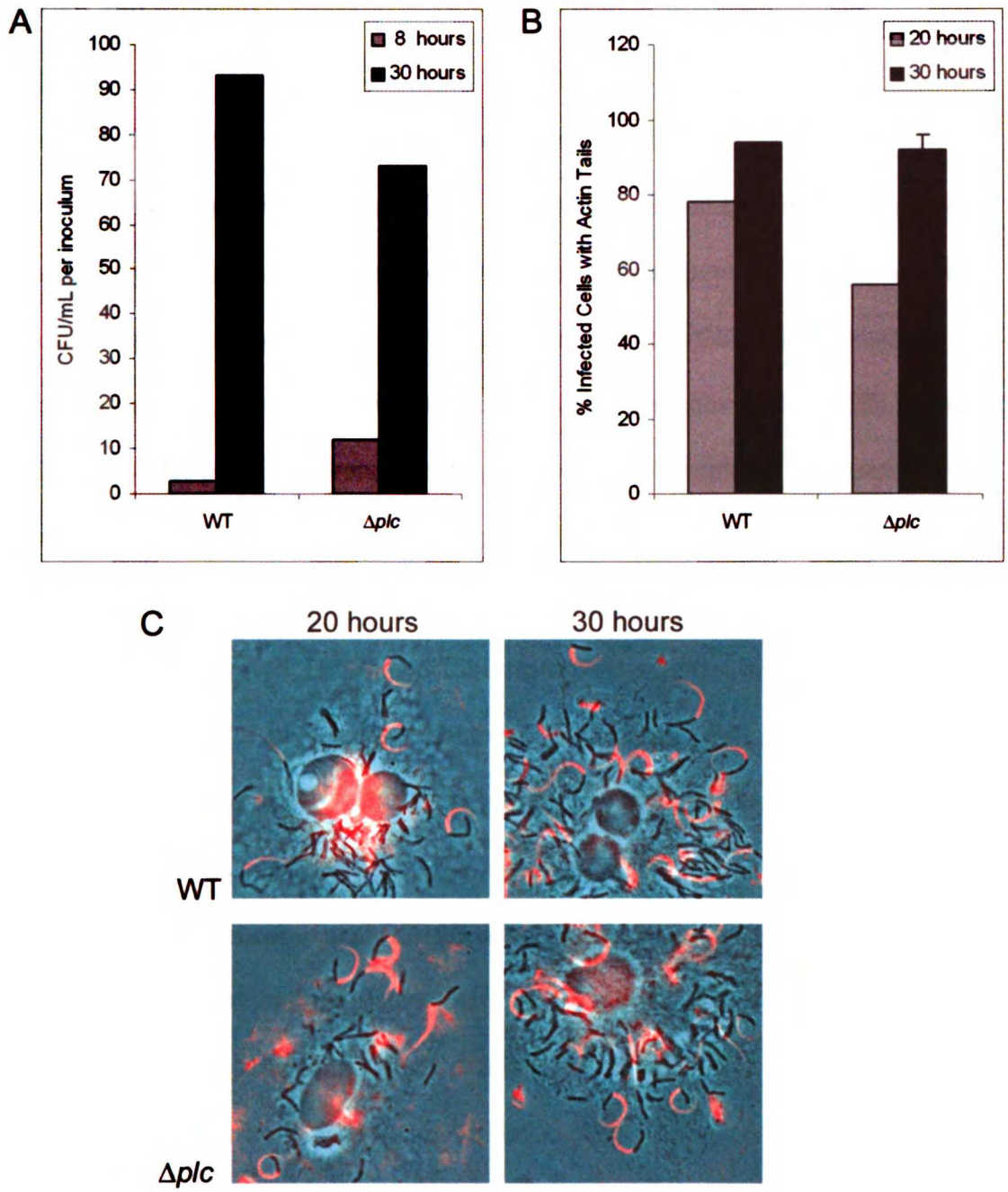

Figure 4.12 *Δplc* strain is similar to wild type in primarily infected macrophages. Macrophages were infected with wild type (WT) and *Δplc M. marinum*. (A) At 8 and 30 hours post-infection, intracellular bacterial growth was measured. (B) At 20 and 30 hours post-infection, the percentage of infected cells with actin tails was quantified. (C) Infected macrophages stained for actin are shown in an overlay on phase contrast.

Materials and Methods

M. marinum *Genomic Prey Library and Yeast Two-Hybrid Baits*

To isolate genomic DNA, log-phase *M. marinum* (Strain M) were freeze-thawed and the cell wall treated with organic extraction (chloroform/methanol, 2:1) followed by enzymatic degradation by lysozyme. Proteinase K and Phenol/Chloroform/Isoamyl alcohol were used to remove proteins and cellular debris from the resultant DNA, and CTAB was used to precipitate contaminating carbohydrate complexes. Genomic DNA was precipitated with isopropanol and resuspended in TE.

To increase the complexity of the library, the *M. marinum* genomic DNA was partially digested with AciI, HinPI, and TaqI, restriction enzymes compatible with the ClaI site in the pGADT7 prey vector (Clontech). Partially digested genomic DNA was size-selected in a range from ~1-4 x 10^3 bp by cutting out of an agarose gel, and ligated overnight into ClaI-digested, phosphatase-treated pGADT7. The ligation products were transformed into electrocompetent DH10B cells (a methylase/restriction-deficient strain) and 2.5x 10^5 total colonies were plated (7x10^3 cfu/150mm plate x 35 plates). The plasmid DNA was prepared using NucleoBond plasmid purification kit (Clontech).

Bait constructs were made by amplification using polymerase chain reaction (PCR) from full-length and mini murine N-WASP and human WASP expression constructs and from *M. marinum* genomic DNA for CFP-10 using the primers described in Table 4.1. As an intermediate step, the PCR products were into pCR-Blunt II-TOPO vector using the Zero Blunt TOPO PCR Cloning Kit (Invitrogen), then cut with the appropriate enzymes and ligated into the digested, phosphatase-treated, bait plasmid

pGBKT7 (Clontech). The bait constructs were tested in the AH109 yeast strain for expression by Western blot and for autoactivation by a β-galactosidase *in vitro* assay.

Yeast Two-Hybrid Screen and Validation

Yeast two-hybrid screens were performed as per the Matchmaker GAL4 Two-Hybrid System 3 (Clontech). This kit utilitizes the yeast strain AH109 that has three reporters (histidine, adenine, and LacZ). Transformations with the bait and prey library were done simultaneously as per the protocol. Positive and negative control plasmids (pCL1, pGADT7-T, pGBKT7-53, and pGBKT7-Lam) were used to determine relative efficiencies. High-stringency screens included nutritional selection for bait (-tryptophan, -T), prey (-leucine, -L), and reporter activation (-histidine-adenine, -H-A). The phenotype of 26 candidates (10 colonies from Screen 1 and 16 colonies from Screen 2) was retested by streaking twice on -L-T, and once on –L-T-H-A. Plasmids were isolated using the YeastMaker Yeast Plasmid Isolation Kit (Clontech), and transformed into *E. coli*. The bacterial plasmids were mini-prepped (Qiagen) and sequenced using the T7 sequencing primer located within the pGADT7 plasmid. These 26 candidates contained 9 unique sequences.

The remaining 343 candidates were screened with yeast colony hybridization as per the Yeast Protocols Handbook (Clontech). In brief, colonies from a master plate were grown in broth and spotted on a Hybond N+ nylon membrane (Amersham), soaked in sorbital/EDTA/DTT and freeze-thawed. The membranes were treated with β-glucuronidase to break cell walls, and UV cross-linked. Probes based upon the 9 unique classes originally identified were labeled using the AlkPhos Direct Labeling System

(Amersham), hybridized and washed as per manufacturer's recommendations. Selection of clones that did not hybridize yielded another 12 classes of candidates by sequence analysis. To validate specific interactions of the 21 candidates with the full-length N-WASP bait, yeast mating was performed using the AD plasmids in AH109 (Mat-a yeast strain) and the BD plasmids in Y187 (Mat-α yeast strain). β-galactosidase assays were performed using CPRG as a substrate as per the Yeast Protocols Handbook.

Overexpression of Mh3405c and Recombinant Protein

Mh3405c was expressed in *M. marinum* using the pLYG206 plasmid that drives overexpression in mycobacteria using the groEL hsp60 promoter. Four different plasmids were made: Mh3405c with no tag, with a 5'V5 tag, with a 3' his tag and a 3'GFP tag (Table 4.1). *M. marinum* were transformed with plasmid as previously described (10). Cell fractionation of transformed *M. marinum* into cell wall and cytoplasmic fractions were carried out as described on the Colorado State University TB Research Materials website (http://www.cvmbs.colostate.edu/microbiology/tb/subcell.html). Approximately 10 μg of the fractions was resolved by SDS-PAGE and by Western blot with anti-V5 antibody (Invitrogen), anti-his antibody (Novagen) and anti-katG (provided by S.T. Cole) antibody as a fractionation control. Cell extract molitity studies using *Xenopus* egg extracts were done as previously published (98).

Recombinant protein was made with the pET-15b plasmid (Novagen) and the *E. coli* strain BL-21-CodonPlus (Stratagene) that has additional tRNAs for GC rich proteins. Protein was induced using 1mM IPTG for 3 hours at 37°C, and purified using the His-

Bind kit (Novagen). Eluted protein was exchange into a neutral buffer (10mM Tris, 100mM NaCl, 2mM EDTA, 2mM DTT) with a PD10 desalting column (Amersham). Pyrene assays were performed as previously described (131).

ΔMh3405c *construction and Additional* M. marinum *Mutant Strains*

The Δ*Mh3405c* strain was made using primers to amplify the 1.5 x 10^3 base-pair regions of the *M. marinum* genome upstream (US) and downstream (DS) of *Mh3405c* (Table 4.1). The resulting PCR products were ligated into pCR-Blunt II-TOPO vector using the Zero Blunt TOPO PCR Cloning Kit (Invitrogen), then cut with the appropriate enzymes and pieced together. The kanamycin resistance gene was inserted between the two cloned fragments using the EcoRV site. This insert (USkanDS) was digested and ligated to digested phosphatase-treated pLYG304, the deletion vector (11), and transformed into DH10B to accommodate the resultant large plasmid (1.5 x 10^4 bp). To select for *E. coli* with the USkanDS/pLYG304 plasmid, a two-step selection was performed: first kanamycin in the insert and then gentamycin in the vector.

USkanDS/pLYG304 with the correct sequence was transformed into *M. marinum* as previously described (11). The transformants were first selected on kan for the presence of the plasmid. Secondarily, colonies were selected on kan with sucrose since pLYG304 contains the *sacB* gene which is lethal mycobacteria in the presence of sucrose. The integration of the insert by homologous recombination via a double-crossover was confirmed by sensitivity to zeocin whose resistance gene is on pLYG304 and by two-sided PCR.

The ΔRD1 strain was kindly provided by L. Ramakrishnan (35). *M. marinum* transposon mutants in the RD1 region were identified previously, and maintained in 7H9

with kanamycin (30 μg/mL) (11). The phospholipase C mutant was constructed by L.Y. Gao and M.A. Pak in a method similar to the Δ*Mh3405c* described above. All strains were tested for intracellular growth and actin tail formation as previously described (9) (98). Briefly, macrophages derived from the bone marrow of 129Sv mice were infected with singly prepared bacteria at an multiplicity of infection of one. Cells were washed after two hours of infection at 32°C, and fixed at 20 or 30 hours post-infection. To assess intracellular growth, infected cells were lysed by 0.1% Triton-X at the indicated times and plated onto Middlebrook 7H10 agar using serially dilutions and evaluated 7-10 days later for growth.

Chapter 5

Concluding Remarks

Model for *M. marinum* Actin-based Motility

Despite the enormous burden of disease in the world caused by the genus *Mycobacterium*, molecular understanding of its pathogenesis is in its infancy. The use of *M. marinum* as a model system has recently provided insight into *M. tuberculosis* (30,31). The work in this dissertation begins to describe *M. marinum* actin-based motility, a novel process potentially involved in virulence but not yet observed with any other mycobacterial species. In the initial characterization (Chapter 2), it was determined that *M. marinum* is capable of phagosome escape and polymerize actin while free in the cytoplasm. Experiments were done to explore the mechanism by determining host factors involved (Chapter 3). These results indicate that *M. marinum* has highjacked an endogenous host signaling pathway leading to actin polymerization (Figure 5.1).

In host cells, initiation of the pathway can begin at the plasma membrane with binding of an extracellular signal, such as bradykinin, to its receptor. The receptor is phosphorylated leading to activation of the guanine exchange factors, such as those of the Dbl family, that activate the rho family of GTPases like Cdc42. GTP-bound Cdc42 together with the anionic lipid PIP_2 fully activate N-WASP at the plasma membrane leading to Arp2/3-mediated actin nucleation and polymerization, which in turn causes filopodia formation (132). M. *marinum* exploits this signaling cascade most likely at the input level, perhaps by mycobacterial lipids that mimic PIP_2 (Chapter 3). *M. marinum* activated N-WASP leads to actin nucleation that, rather than pushing the membrane and forming a filopodia, propels the bacterium through the cytoplasm. It is quite remarkable that multiple pathogens besides *M. marinum* have converged on this single pathway (43,92).

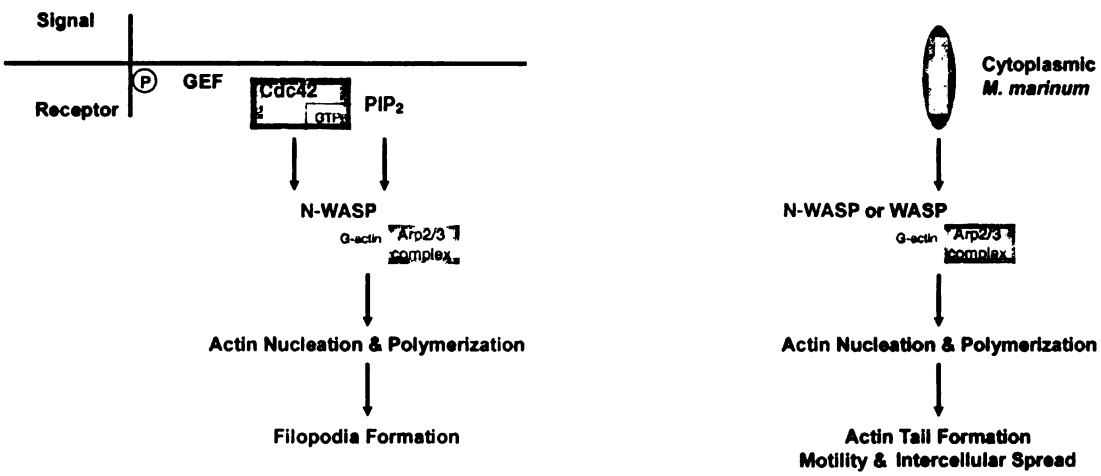

Figure 5.1 ***M. marinum*** **actin polymerization exploits a host signaling pathway.** An endogenous host signaling pathway involving GTP-Cdc42 and PIP_2 at the plasma membrane results in activation of N-WASP leading to Arp2/3-dependent actin nucleation and polymerization and filopodia formation. *M. marinum* intercepts this pathway by initiating it on the bacterial surface most likely at the level of N-WASP. Here the resultant actin polymerization leads to actin tail formation, intracellular motility and direct intercellular spread.

Based on a subtle difference in efficiency of actin tail restoration in N-WASP$^{-/-}$ fibroblasts we speculate that *M. marinum* has a higher affinity for N-WASP than WASP. In addition, a relatively small amount of N-WASP in WASP$^{-/-}$ macrophages supports 50% of the actin tail formation present in WASP$^{+/+}$ macrophages (Chapter 3). Differences between the two overall highly homologous proteins may explain this apparent variation in affinity. For example, the basic motif of N-WASP contains nine lysines whereas WASP contains six. This may be particularly relevant since we believe the basic motif to be critical in efficient *M. marinum* actin tail formation (Chapter 3). It has been shown that PIP_2-containing vesicles binding to N-WASP and motility is abrogated when the basic charge is decreased (106,110). In addition, the N-WASP acidic region, to which Arp2/3 binds, has a higher net negative charge than that of WASP, the N-WASP polyproline region is larger than that of WASP, and N-WASP has two, rather than one, verprolin actin-binding regions; all of these may contribute to the higher efficiency of N-WASP-mediated *M. marinum* actin tail formation.

Role of Actin-based Motility in *M. marinum* Pathogenicity

It is interesting to consider where and when in *M. marinum* pathogenesis actin based-motility is important, particularly since this pathogenic strategy seems to be absent in other mycobacteria including *M. tuberculosis* and *M. ulcerans*. There are two distinct possibilities: actin-based motility is utilized in the initial establishment of infection or in the persistence of infection. Comparing the lifecycle of the two pathogenic mycobacteria (Chapter 1), it is clear that *M. marinum* has less in common with *M. tuberculosis* in the early steps of infection, such as transmission, than in the later steps, such as granuloma formation. The adaptation of *M. marinum* to being a pathogen transmitted from a water source to fish may have placed a unique evolutionary pressure on the species in contrast to *M. tuberculosis* that is transmitted directly from host-to-host via the aerosol route.

Inhaled *M. tuberculosis* is most likely phagocytosed by macrophages lining the distal epithelium of the lung alveoli. These *M. tuberculosis*-infected avelolar macrophages traffic to lymph nodes and are critical for establishment of infection. In contrast, little is known regarding the establishment of *M. marinum* infection in fish. It is thought that a common mode of transmission of *M. marinum* in fish is oral, and so it is possible that *M. marinum* may utilize actin-based motility within the gut epithelia, as do the gut pathogens *Listeria* and *Shigella*. This establishment of infection within the gut of fish may be important for later systemic infection, and perhaps is required to cross the epithelial surface without the aid of lumenal macrophages. *M. marinum* infection may also be established through invasion of gill epithelia; in this case, actin-based motility could have a similar role in initiation of infection. Another intriguing possibility is that *M. marinum*-infected amoebae are a vector in fish infection; if so, *M. marinum* might use

actin based motility to escape from amoebae into fish cells in proximity. Use of actin-based motility for intercellular spread between macrophages either during establishment of systemic infection or within a granuloma later in infection also remains possible. Clearly, more must be learned about *M. marinum* transmission and infection before these hypotheses can be tested adequately.

At the cellular level, only a portion of intracellular *M. marinum* ever produces actin tails, and whether this is because only this minority escapes phagosomes is not certain (Chapter 2). Electron microscopy has shown that even at times when bacteria are cytoplasmlic, there are still many within phagosomes. Perhaps only some of the intracellular bacterial population may express the molecules necessary for actin polymerization, as these apparently are induced during intracellular infection. If the *M. marinum* actin polymerizing activity is a lipid, it may be accessibility rather than expression that is regulated during intracellular infection. For other species, actin-based motility is used as a way to spread from cell to cell directly without being exposed to the extracellular milieu. One may speculate that the heterogeneity of intracellular *M. marinum* may be part of a strategy on the part of the organism to maintain viable bacteria in several intracellular compartments, perhaps as a way of foiling specific host defense strategies.

Of course, the role of actin-based motility will be most directly addressed when the molecule(s) have been identified, and the phenotypes of the deletion mutants are evaluated *in vivo* using the established zebrafish model (11,133). These experiments would also be informative to understand the disease caused by *M. marinum* in its natural host, and to test some of the above hypotheses. For example, one could assess a mutant's

ability to establish infection following various routes of bacterial delivery; Attenuation following oral, but not intraperitoneal, administration would support that *M. marinum* actin polymerization is important in penetrating gut epithelial layers. In addition to *in vivo* studies, it would be important to look for the presence, sequence and expression of the *M. tuberculosis* homologue to understand if actin polymerization has relevance to tuberculosis in humans that has never been appreciated.

Future Directions

Testing Mycobacterial Lipids in Pyrene Assays

The microbial molecules required for *M. marinum* phagosome escape, actin-based motility, and intercellular spread remain to be elusive (Chapter 4). Future directions for related research focus on identifying these factors. Results with reconstitution of N-WASP$^{-/-}$ fibroblasts indicate that the basic region of N-WASP is required for M. marinum actin tail formation (Chapter 3). Because host cell lipids bind to this area, it would be interesting to test if *M. marinum* lipids activate N-WASP-dependent actin polymerization in vitro in a pyrene assay. To start, mycobacterial lipids could be extracted from broth-grown bacteria gently by using glass beads or more aggressively by incubating in Tween 80. These two techniques to isolate surface and capsular lipids, respectively, have been used to identify phosphatidylinositol mannosides, potential candidates for binding to the N-WASP basic motif (112). It would also be possible to use more complete extraction procedures, such as treatment with hexane, which removes most non-covalently bound lipids. However, our data have shown that broth-grown bacteria do not form tail in extracts (Chapter 2), and it will be a challenge to isolate mycobacterial lipids away from host cell lipids from bacteria grown intracellularly.

Transposon mutagenesis

To identify *M. marinum* molecules involved in actin tail formation, one could use efficient mutagenesis of the genome with a mariner-based transposon system adapted for use in *M. marinum* on our lab (9). Following creation of a saturating library, mutants could be screened for a loss of function microscopically by staining infected

macrophages for F-actin with phalloidin and evaluating mutants for the inability to form tails. The screen of individual mutants would be rather labor intensive, but necessary as mycobacteria grown together form clumps and pooling of mutants could lead, even at low multiplicities of infection, to failure to discover individual mutants that do not to polymerize actin in the assay. Alternatively, one could assay individual mutants for the inability to form plaques or foci of infection in cell monolayers. This approach would yield other interesting mutants such as those that do not grow intracellularly or do not escape the phagosome, in addition to those that have mutations in transcription, production and secretion of the actual factor required for actin polymerization. Either way, the original screen would require additional, secondary assays to sort through the potentially interesting, different kinds of mutants.

Expressing M. marinum *DNA in* M. ulcerans

M. marinum is most closely related to *M. ulcerans* (discussed in Chapter 1). However, intracellular *M. ulcerans* failed to form actin tails in all our assays (Chapters 2 and 4). One approach to identifying the *M. marinum* genes involved in phagosome escape and actin polymerization would be to add the cosmid library generated by L. Ramakrishnan to *M. ulcerans* and screen transformants for their ability to form tails. The library consists of 380 cosmids harboring 30-35 kbp of *M. marinum* genomic DNA in the mycobacterial expression vector pYUB18 (29). Because the screen is based on a gain of function (actin tail formation), we need not test individual transformants and could pool them. Since it is assumed that the all non-motile intracellular *M. ulcerans* are in a membrane-bound compartment, this approach critically depends on the assumption that

the genes involved in phagsome escape and actin tail formation are together in a pathogenicity island or at least together on a cosmid. There is a precedent for this in *Listeria* where LLO, ActA and the phospholipases are all in an operon. There is an additional technical difficulty because transformation of the *M ulcerans* is known to be highly inefficient (1 CFU/μg DNA; P.L. Small, unpublished results). Alternatively, one could use subtractive hybridation to find genes present in *M. marinum* that were not in M. *ulcerans*. This technique was used to identify the polyketide locus in *M. ulcerans*, but not in *M. marinum*, that is involved in mycolactone production (134).

Biochemical approaches

Biochemical approaches to identifying the microbial molecule(s) required for *M. marinum* actin tail formation remain largely unexplored due to technical issues. Our results with the cell extract assay suggest that the protein is not expressed at a high level in broth-grown bacteria, and is upregulated in cells (Chapter 2). Therefore, for any biochemical approach, we would have to produce a large quantity of intracellularly grown bacteria. The challenge is to isolate pure bacterial molecules from cells away from host cell contaminants. If this could be achieved, perhaps by optimizing detergent conditions, it would be possible to do pull-downs or column chromatography with N-WASP to identify *M. marinum* binding partners. We attempted two biochemical approaches focusing on *M. marinum* proteins involved in actin tail formation that never succeeded. The first was to metabolically label *M. marinum* proteins induced intracellularly by adding eukaryotic protein synthesis inhibitors, cycloheximide and anisomycin, to *M. marinum* infected macrophages in the presences of ^{35}S-methionine.

This technique was previously used to identify ActA expressed by *Listeria* intracellularly (74). In addition, we tried far Western blots with tagged ΔWH1 N-WASP recombinant protein on cell wall proteins from bacteria grown in macrophages. In our hands, neither of these techniques produced reproducible results. Of course, if the relevant molecule is a lipid, these techniques would not work. Instead bacterial lipids could be labeled with acetate to try to identify lipids that interact with N-WASP. This approach would be difficult because of the notorious difficulties of establishing robust lipid binding assays *in vitro*. For this reason, an assay for functional N-WASP activation by *M. marinum* lipids, as described above, would be preferable.

Discovery of the molecule(s) involved in *M. marinum* actin polymerization by the above proposed methods or others would ultimately be useful for increasing our understanding of mycobacterial pathogenesis. In addition, it would provide insights into cell biology of the actin cytoskeleton by elucidating how another pathogen have manipulated the endogenous pathway for its own purposes.

References

1. WHO (2003) http://www.who.int/mediacentre/factsheets/fs104/en/.

2. Salo W.L., Aufderheide A.C., Buikstra J., Holcomb T.A. (1994) Identification of *Mycobacterium tuberculosis* DNA in a pre-Columbian Peruvian mummy. *Proc Natl Acad Sci U S A* 91: 2091-2094.

3. Clark H.F., Shepard C.C. (1963) Effect of environmental temperatures on infection with *Mycobacterium marinum* (balnei) of mice and a number of poikilothermic species. *J Bacteriol* 86: 1057-1069.

4. Parent L.J., Salam M.M., Appelbaum P.C., Dossett J.H. (1995) Disseminated *Mycobacterium marinum* infection and bacteremia in a child with severe combined immunodeficiency. *Clin Infect Dis* 21: 1325-1327.

5. Cole S.T., Brosch R., Parkhill J., Garnier T., Churcher C. et al. (1998) Deciphering the biology of *Mycobacterium tuberculosis* from the complete genome sequence. *Nature* 393: 537-544.

6. The Sanger Institute (2003) The *M. marinum* genome project. http://www.sanger.ac.uk/Projects/M_marinum/.

7. The Institut Pasteur (2004) . The *M. ulcerans* genome project. http://genopole.pasteur.fr/Mulc/BuruList html .

8. Tonjum T., Welty D.B., Jantzen E., Small P.L. (1998) Differentiation of *Mycobacterium ulcerans*, *M. marinum*, and *M. haemophilum*: mapping of their relationships to *M. tuberculosis* by fatty acid profile analysis, DNA-DNA hybridization, and 16S rRNA gene sequence analysis. *J Clin Microbiol* 36: 918-925.

9. Gao L.Y., Groger R., Cox J.S., Beverley S.M., Lawson E.H. et al. (2003) Transposon mutagenesis of *Mycobacterium marinum* identifies a locus linking pigmentation and intracellular survival. *Infect Immun* 71: 922-929.

10. Gao L.Y., Laval F., Lawson E.H., Groger R.K., Woodruff A. et al. (2003) Requirement for kasB in *Mycobacterium* mycolic acid biosynthesis, cell wall impermeability and intracellular survival: implications for therapy. *Mol Microbiol* 49: 1547-1563.

11. Gao L.Y., Guo S., McLaughlin B., Morisaki J.H., Engele M. et al. (2004) A mycobacterial virulence gene cluster extending RD1 is required for cytolosis, bacterial spreading, and ESAT-6 secretion. *Mol Microbiol* 53: 1677-1693.

12. Cirillo J.D., Falkow S., Tompkins L.S., Bermudez L.E. (1997) Interaction of *Mycobacterium avium* with environmental amoebae enhances virulence. *Infect Immun* 65: 3759-3767.

13. Portaels F., Elsen P., Guimaraes-Peres A., Fonteyne P.A., Meyers W.M. (1999) Insects in the transmission of *Mycobacterium ulcerans* infection. *Lancet* 353: 986-ortaels, F.

14. George K.M., Chatterjee D., Gunawardana G., Welty D., Hayman J. et al. (1999) Mycolactone: a polyketide toxin from *Mycobacterium ulcerans* required for virulence. *Science* 283: 854-857.

15. George K.M., Pascopella L., Welty D.M., Small P.L. (2000) A *Mycobacterium ulcerans* toxin, mycolactone, causes apoptosis in guinea pig ulcers and tissue culture cells. *Infect Immun* 68: 877-883.

16. Daniel A.K., Lee R.E., Portaels F., Small P.L. (2004) Analysis of *Mycobacterium* species for the presence of a macrolide toxin, mycolactone. *Infect Immun* 72: 123-132.

17. Stinear T.P., Mve-Obiang A., Small P.L., Frigui W., Pryor M.J. et al. (2004) Giant plasmid-encoded polyketide synthases produce the macrolide toxin of *Mycobacterium ulcerans*. *Proc Natl Acad Sci U S A* 101: 1345-1349.

18. Delogu G., Brennan M.J. (2001) Comparative immune response to PE and PE_PGRS antigens of *Mycobacterium tuberculosis*. *Infect Immun* 69: 5606-5611.

19. Banu S., Honore N., Saint-Joanis B., Philpott D., Prevost M.C. et al. (2002) Are the PE-PGRS proteins of *Mycobacterium tuberculosis* variable surface antigens? *Mol Microbiol* 44: 9-19.

20. Brennan M.J., Delogu G., Chen Y., Bardarov S., Kriakov J. et al. (2001) Evidence that mycobacterial PE_PGRS proteins are cell surface constituents that influence interactions with other cells. *Infect Immun* 69: 7326-7333.

21. Delogu G., Pusceddu C., Bua A., Fadda G., Brennan M.J. et al. (2004) Rv1818c-encoded PE_PGRS protein of *Mycobacterium tuberculosis* is surface exposed and influences bacterial cell structure. *Mol Microbiol* 52: 725-733.

22. Barker L.P., Brooks D.M., Small P.L. (1998) The identification of *Mycobacterium marinum* genes differentially expressed in macrophage phagosomes using promoter fusions to green fluorescent protein. *Mol Microbiol* 29: 1167-1177.

23. Ramakrishnan L., Federspiel N.A., Falkow S. (2000) Granuloma-specific expression of *Mycobacterium* virulence proteins from the glycine-rich PE-PGRS family. *Science* 288: 1436-1439.

24. Chan K., Knaak T., Satkamp L., Humbert O., Falkow S. et al. (2002) Complex pattern of *Mycobacterium marinum* gene expression during long-term granulomatous infection. *Proc Natl Acad Sci U S A* 99: 3920-3925.

25. Schaeffer M.L., Agnihotri G., Volker C., Kallender H., Brennan P.J. et al. (2001) Purification and biochemical characterization of the *Mycobacterium tuberculosis* beta-ketoacyl-acyl carrier protein synthases KasA and KasB. *J Biol Chem* 276: 47029-47037.

26. Hsu T., Hingley-Wilson S.M., Chen B., Chen M., Dai A.Z. et al. (2003) The primary mechanism of attenuation of bacillus Calmette-Guerin is a loss of secreted lytic function required for invasion of lung interstitial tissue. *Proc Natl Acad Sci U S A* 100: 12420-12425.

27. Stanley S.A., Raghavan S., Hwang W.W., Cox J.S. (2003) Acute infection and macrophage subversion by *Mycobacterium tuberculosis* require a specialized secretion system. *Proc Natl Acad Sci U S A* 100: 13001-13006.

28. Guinn K.M., Hickey M.J., Mathur S.K., Zakel K.L., Grotzke J.E. et al. (2004) Individual RD1-region genes are required for export of ESAT-6/CFP-10 and for virulence of *Mycobacterium tuberculosis*. *Mol Microbiol* 51: 359-370.

29. Ramakrishnan L., Tran H.T., Federspiel N.A., Falkow S. (1997) A crtB homolog essential for photochromogenicity in *Mycobacterium marinum*: isolation, characterization, and gene disruption via homologous recombination. *J Bacteriol* 179: 5862-5868.

30. Ramakrishnan L. (2004) Using *Mycobacterium marinum* and its hosts to study tuberculosis. *Current science* 86: 82-92.

31. Pozos T.C., Ramakrishan L. (2004) New models for the study of *Mycobacterium*-host interactions. *Curr Opin Immunol* 16: 499--505.

32. The Sanger Institute (2004) The zebrafish genome project. http://www.sanger.ac.uk/Projects/D_rerio/.

33. Trede N.S., Langenau D.M., Traver D., Look A.T., Zon L.I. (2004) The use of zebrafish to understand immunity. *Immunity* 20: 367-379.

34. Davis J.M., Clay H., Lewis J.L., Ghori N., Herbomel P. et al. (2002) Real-time visualization of mycobacterium-macrophage interactions leading to initiation of granuloma formation in zebrafish embryos. *Immunity* 17: 693-702.

35. Volkman H.E., Clay H., Beery D., Chang J.C., Sherman D.R. et al. (2004) Tuberculous granuloma formation is enhanced by a mycobacterium virulence determinant. *PLoS Biol* 2: e367.

36. Solomon J.M., Leung G.S., Isberg R.R. (2003) Intracellular Replication of *Mycobacterium marinum* within *Dictyostelium discoideum*: Efficient replication in the absence of host coronin. *Infect Immun* 71: 3578-3586.

37. Dionne M.S., Ghori N., Schneider D.S. (2003) *Drosophila melanogaster* is a genetically tractable model host for *Mycobacterium marinum*. *Infect Immun* 71: 3540-3550.

38. Russell D.G. (2001) *Mycobacterium tuberculosis*: here today, and here tomorrow. *Nat Rev Mol Cell Biol* 2: 569-577.

39. El-Etr S.H., Yan L., Cirillo J.D. (2001) Fish monocytes as a model for mycobacterial host-pathogen interactions. *Infect Immun* 69: 7310-7317.

40. Barker L.P., George K.M., Falkow S., Small P.L. (1997) Differential trafficking of live and dead *Mycobacterium marinum* organisms in macrophages. *Infect Immun* 65: 1497-1504.

41. Via L.E., Fratti R.A., McFalone M., Pagan-Ramos E., Deretic D. et al. (1998) Effects of cytokines on mycobacterial phagosome maturation. *J Cell Sci* 111 (Pt 7): 897-905.

42. Chua J., Vergne I., Master S., Deretic V. (2004) A tale of two lipids: *Mycobacterium tuberculosis* phagosome maturation arrest. *Curr Opin Microbiol* 7: 71-77.

43. Goldberg M.B. (2001) Actin-based motility of intracellular microbial pathogens. *Microbiol Mol Biol Rev* 65: 595-626, table.

44. Brzychcy M., Andrzejczyk Z., Zalewska N., Zwolska Z., Rudnicka W. (1997) Haemolytic activity of *Mycobacterium* spp. *Acta Microbiol Pol* 46: 377-385.

45. McDonough K.A., Kress Y., Bloom B.R. (1993) Pathogenesis of tuberculosis: interaction of *Mycobacterium tuberculosis* with macrophages. *Infect Immun* 61: 2763-2773.

46. Myrvik Q.N., Leake E.S., Wright M.J. (1984) Disruption of phagosomal membranes of normal alveolar macrophages by the H37Rv strain of *Mycobacterium tuberculosis*. A correlate of virulence. *Am Rev Respir Dis* 129: 322-328.

47. Teitelbaum R., Cammer M., Maitland M.L., Freitag N.E., Condeelis J. et al. (1999) Mycobacterial infection of macrophages results in membrane-permeable phagosomes. *Proc Natl Acad Sci U S A* 96: 15190-15195.

48. Clemens D.L., Lee B.Y., Horwitz M.A. (2002) The *Mycobacterium tuberculosis* phagosome in human macrophages is isolated from the host cell cytoplasm. *Infect Immun* 70: 5800-5807.

49. Schaible U.E., Winau F., Sieling P.A., Fischer K., Collins H.L. et al. (2003) Apoptosis facilitates antigen presentation to T lymphocytes through MHC-I and CD1 in tuberculosis. *Nat Med* 9: 1039-1046.

50. Flynn J.L., Goldstein M.M., Triebold K.J., Koller B., Bloom B.R. (1992) Major histocompatibility complex class I-restricted T cells are required for resistance to *Mycobacterium tuberculosis* infection. *Proc Natl Acad Sci U S A* 89: 12013-12017.

51. Mazzaccaro R.J., Gedde M., Jensen E.R., van Santen H.M., Ploegh H.L. et al. (1996) Major histocompatibility class I presentation of soluble antigen facilitated by *Mycobacterium tuberculosis* infection. *Proc Natl Acad Sci U S A* 93: 11786-11791.

52. Ramirez M.C., Sigal L.J. (2004) The multiple routes of MHC-I cross-presentation. *Trends Microbiol* 12: 204-207.

53. Gedde M.M., Higgins D.E., Tilney L.G., Portnoy D.A. (2000) Role of listeriolysin O in cell-to-cell spread of *Listeria monocytogenes*. *Infect Immun* 68: 999-1003.

54. Barzu S., Benjelloun-Touimi Z., Phalipon A., Sansonetti P., Parsot C. (1997) Functional analysis of the *Shigella flexneri* IpaC invasin by insertional mutagenesis. *Infect Immun* 65: 1599-1605.

55. Raynaud C., Guilhot C., Rauzier J., Bordat Y., Pelicic V. et al. (2002) Phospholipases C are involved in the virulence of *Mycobacterium tuberculosis*. *Mol Microbiol* 45: 203-217.

56. Gouin E., Egile C., Dehoux P., Villiers V., Adams J. et al. (2004) The RickA protein of *Rickettsia conorii* activates the Arp2/3 complex. *Nature* 427: 457-461.

57. Jeng R.L., Goley E.D., D'Alessio J.A., Chaga O.Y., Svitkina T.M. et al. (2004) A Rickettsia WASP-like protein activates the Arp2/3 complex and mediates actin-based motility. *Cell Microbiol* 6: 761-769.

58. Stevens M.P., Stevens J.M., Jeng R.L., Taylor L.A., Wood M.W. et al. (2005) Identification of a bacterial factor required for actin-based motility of *Burkholderia pseudomallei*. *Mol Microbiol* 56: 40-53.

59. Snapper S.B., Takeshima F., Anton I., Liu C.H., Thomas S.M. et al. (2001) N-WASP deficiency reveals distinct pathways for cell surface projections and microbial actin-based motility. *Nat Cell Biol* 3: 897-904.

60. Lommel S., Benesch S., Rottner K., Franz T., Wehland J. et al. (2001) Actin pedestal formation by enteropathogenic *Escherichia coli* and intracellular motility of *Shigella flexneri* are abolished in N-WASP-defective cells. *EMBO Rep* 2: 850-857.

61. Lommel S., Benesch S., Rohde M., Wehland J., Rottner K. (2004) Enterohaemorrhagic and enteropathogenic *Escherichia coli* use different mechanisms for actin pedestal formation that converge on N-WASP. *Cell Microbiol* 6: 243-254.

62. Frischknecht F., Moreau V., Rottger S., Gonfloni S., Reckmann I. et al. (1999) Actin-based motility of vaccinia virus mimics receptor tyrosine kinase signalling. *Nature* 401: 926-929.

63. Gruenheid S., DeVinney R., Bladt F., Goosney D., Gelkop S. et al. (2001) Enteropathogenic *E. coli* Tir binds Nck to initiate actin pedestal formation in host cells. *Nat Cell Biol* 3: 856-859.

64. Moreau V., Frischknecht F., Reckmann I., Vincentelli R., Rabut G. et al. (2000) A complex of N-WASP and WIP integrates signalling cascades that lead to actin polymerization. *Nat Cell Biol* 2: 441-448.

65. Campellone K.G., Robbins D., Leong J.M. (2004) EspFU is a translocated EHEC effector that interacts with Tir and N-WASP and promotes Nck-independent actin assembly. *Dev Cell* 7: 217-228.

66. Springer B., Stockman L., Teschner K., Roberts G.D., Bottger E.C. (1996) Two-laboratory collaborative study on identification of mycobacteria: molecular versus phenotypic methods. *J Clin Microbiol* 34: 296-303.

67. Ramakrishnan L., Falkow S. (1994) *Mycobacterium marinum* persists in cultured mammalian cells in a temperature-restricted fashion. *Infect Immun* 62: 3222-3229.

68. Gouin E., Gantelet H., Egile C., Lasa I., Ohayon H. et al. (1999) A comparative study of the actin-based motilities of the pathogenic bacteria *Listeria monocytogenes*, *Shigella flexneri* and *Rickettsia conorii*. *J Cell Sci* 112 (Pt 11): 1697-1708.

69. Moors M.A., Levitt B., Youngman P., Portnoy D.A. (1999) Expression of listeriolysin O and ActA by intracellular and extracellular *Listeria monocytogenes*. *Infect Immun* 67: 131-139.

70. Goldberg M.B., Theriot J.A., Sansonetti P.J. (1994) Regulation of surface presentation of IcsA, a *Shigella* protein essential to intracellular movement and spread, is growth phase dependent. *Infect Immun* 62: 5664-5668.

71. Van Kirk L.S., Hayes S.F., Heinzen R.A. (2000) Ultrastructure of *Rickettsia rickettsii* actin tails and localization of cytoskeletal proteins. *Infect Immun* 68: 4706-4713.

72. Suzuki T., Mimuro H., Suetsugu S., Miki H., Takenawa T. et al. (2002) Neural Wiskott-Aldrich syndrome protein (N-WASP) is the specific ligand for *Shigella* VirG among the WASP family and determines the host cell type allowing actin-based spreading. *Cell Microbiol* 4: 223-233.

73. Skoble J., Portnoy D.A., Welch M.D. (2000) Three regions within ActA promote Arp2/3 complex-mediated actin nucleation and *Listeria monocytogenes* motility. *J Cell Biol* 150: 527-538.

74. Brundage R.A., Smith G.A., Camilli A., Theriot J.A., Portnoy D.A. (1993) Expression and phosphorylation of the *Listeria monocytogenes* ActA protein in mammalian cells. *Proc Natl Acad Sci U S A* 90: 11890-11894.

75. Byrd T.F., Green G.M., Fowlston S.E., Lyons C.R. (1998) Differential growth characteristics and streptomycin susceptibility of virulent and avirulent *Mycobacterium tuberculosis* strains in a novel fibroblast-mycobacterium microcolony assay. *Infect Immun* 66: 5132-5139.

76. Roach T.I., Slater S.E., White L.S., Zhang X., Majerus P.W. et al. (1998) The protein tyrosine phosphatase SHP-1 regulates integrin-mediated adhesion of macrophages. *Curr Biol* 8: 1035-1038.

77. Castro-Garza J., King C.H., Swords W.E., Quinn F.D. (2002) Demonstration of spread by *Mycobacterium tuberculosis* bacilli in A549 epithelial cell monolayers. *FEMS Microbiol Lett* 212: 145-149.

78. May R.C., Hall M.E., Higgs H.N., Pollard T.D., Chakraborty T. et al. (1999) The Arp2/3 complex is essential for the actin-based motility of *Listeria monocytogenes*. *Curr Biol* 9: 759-762.

79. Yarar D., D'Alessio J.A., Jeng R.L., Welch M.D. (2002) Motility determinants in WASP family proteins. *Mol Biol Cell* 13: 4045-4059.

80. Welch M.D., Iwamatsu A., Mitchison T.J. (1997) Actin polymerization is induced by Arp2/3 protein complex at the surface of *Listeria monocytogenes*. *Nature* 385: 265-269.

81. Welch M.D., DePace A.H., Verma S., Iwamatsu A., Mitchison T.J. (1997) The human Arp2/3 complex is composed of evolutionarily conserved subunits and is localized to cellular regions of dynamic actin filament assembly. *J Cell Biol* 138: 375-384.

82. Smith G.A., Theriot J.A., Portnoy D.A. (1996) The tandem repeat domain in the *Listeria monocytogenes* ActA protein controls the rate of actin-based motility, the percentage of moving bacteria, and the localization of vasodilator-stimulated phosphoprotein and profilin. *J Cell Biol* 135: 647-660.

83. Taunton J., Rowning B.A., Coughlin M.L., Wu M., Moon R.T. et al. (2000) Actin-dependent propulsion of endosomes and lysosomes by recruitment of N-WASP. *J Cell Biol* 148: 519-530.

84. Heuser J. (1981) Preparing biological samples for stereomicroscopy by the quick-freeze, deep-etch, rotary-replication technique. *Methods Cell Biol* 22: 97-122.

85. Takenawa T., Miki H. (2001) WASP and WAVE family proteins: key molecules for rapid rearrangement of cortical actin filaments and cell movement. *J Cell Sci* 114: 1801-1809.

86. Beuzon C.R., Salcedo S.P., Holden D.W. (2002) Growth and killing of a *Salmonella enterica* serovar *Typhimurium* sifA mutant strain in the cytosol of different host cell lines. *Microbiology* 148: 2705-2715.

87. Prehoda K.E., Scott J.A., Mullins R.D., Lim W.A. (2000) Integration of multiple signals through cooperative regulation of the N-WASP-Arp2/3 complex. *Science* 290: 801-806.

88. Kim A.S., Kakalis L.T., Abdul-Manan N., Liu G.A., Rosen M.K. (2000) Autoinhibition and activation mechanisms of the Wiskott-Aldrich syndrome protein. *Nature* 404: 151-158.

89. Rohatgi R., Nollau P., Ho H.Y., Kirschner M.W., Mayer B.J. (2001) Nck and phosphatidylinositol 4,5-bisphosphate synergistically activate actin polymerization through the N-WASP-Arp2/3 pathway. *J Biol Chem* 276: 26448-26452.

90. Carlier M.F., Nioche P., Broutin-L'Hermite I., Boujemaa R., Le Clainche C. et al. (2000) GRB2 links signaling to actin assembly by enhancing interaction of neural

Wiskott-Aldrich syndrome protein (N-WASp) with actin-related protein (ARP2/3) complex. *J Biol Chem* 275: 21946-21952.

91. Miki H., Suetsugu S., Takenawa T. (1998) WAVE, a novel WASP-family protein involved in actin reorganization induced by Rac. *EMBO J* 17: 6932-6941.

92. Frischknecht F., Way M. (2001) Surfing pathogens and the lessons learned for actin polymerization. *Trends Cell Biol* 11: 30-38.

93. Breitbach K., Rottner K., Klocke S., Rohde M., Jenzora A. et al. (2003) Actin-based motility of *Burkholderia pseudomallei* involves the Arp 2/3 complex, but not N-WASP and Ena/VASP proteins. *Cell Microbiol* 5: 385-393.

94. Egile C., Loisel T.P., Laurent V., Li R., Pantaloni D. et al. (1999) Activation of the Ccd42 effector N-WASP by the *Shigella flexneri* IcsA protein promotes actin nucleation by Arp2/3 complex and bacterial actin-based motility. *J Cell Biol* 146: 1319-1332.

95. Garmendia J., Phillips A.D., Carlier M.F., Chong Y., Schuller S. et al. (2004) TccP is an enterohaemorrhagic *Escherichia coli* O157:H7 type III effector protein that couples Tir to the actin-cytoskeleton. *Cell Microbiol* 6: 1167-1183.

96. Scaplehorn N., Holmstrom A., Moreau V., Frischknecht F., Reckmann I. et al. (2002) Grb2 and Nck act cooperatively to promote actin-based motility of vaccinia virus. *Curr Biol* 12: 740-745.

97. Kenny B. (1999) Phosphorylation of tyrosine 474 of the enteropathogenic Escherichia coli (EPEC) Tir receptor molecule is essential for actin nucleating activity and is preceded by additional host modifications. *Mol Microbiol* 31: 1229-1241.

98. Stamm L.M., Morisaki J.H., Gao L.Y., Jeng R.L., McDonald K.L. et al. (2003) *Mycobacterium marinum* escapes from phagosomes and is propelled by actin-based motility. *J Exp Med* 198: 1361-1368.

99. Kenny B., DeVinney R., Stein M., Reinscheid D.J., Frey E.A. et al. (1997) Enteropathogenic *E. coli* (EPEC) transfers its receptor for intimate adherence into mammalian cells. *Cell* 91: 511-520.

100. Phillips N., Hayward R.D., Koronakis V. (2004) Phosphorylation of the enteropathogenic *E. coli* receptor by the Src-family kinase c-Fyn triggers actin pedestal formation. *Nat Cell Biol* 6: 618-625.

101. Swimm A., Bommarius B., Li Y., Cheng D., Reeves P. et al. (2004) Enteropathogenic *Escherichia coli* use redundant tyrosine kinases to form actin pedestals. *Mol Biol Cell* 15: 3520-3529.

102. Cory G.O., Garg R., Cramer R., Ridley A.J. (2002) Phosphorylation of tyrosine 291 enhances the ability of WASP to stimulate actin polymerization and filopodium formation. *J Biol Chem* 277: 45115-45121.

103. Suetsugu S., Hattori M., Miki H., Tezuka T., Yamamoto T. et al. (2002) Sustained activation of N-WASP through phosphorylation is essential for neurite extension. *Dev Cell* 3: 645-658.

104. Benesch S., Lommel S., Steffen A., Stradal T.E., Scaplehorn N. et al. (2002) Phosphatidylinositol 4,5-biphosphate (PIP_2)-induced vesicle movement depends on N-WASP and involves Nck, WIP, and Grb2. *J Biol Chem* 277: 37771-37776.

105. Zettl M., Way M. (2002) The WH1 and EVH1 domains of WASP and Ena/VASP family members bind distinct sequence motifs. *Curr Biol* 12: 1617-1622.

106. Rohatgi R., Ho H.Y., Kirschner M.W. (2000) Mechanism of N-WASP activation by Cdc42 and phosphatidylinositol 4, 5-bisphosphate. *J Cell Biol* 150: 1299-1310.

107. Higgs H.N., Pollard T.D. (2000) Activation by Cdc42 and PIP_2 of Wiskott-Aldrich syndrome protein (WASp) stimulates actin nucleation by Arp2/3 complex. *J Cell Biol* 150: 1311-1320.

108. Nakanishi S., Catt K.J., Balla T. (1995) A wortmannin-sensitive phosphatidylinositol 4-kinase that regulates hormone-sensitive pools of inositolphospholipids. *Proc Natl Acad Sci U S A* 92: 5317-5321.

109. Ho H.Y., Rohatgi R., Lebensohn A.M., Le M., Li J. et al. (2004) Toca-1 Mediates Cdc42-Dependent Actin Nucleation by Activating the N-WASP-WIP Complex. *Cell* 118: 203-216.

110. Papayannopoulos V., Co C., Prehoda K.E., Snapper S., Taunton J. et al. (2005) A polybasic motif allows N-WASP to act as a sensor of PIP_2 density. *Mol Cell* 17: 181-191.

111. Strohmeier G.R., Fenton M.J. (1999) Roles of lipoarabinomannan in the pathogenesis of tuberculosis. *Microbes Infect* 1: 709-717.

112. Ortalo-Magne A., Lemassu A., Laneelle M.A., Bardou F., Silve G. et al. (1996) Identification of the surface-exposed lipids on the cell envelopes of *Mycobacterium tuberculosis* and other mycobacterial species. *J Bacteriol* 178: 456-461.

113. Pizarro-Cerda J., Cossart P. (2004) Subversion of phosphoinositide metabolism by intracellular bacterial pathogens. *Nat Cell Biol* 6: 1026-1033.

114. Snapper S.B., Rosen F.S., Mizoguchi E., Cohen P., Khan W. et al. (1998) Wiskott-Aldrich syndrome protein-deficient mice reveal a role for WASP in T but not B cell activation. *Immunity* 9: 81-91.

115. Bladt F., Aippersbach E., Gelkop S., Strasser G.A., Nash P. et al. (2003) The murine Nck SH2/SH3 adaptors are important for the development of mesoderm-derived embryonic structures and for regulating the cellular actin network. *Mol Cell Biol* 23: 4586-4597.

116. Anton I.M., Saville S.P., Byrne M.J., Curcio C., Ramesh N. et al. (2003) WIP participates in actin reorganization and ruffle formation induced by PDGF. *J Cell Sci* 116: 2443-2451.

117. Cosma C.L., Humbert O., Ramakrishnan L. (2004) Superinfecting mycobacteria home to established tuberculous granulomas. *Nat Immunol* 5: 828-835.

118. Lett M.C., Sasakawa C., Okada N., Sakai T., Makino S. et al. (1989) virG, a plasmid-coded virulence gene of *Shigella flexneri*: identification of the virG protein and determination of the complete coding sequence. *J Bacteriol* 171: 353-359.

119. Bernardini M.L., Mounier J., d'Hauteville H., Coquis-Rondon M., Sansonetti P.J. (1989) Identification of IcsA, a plasmid locus of *Shigella flexneri* that governs

bacterial intra- and intercellular spread through interaction with F-actin. *Proc Natl Acad Sci U S A* 86: 3867-3871.

120. Kocks C., Gouin E., Tabouret M., Berche P., Ohayon H. et al. (1992) *L. monocytogenes*-induced actin assembly requires the ActA gene product, a surface protein. *Cell* 68: 521-531.

121. Loisel T.P., Boujemaa R., Pantaloni D., Carlier M.F. (1999) Reconstitution of actin-based motility of *Listeria* and *Shigella* using pure proteins. *Nature* 401: 613-616.

122. Frischknecht F., Cudmore S., Moreau V., Reckmann I., Rottger S. et al. (1999) Tyrosine phosphorylation is required for actin-based motility of vaccinia but not *Listeria* or *Shigella*. *Curr Biol* 9: 89-92.

123. DeVinney R., Stein M., Reinscheid D., Abe A., Ruschkowski S. et al. (1999) Enterohemorrhagic *Escherichia coli* O157:H7 produces Tir, which is translocated to the host cell membrane but is not tyrosine phosphorylated. *Infect Immun* 67: 2389-2398.

124. DeVinney R., Puente J.L., Gauthier A., Goosney D., Finlay B.B. (2001) Enterohaemorrhagic and enteropathogenic *Escherichia coli* use a different Tir-based mechanism for pedestal formation. *Mol Microbiol* 41: 1445-1458.

125. Renzoni A., Cossart P., Dramsi S. (1999) PrfA, the transcriptional activator of virulence genes, is upregulated during interaction of *Listeria monocytogenes* with mammalian cells and in eukaryotic cell extracts. *Mol Microbiol* 34: 552-561.

126. Vazquez-Boland J.A., Kocks C., Dramsi S., Ohayon H., Geoffroy C. et al. (1992) Nucleotide sequence of the lecithinase operon of *Listeria monocytogenes* and possible role of lecithinase in cell-to-cell spread. *Infect Immun* 60: 219-230.

127. Middlebrook G., Dubos R.J., Pierce C. (1947) Virulence and morphological characteristics of mammalian tubercle bacilli. *J Exp Med* 86: 175-184.

128. Glickman M.S., Cox J.S., Jacobs W.R.J. (2000) A novel mycolic acid cyclopropane synthetase is required for cording, persistence, and virulence of *Mycobacterium tuberculosis*. *Mol Cell* 5: 717-727.

129. Glomski I.J., Gedde M.M., Tsang A.W., Swanson J.A., Portnoy D.A. (2002) The *Listeria monocytogenes* hemolysin has an acidic pH optimum to compartmentalize activity and prevent damage to infected host cells. *J Cell Biol* 156: 1029-1038.

130. Smith G.A., Marquis H., Jones S., Johnston N.C., Portnoy D.A. et al. (1995) The two distinct phospholipases C of *Listeria monocytogenes* have overlapping roles in escape from a vacuole and cell-to-cell spread. *Infect Immun* 63: 4231-4237.

131. Dueber J.E., Yeh B.J., Chak K., Lim W.A. (2003) Reprogramming control of an allosteric signaling switch through modular recombination. *Science* 301: 1904-1908.

132. Welch M.D., Mullins R.D. (2002) Cellular control of actin nucleation. *Annu Rev Cell Dev Biol* 18: 247-288.

133. Prouty M.G., Correa N.E., Barker L.P., Jagadeeswaran P., Klose K.E. (2003) Zebrafish-*Mycobacterium marinum* model for mycobacterial pathogenesis. *FEMS Microbiol Lett* 225: 177-182.

134. Jenkin G.A., Stinear T.P., Johnson P.D., Davies J.K. (2003) Subtractive hybridization reveals a type I polyketide synthase locus specific to *Mycobacterium ulcerans*. *J Bacteriol* 185: 6870-6882.